NATIONAL TRANSPORTATION SAFETY BOARD

Office of Research and Engineering
Washington, D.C. 20594

July 16, 2015

Vehicle Performance Study

by John O'Callaghan

ACCIDENT:

Location:	Koehn Lake, CA
Date:	October 31, 2014
Time:	10:07 Pacific Daylight Time (PDT) (17:07 Universal Coordinated Time (UTC))
Vehicle:	Scaled Composites SpaceShipTwo (SS2) rocket plane, N339SS
NTSB#:	DCA15MA019

TABLE OF CONTENTS

NATIONAL TRANSPORTATION SAFETY BOARD

Office of Research and Engineering
Washington, D.C. 20594

July 16, 2015

Vehicle Performance Study

by John O'Callaghan

A. ACCIDENT

Location: Koehn Lake, CA
Date: October 31, 2014
Time: 10:07 Pacific Daylight Time (PDT)
(17:07 Universal Coordinated Time (UTC))[1]
Vehicle: Scaled Composites SpaceShipTwo (SS2) rocket plane, N339SS
NTSB#: DCA15MA019

B. GROUP

Chairman: John O'Callaghan
National Resource Specialist - Aircraft Performance
National Transportation Safety Board (NTSB)
490 L'Enfant Plaza E, SW
Washington, DC 20594

Members: Mark Bassett
Design Engineer
Scaled Composites
Hangar 78 Airport, 1624 Flight Line
Mojave, CA 93501-1663

Mark Beyer
Engineering Manager of Flight Sciences
The Spaceship Company
Building 79, 1223 Sabovich St.
Mojave, CA 93501

Jennifer Bailey[2]
Aerospace Engineer
Federal Aviation Administration
Office of Commercial Space Transportation
800 Independence Ave SW, Rm 325
Washington, DC 22315

[1] Local time at Mojave on the day of the accident was Pacific Daylight Time (PDT). PDT = UTC - 7 hours. Times in this *Study* use the telemetry data time in PDT unless otherwise noted.
[2] Jennifer Bailey replaced Brett Vance as the FAA Group Member on November 14, 2014.

C. HISTORY OF FLIGHT

On October 31, 2014, about 10:07 PDT, a Scaled Composites (SC) SpaceShipTwo (SS2) reusable suborbital rocket, N339SS, experienced an in-flight anomaly during a rocket-powered flight test, resulting in loss of control of the vehicle. SS2 broke up into multiple pieces and impacted terrain over a 5-mile area near Koehn Dry Lake, California. One test pilot (the copilot) was fatally injured, and the other test pilot was seriously injured. SS2 had launched from the WhiteKnightTwo (WK2) carrier aircraft, N348MS, about 12 seconds before the loss of control. SS2 was destroyed, and WK2 made an uneventful landing. Scaled Composites was operating SS2 under an experimental permit issued by the Federal Aviation Administration's (FAA) Office of Commercial Space Transportation under the provisions of 14 *Code of Federal Regulations* (CFR) Part 437.

The objective of this *Vehicle Performance Study* (*Study*) is to determine and analyze the motion of the vehicle and the physical forces that produce that motion. In particular, the *Study* attempts to define SS2's position and orientation throughout its trajectory, and determine its response to control inputs, external disturbances, and other factors that could affect its trajectory.

The data the *Study* uses to determine and analyze the vehicle motion includes:

- Ground scars, markings, and debris locations.
- Recorded flight data (from both WK2 and SS2).
- Ground and vehicle-based video data.
- Radar data.
- Weather information.
- SS2 documentation, including the Pilot's Operating Handbook (POH) (Reference 1) and SC's Experimental Permit Application for SS2 (Reference 2).
- SS2 trajectory and loads prediction computer programs provided by SC.
- Personnel statements and interviews.

This *Study* describes the results of using the data listed above in defining the position of WK2 and SS2 relative to the Mohave Air and Space Port (KMHV) runway 30 threshold throughout the mission, and in particular during SS2's release from WK2, in-flight breakup, and descent. The *Study* describes the WK2/SS2 system briefly, introduces the vehicle motion data collected during the investigation, describes the methods used to extract additional vehicle motion information from the recorded data, and presents the results of these calculations.

In addition, this *Study* examines the aerodynamic and inertial moments about SS2's feather hinge ("feather moments"), particularly following the moment when recorded data and cockpit video evidence indicates that the co-pilot unlocked the feather (at Mach 1.0, instead of at Mach 1.4 as called for in the test plan). Finally, the *Study* presents the dispersion and impact locations of the major components and smaller debris from SS2, and compares this information with the operating area containment and exclusion zone requirements of 14 CFR Part 437, as specified in Reference 2.

The results presented in the *Study* indicate that the predicted aerodynamic feather moments shortly after the feather was unlocked were sufficient to overcome the closing moment provided by the feather actuators and inertia, and open the feather. Additionally, the flight path of WK2 and SS2, and the debris from the breakup of SS2, remained within the mission's operating area (Restricted Area R2508). The key flight safety events (release from WK2 and rocket-powered flight), and SS2's predicted instantaneous impact point (IIP), remained within the operating area and outside of the mission's exclusion zones.[3]

D. DETAILS OF THE INVESTIGATION

I. The Scaled Composites Tier 1B Suborbital Commercial Space Launch System

Tier 1B design mission

WK2 and SS2 are the two vehicles that comprise SC's "Tier 1B" project to develop a prototype suborbital commercial space launch system. The system's design mission is illustrated in Figure 1 (taken from Reference 2). SS2 is mated to WK2 on the ground (see Figure 2), and is carried by WK2 to altitude. At about 50,000 ft., SS2 is released from WK2, and its rocket motor ignited. SS2 then climbs under rocket thrust to approximately 150,000 ft. After the rocket fuel is exhausted, SS2 coasts to a maximum altitude (apogee) of approximately 360,000 ft. The vehicle is then "feathered" (see Figure 3) to provide a stable attitude for reentry and increase drag so as to reduce reentry speeds and associated structural loads and heating. At the appropriate time, the vehicle is returned to the "unfeathered" configuration and glides to a landing.

This system is further described in Reference 2, as follows:

> Scaled Composites (Scaled) is a proof-of-concept and prototyping aerospace company tasked with developing a reliable, reusable, and affordable suborbital commercial space tourism system for Virgin Galactic (Galactic). This program is called "Tier 1B". The goals for the Tier 1B program are to test and evaluate the vehicles and the systems and thus to improve safety and reliability of manned commercial space flight. Scaled is developing and testing the vehicles in support of this program.
>
> Scaled has developed two vehicles for the Tier 1B program in order to meet the goals of future space flight tourism:
>
> - The WhiteKnightTwo mother ship (WK2)
> - The SpaceShipTwo (SS2) space plane
>
> WK2 has been in flight test since December 2008 and SS2 since March 2010.
>
> …
>
> A nominal (design) altitude mission (shown in Figure 1) includes these phases or events (all times are approximate and will vary from flight-to-flight):

[3] The mission operating area, key flight safety events, exclusion zones, and IIP are described in Section D-VI.

- T = 0:00 –Air release [from WK2] at approximately 50,000 feet
- T = 0:04 –Boost phase beginning in gliding flight attitude and ending in a nearly vertical attitude.
- T = 0:23–Max Q at approximately 63,000 feet.
- T = 1:08–Engine cut-off at approximately 150,000 feet. The craft will then coast to apogee.
- T = 2:59–Apogee at approximately or above 360,000 feet.
- T = 5:13–Max Q at approximately 100,000 feet during reentry in care-free feathered configuration.
- T = 5:41–Transition to normal configuration (un-feathered) and beginning the glide phase.
- T = 18:00 –Landing at Mojave Air and Space Port

Other kinds of design missions are possible, including, but not limited to, a "down range" mission.

The accident occurred on the fourth "powered" (rocket motor ignited) test flight of SS2 (powered flight #4, or PF04), and the first powered flight with "RocketMotorTwo," a higher-thrust version of the rocket motor with a different kind of solid fuel and a newly-introduced (b) (4) system to stabilize rocket combustion.[4] The in-flight breakup occurred during the boost phase of PF04, about 12 seconds after the ignition of the rocket motor.

SS2 vehicle description

Reference 2 describes SS2 as follows:

> The Scaled Model 339 SpaceShipTwo (SS2) is an eight-seat,[5] hybrid-rocket powered, multi-configuration aircraft of composite construction. It has a low-wing, twin-tail boom, outboard horizontal tail, "extension-only" tricycle landing gear configuration. The vehicle was designed and built to provide regular suborbital space access for the general public.
>
> Key features of the design are:
>
> - All composite primary airframe structure
> - Two configurations, carry/boost/glide and reentry
> - Horizontal landing capability
> - Vertical and downrange trajectory capability
> - Redundant, custom-built avionics and inertial navigation units
> - Care Free "feather" reentry system
> - 361,000 feet to 427,000 feet altitude capability with six (6) passengers and two crew
> - Proprietary, custom-designed, hybrid rocket motor

Three-view drawings of SS2 in its unfeathered and feathered configurations are shown in Figure 3.

Table 1 presents some of SS2's dimensions, as well as relevant mass properties for PF04.

[4] Prior to PF04, SC conducted 17 "captive carry flights" (SS2 coupled to WK2 but not released), 30 "glide flights" (SS2 released from WK2, but without igniting the rocket motor), and 3 powered flights. See Reference 3 for more information about the development of the rocket motor.
[5] The six passenger seats were not installed on the accident flight.

Item	Value
Reference dimensions:[6]	
Wing area	449 ft^2
Wing span	23 ft.
Mean Aerodynamic Chord (MAC)	20.4 ft.
Mass properties for PF04:[7]	
Drop (release from WK2) weight	(b) (4)
Drop center of gravity (CG)	
Full burn landing weight	
Full burn landing CG	

Table 1. Dimensions of SS2, and mass properties for PF04.

II. Debris fields and major vehicle component locations

As noted above, starting about 11 seconds after the ignition of the rocket motor, SS2 broke up into multiple pieces, with the largest of these impacting terrain over a 5-mile area near Koehn Dry Lake. The locations of the multiple debris fields and major vehicle components were surveyed by the Kern County Sheriff's office using hand-held GPS devices, and more precisely by Federal Bureau of Investigation (FBI) Emergency Response Teams (ERTs) using a Total Station system. The results of the FBI survey of the major vehicle component locations are presented in Table 2 and Figures 5-7, in terms of a Cartesian coordinate system centered on the KMHV runway 30 threshold, with axes extending north and east.

Site number	Coordinates (latitude & longitude)	Coordinates (nmi north & east of KMHV rwy 30)	General Description
1	35°20'31.63"N 117°55'8.45"W	17.8240 north 10.4049 east	Right boom
2	35°19'34.34"N 117°56'42.85"W	16.8680 north 9.1194 east	Main oxidizer tank and wings
3	35°20'31.84"N 117°55'29.93"W	17.8269 north 10.1120 east	Left boom
4	35°18'15.10"N 117°58'31.31"W	15.5468 north 7.6422 east	Cockpit and nose section
5	35°17'33.59"N 117°59'16.01"W	14.8550 north 7.0334 east	Rocket Engine
6	35°21'20.15"N 117°55'12.47"W	18.6313 north 10.3483 east	Parachute
8	35°20'05.02"N 117°56'14.05"W	17.3793 north 9.5112 east	Seat

Table 2. Results of FBI survey of vehicle component debris field locations. *Note:* Site 7 was the wreckage site command post and contained no wreckage.

In addition to the major wreckage areas defined in Table 2, numerous small and light pieces of vehicle debris (such as skin fragments) were recovered by the Kern County's Sheriff's office, representatives of SC, and the general public in the area downwind (northeast) of the breakup point over the course of several days following the accident (see Figure 7). The most distant fragment was found on the China Lake Golf Course, about 27 nmi northeast of the breakup point. Descriptions of these items, as well as additional details regarding items located in the debris fields listed in Table 2, are provided in Reference 5.

[6] From Reference 1.
[7] Mass properties from the PF04 test card (see Reference 4).

III. Radar data

A RIR-716C Range Instrumentation Radar (RIR) located on Edwards Air Force Base (EDW AFB) tracked WK2 with SS2 attached, and SS2 itself following release from WK2, from shortly after takeoff from KMHV until the impact of the SS2 main oxidizer tank (MOT) and wings with the ground (at site 2 in Table 2). In addition, WK2, SS2, and the Extra 300 airplane (registration N24GA) that SC used as a chase plane during the flight test were tracked by a number of FAA and military Airport Surveillance Radars (ASRs). The ASRs also detected primary radar returns from SS2 debris starting at the break-up time and continuing for over an hour, as lightweight pieces from the vehicle drifted northeast carried by the wind. Data from the ASR located on EDW AFB (EDW) are used in this *Study.* The RIR and ASR data are described further below.

Range Instrumentation Radars

The RIR-716C located on EDW AFB (RIR) is part of the NASA/Dryden Flight Research Test Center (DFRC) Western Aeronautical Test Range (WATR). The DFRC website[8] describes the RIR-716C radar as follows:

> The WATR RADAR systems include two highly accurate RIR-716 C-band instrumentation radars, providing Time Space Positioning Information (TSPI) of research aircraft and Low Earth Orbiting (LEO) space vehicles. Each RADAR system has a 1-megawatt transmitter and can track targets with accuracies to 0.0006 degrees in angle and 30 feet in range - depending on supporting mode (skin or beacon).

Unlike surveillance radars (described below), tracking radars keep their radar beams focused on the target of interest, and so returns from the target are received at a much higher frequency than with surveillance radars. However, this also means that tracking radars can only track one target at a time, while surveillance radars, which sweep the horizon while rotating about a vertical axis, can track all targets within their field of coverage.

Personnel from EDW AFB provided the recorded RIR data from the WK2 / SS2 accident mission to the NTSB. The data were recorded at 20 Hz and include the following parameters:

- UTC time of the radar return, in hours, minutes, and seconds.
- Slant range from the radar antenna to the target, in yards.
- Azimuth relative to True North from the radar antenna to the target, in degrees.
- Elevation from the radar antenna to the target, in degrees.

The geographic location of the radar antenna must be known in order to determine the latitude and longitude of the target from the range, azimuth, and elevation data recorded by the radar. The RIR antenna coordinates are:

Latitude:	N 34° 57’ 38.89931”
Longitude:	W 117° 54’ 41.40755”
Elevation:	2666.1 ft.

The positions of WK2, SS2, and N24GA are most conveniently expressed in rectangular Cartesian coordinates. As mentioned above, the Cartesian coordinate system used in this

[8] See http://www.nasa.gov/centers/dryden/capabilities/CodeM/CodeMR/watr_systems_overview_prt.htm.

Study is centered at the KMHV runway 30 threshold, with axes extending east, north, and up from the center of the Earth. The data from the RIR are converted into this coordinate system by first computing the latitude, longitude, and altitude of the target using the WGS84 ellipsoid model of the Earth, and then computing the coordinates east and north of the KMHV runway 30 threshold. The coordinates of the runway 30 threshold are:

Latitude:	N 35° 02' 41.2716"
Longitude:	W 118° 07' 51.4825"
Elevation:	2680.3 ft.

The RIR data for WK2 and SS2 are presented in Figures 4-10. Figure 8 presents two altitude calculations based on the RIR data: one that does not include any corrections for atmospheric refraction of radar beam, and one that incorporates an approximate correction by using an altered radius of the Earth when accounting for the Earth's curvature in the altitude calculation. This altered radius is 4/3 times the actual Earth radius at the latitude of the RIR antenna (using the WGS84 ellipsoid model).[9] The approximate correction does not account for the effects of actual atmospheric moisture, temperature, and pressure at the time of the flight, which affect the refraction of the radar beam. Nonetheless, since the approximate correction makes the RIR altitude match the WK2 inertial altitude better than the uncorrected RIR altitude, the corrected RIR altitude is shown in Figures 4-10. The difference between the (corrected) RIR altitude and WK2 inertial altitude increases with range from the radar antenna, and is a maximum of about 550 ft. at a range of 80 nmi. This is equivalent to about a 0.065° error in the elevation of the radar beam.

Airport Surveillance Radars

Airport Surveillance Radars (ASRs) are short range (60 nmi) radars used to provide air traffic control services in terminal areas. ASR antennas rotate at 13 to 14 RPM, resulting in a radar return every 4.3 to 4.6 seconds. In addition to detecting radar energy reflected from aircraft surfaces (primary returns), the radars also emit transponder interrogations and detect the corresponding transponder replies from aircraft (secondary returns), which contain identifying beacon code (Mode A) and altitude (Mode C) information. Secondary radar returns from WK2, SS2, and N24GA were recorded by several FAA and military ASRs during the accident mission. In addition, numerous primary returns that are consistent with debris shed from SS2 during the in-flight breakup were recorded after secondary returns were no longer received.

Recorded data from these ASRs were provided to the NTSB by personnel from the FAA Joshua Air Traffic Control Facility (Joshua). For this *Study,* data from the EDW ASR11 and the Fremont Valley Common Digitizer (QFV CD2) radars are presented. Specifically, secondary returns from N24GA and primary returns following the break-up of SS2 recorded by the EDW ASR11 are presented in Figures 4-10. In addition, secondary returns from the helicopters involved in the rescue of the surviving pilot, as recorded by the QFV CD2, are presented in Figures 11 and 12.[10] ASR returns from WK2 and SS2 are not presented, since higher-quality position data for these vehicles is available from the RIR and recorded or telemetered inertial data (see Section D-IV).

[9] See http://www.radartutorial.eu/01.basics/Calculation%20of%20height.en.html.
[10] The QFV CD2 radar did not record primary returns.

The EDW ASR11 and QFV CD2 data include the following parameters:

- UTC time of the radar return, in hours, minutes, and seconds.

- Transponder beacon code associated with the return (secondary returns only). The Scaled Composites vehicles involved in the accident mission used the following transponder codes:

  - WK2 (with and without SS2 attached) = transponder code 0401. Secondary returns from WK2 stopped (the last return was received) at 17:04:34, 24 seconds before transponder returns started be received from SS2 in preparation for SS2's release from WK2. Secondary returns from WK2 (with transponder code 0401) resumed at 17:08:50.
  - SS2 = transponder code 0402. Secondary returns from SS2 were received starting at 17:04:58. The last return was received at 17:07:32.6.
  - N24GA = transponder code 0403. Following the breakup of SS2, secondary returns from N24GA were interrupted for brief periods as the airplane was maneuvering near the accident site. These gaps are apparent in Figures 4-10, and may be the result of radar line-of-sight interruptions due to N24GA's relatively low altitude (below 4000 ft. MSL) during the interruptions.

  The helicopters involved in the rescue of the surviving pilot used the following call signs and transponder codes, as determined by a review of the recorded radar data, Air Traffic Control (ATC) communications with the FAA Joshua High Desert Terminal Radar Approach Control (TRACON) facility, and transcripts of personnel on board the helicopters (References 6-9):[11]

  - Call sign "Tiger 1" (National Test Pilot School UH-1) = transponder code 0444.
  - Call sign "Helo 408" (Kern County Fire Department [KCFD]) UH-1 = transponder code 1255.
  - Call sign "Mercy 14" (Mercy Air medical evacuation helicopter) = transponder code 0447.

- Transponder reported altitude in hundreds of feet MSL (secondary returns only). This altitude is pressure altitude, and must be corrected for the local altimeter setting (29.96 "Hg) to obtain true altitude.[12] The resolution of the altitude data is ± 50 ft.

- Slant Range from the radar antenna to the return, in 1/128^{ths} of a nautical mile. The accuracy of this data is ± 1/16 nmi or about ± 380 ft.

- Azimuth relative to Magnetic or True North from the radar antenna to the return[13]. The azimuth is reported in 1/16^{ths} of an Azimuth Change Pulse (ACPs). ACPs range from 0 to

[11] The radar data indicates that two more helicopters, on transponder codes 1203 and 1277, were also operating in the area of the wreckage sites. However, these helicopters do not appear to have been involved in the rescue of the surviving pilot, and their tracks are not plotted here.
[12] An altimeter setting of 29.96 "Hg will result in a true altitude about 37 ft. higher than the pressure altitude.
[13] The magnetic variation used by the EDW ASR11 to determine magnetic azimuth is 14.5° W. The QFV CD2 recorded azimuth relative to True North, and no correction for magnetic variation is required.

4096, where 0 = 0° magnetic and 4096 = 360° magnetic. Thus, the azimuth to the target in degrees is:

(Azimuth in degrees) = (360/4096) x (Azimuth in ACPs) = (0.08789) x (Azimuth in ACPs)

The accuracy of azimuth data is ± 2 ACP or ± 0.176°.

The geographic location of the radar antenna must be known to determine the latitude and longitude of radar returns from the range and azimuth data recorded by the radar. The EDW ASR11 antenna coordinates are:

Latitude: N 34° 52' 22.6"
Longitude: W 117° 54' 32.5"
Elevation: 2408 ft.

The QFV CD2 antenna coordinates are:

Latitude: N 35° 13' 01.07"
Longitude: W 118° 00' 44.27"
Elevation: 2178 ft.

The EDW ASR11 secondary returns from N24GA and primary returns consistent with debris from SS2 are presented in Figures 4-10. The QFV CD2 secondary returns from the helicopters involved in the rescue of the surviving pilot are presented in Figures 11 and 12.

Note in Figures 7 and 10 that the EDW ASR11 primary returns originating at the site of the in-flight breakup drift towards the northeast in what appears to be two distinct groups. Using linear fits through the north and east positions of these groups as shown in Figure 10, the average speed and direction of the groups can be computed.

The faster group is drifting at 74 kts. from 223° (on a track of 43°); the slower group is drifting at 45 kts. from 219° (on a track of 39°). The speed and direction of drift is generally consistent with the wind speeds at various altitudes computed from inertial and airspeed data recorded by WK2 (see Section D-V and Figure 24). Based on these wind calculations, the faster group of primaries is consistent with lighter debris remaining at higher altitudes with stronger winds, and the slower group is consistent with heavier items that descend more quickly to lower altitudes and weaker winds. Note that the locations of the numerous pieces of small debris documented in Reference 5 (and plotted in Figure 7) are consistent with the track of the primary returns.

The tracks of the rescue helicopters are plotted in Figure 11, and the helicopter altitudes are plotted vs. time in Figure 12. The times of the returns in Figure 11 are indicated by the symbol colors, as noted in the color scale in the bottom right. Specific times of the beginning and end of the tracks plotted in the Figure are also shown (the NTSB only requested data through 11:30 PDT, so all the tracks end near that time).

The "Site 6 landing & takeoff times" noted in Figure 11 are the times that the radar returns descend to the lowest recorded altitude and remain steady or disappear, and then reappear and increase in altitude (see Figure 12). These times should be close to the actual helicopter touchdown and liftoff times, since the QFV CD2 apparently "sees" the helicopters all the way to the elevation of wreckage site 6 (1976 ft., per *Google Earth*).

IV. Recorded flight data

Description of data sources

PF04 was a developmental flight test of SS2, and consequently the vehicle was fitted with extensive instrumentation for sensing, recording, and transmitting numerous parameters describing the states of the vehicle's motion and systems. In addition, video and audio recordings from an over-the-shoulder camera mounted in the cockpit, a video recording from a camera mounted on SS2's left tail boom, and video recordings from several ground-based cameras captured data from the accident flight. These data sources, and the procedures used to recover the information retained by them, are described in References 10-12. Reference 12 also describes additional video cameras that were aboard SS2 and WK2.

This *Study* presents data (referred to here as "TM data") telemetered from SS2's Strap-On Data Acquisition System (SODAS) to a ground station, and recorded on a computer in SC's Mission Control Room. This data includes numerous vehicle motion and system parameters. Audio and video information telemetered from the over-the-shoulder cockpit video camera and recorded on the ground is also presented. Additional parameters computed using the TM data are described in Section D-V.

Motion data for WK2 (including inertial-derived position, attitude, and speed, and pitot-static airspeeds) were used to compute the winds encountered by the airplane during its climb from KMHV to the peak altitude it obtained following the release of SS2 (about 46,600 ft. MSL). These winds are used along with the inertial parameters telemetered by SS2 to compute SS2's actual airspeed and Mach number following release from WK2 (see Section D-V).

SS2 telemetered parametric data (TM data)

Reference 10 describes the TM data recovery process used by the investigation Data Group, and the resulting data set provided by that Group.[14] During the investigation, the Vehicle Performance Group Chairman (VPGC) requested additional parameters that were not in the original set from SC and The Spaceship Company (TSC), which were provided directly by those companies. These additional parameters included "raw" (unfiltered) inertial load factors and angular rates for SS2, and position, attitude, and airspeed data for WK2.

The parameters of most interest in this *Study* concern the motion of SS2 and the timing of significant events associated with the rocket motor (rocket motor arming and firing), and the feather system (feather unlocking and the start of feather motion). Parameters describing the cockpit control and aerodynamic control surface positions are also of interest. Plots of these parameters, focusing on the approximately 14 seconds between the release of SS2 from WK2 and the end of TM data from SS2, are presented in Figures 13 - 22.[15] The parameter names are identified in the plot legends, and the source and meaning of the parameters themselves are described briefly in Tables 3-10.

The source of the SS2 motion parameters (linear and angular positions, speeds, and accelerations) are the two Inertial Navigation Systems (INSs) and two Air Data Computers (ADCs) on SS2. Reference 1 describes these systems as follows:

[14] The Data Group provided the TM data in the following *Microsoft Excel* file:
"TestPointExport_PF04 L-10 - END_NTSB_20141105_export_304_16_57_30.csv."
[15] The x-axis parameter in these Figures is the recorded TM data inter-range instrumentation group (IRIG) time.

Inertial Navigation System (INS)
The Avionics System utilizes two INS LRUs [Line-Replaceable Units], based on the (b) (4) system. Each INS is capable of providing vehicle attitude, velocity and position information. INS data can be displayed on any of the three MFDs [Multi-Functional Displays] and the pilots can select either INS source as desired on each MFD. (b) (4)

Air Data Systems
There are three independent air data systems. The first consists of conventional side-mounted fuselage pitot L-probes and flush static ports. Each L-probe provides pitot air data to its respective air data computer. Below each probe is a button-style flush static port. The two ports are teed together and the combined pressure is the reference input to both ADCs. A third L-probe mounted below the primary right-side L-probe provides pitot information to the L3 Standby All Directional Indicator (b) (4) Static pressure for the ESIS is provided by a second set of left and right side flush ports (mounted just below the primary static ports) that are teed together to provide a common reference source. Additionally, a Flush Air Data System (FADS) is built into the nose cone. The six FADS sensors feed an algorithm that derives conventional pitot-static information as well as angle of attack and sideslip. (b) (4)

Of note, SS2 is not equipped with angle of attack (α) vanes or a supersonic air data system. An inertial is computed from the INS data, (b) (4)

The FADS mentioned in Reference 1 has been used by SC during subsonic flight tests, but is not included in the TM data set for PF04 provided by the Data Group.

SS2's ADC data starts to become unreliable due to compressibility and shock effects starting at about Mach 0.8 (see the plots of ADC-based barometric altitude and rate-of-climb, in Figures 14 and 15). For this reason, under normal conditions the pilots' MFD displays switch from displaying airspeed and altitude data based on ADC parameters to those based on INS parameters. As described in Reference 1,

> **Air Data Display Source:** Allows the pilot to select if the ADC or INS should drive the altimeter and airspeed data groups. Under normal operating conditions, both pilots should use SRC AUTO. This mode defaults to the ADC and automatically select the INS as the air data source when any of the following conditions exist:
> - Airspeed above 0.80M
> - Altitude above 60,000 feet
> - Feather not down

When the MFD airspeed group is driven by the INS, the speeds and Mach numbers displayed are relative to the Earth, not the air mass. Hence, they will be in error by the difference (due to winds) between the vehicle's total inertial speed relative to Earth, and its total speed relative to the air mass. On PF04, this difference is about 62 to 66 KTAS or about 0.12 to 0.13 Mach (with speeds relative to the air mass being higher; see Section D-V and Figure 15). The speed of sound used to compute the INS-based Mach number from the INS speed is determined using the static temperature at the current inertial altitude in the standard atmosphere. On PF04, the actual speed of sound corresponding to the ambient static temperature was about 1.3% to 1.6% lower than the standard-atmosphere speed of sound.

(b) (4)

For a nominal mission, as the vehicle pitches up towards the vertical and accelerates, the effect of winds on the difference between the total speeds relative to the air mass and the Earth decreases significantly.

SS2 Release, Rocket Motor, and Feather System Parameters		
Parameter description	**Parameter name (plot label)**	**Figure #**
SS2 release from WK2 discrete	SS2_RMC_carrier_separated	13
Distance between SS2 and WK2 from left INSs	SS2_WK2_Seperation	13
Rocket arm switch on	SS2_RMC_arm_switch_on	13
Rocket Arm - pilot valve position feedback	SS2_RMC_SV_A2_arm_pilot_open	13
Verifies signal command to main oxidizer valve	SS2_RMC_SV_A1_open_fire_pilot_cmd	13
Rocket Fire - Pilot valve position feedback	SS2_RMC_SV_A1_fire_pilot_open	13
Right feather locked discrete (1=locked)	SS2_Right_Feather_Lock_Position_Switch	13
Right feather unlocked discrete (1=unlocked)	SS2_Right_Feather_UNLock_Position_Switch	13
R feather lock discrete (1=locked, -1=unlocked)	SS2_Right_Feather_Lock_State	13
Left feather locked discrete (1=locked)	SS2_Left_Feather_Lock_Position_Switch	13
Left feather unlocked discrete (1=unlocked)	SS2_Left_Feather_UNLock_Position_Switch	13
R feather lock discrete (1=locked, -1=unlocked)	SS2_Left_Feather_Lock_State	13
Feather position (%)	SS2_Feather_Position	13

Table 3. SS2 release, rocket motor, and feather system parameters from TM data set presented in this *Study.*

SS2 Position Parameters		
Parameter description	**Parameter name (plot label)**	**Figure #**
GPS latitude	SS2_LAT_GPS	14a
GPS longitude	SS2_LONG_GPS	14a
GPS altitude	SS2_ALT_FT_GPS	14a,b
Latitude from left INS	SS2_Left_Latitude	14a
Longitude from left INS	SS2_Left_Longitude	14a
Altitude from left INS	SS2_Left_Altitude	14a,b
Latitude from right INS	SS2_Right_Latitude	14a
Longitude from right INS	SS2_Right_Longitude	14a
Altitude from right INS	SS2_Right_Altitude	14a
Barometric altitude from left ADC	SS2_Left_Baro_Alt	14a
Pressure altitude from left ADC	SS2_Left_Pressure_Alt	14a
Left ADC barometric altimeter setting	SS2_Left_Baro_Setting	14a
Barometric altitude from right ADC	SS2_Right_Baro_Alt	14a
Pressure alt from right ADC	SS2_Right_Pressure_Alt	14a
Right ADC barometric altimeter setting	SS2_Right_Baro_Setting	14a
Flush Air Data System derived pressure altitude	FADS_P_Alt	14a

Table 4. SS2 position parameters from TM data set presented in this *Study.*

SS2 Speed Parameters		
Parameter description	**Parameter name (plot label)**	**Figure #**
Groundspeed from GPS	SS2_BNR_VELOC_KTS	15
Equivalent airspeed from left ADC	SS2_Left_KEAS	15
True airspeed from left ADC	SS2_Left_TAS	15
Equivalent airspeed from right ADC	SS2_Right_KEAS	15
True airspeed from right ADC	SS2_Right_TAS	15
Mach number from left ADC	SS2_Left_Mach	15
Mach number from right ADC	SS2_Right_Mach	15
Ground speed from left INS	SS2_L_Groundspeed	15
Ground speed from right INS	SS2_R_Groundspeed	15
Flush Air Data System derived calibrated Airspeed	FADS Calibrated Airspeed	15
Flush Air Data System derived equivalent Airspeed	FADS Equivalent Airspeed	15
Rate of climb from left ADC	SS2_Left_VSI	15
Rate of climb from left INS	SS2_Left_Vertical_Vel	15
Rate of climb from right ADC	SS2_Right_VSI	15
Rate of climb from right INS	SS2_Right_Vertical_Vel	15
Mach number estimate from right INS	SS2_Right_INS_Mach_Est	15
Mach number estimate from left INS	SS2_Left_INS_Mach_Est	15

Table 5. SS2 speed parameters from TM data set presented in this *Study.*

SS2 Flight Angle Parameters		
Parameter description	**Parameter name (plot label)**	**Figure #**
Flight path angle from left INS	SS2_Left_INS_Derived_Gama	16
Flight path angle from right INS	SS2_Right_INS_Derived_Gama	16
Angle of attack from left INS	SS2_Left_INS_Derived_Alpha	16
Angle of attack from right INS	SS2_Right_INS_Derived_Alpha	16
Left ADC Angle of Attack	SS2_Left_Angle_of_Attack	16
Right ADC Angle of Attack	SS2_Right_Angle_of_Attack	16
Left ADC derived flight path angle	GammaADCleft	16
Right ADC derived flight path angle	GammaADCright	16
Ground track from left INS	Left_Track	16
Ground track from right INS	Right_Track	16

Table 6. SS2 flight angle parameters from TM data set presented in this *Study.*

SS2 Euler Angle and Angular Rate Parameters		
Parameter description	**Parameter name (plot label)**	**Figure #**
True heading displayed on MFD	DisplayedYaw	16
Pitch angle displayed on MFD	DisplayedPitch	16
Roll angle displayed on MFD	DisplayedRoll	16
Left INS pitch indication	SS2_Left_Pitch	16
Left INS roll indication	SS2_Left_Roll	16
Left INS Heading	SS2_Left_Yaw	16
Right INS pitch indication	SS2_Right _Pitch	16
Right INS roll indication	SS2_Right _Roll	16
Right INS Heading	SS2_Right _Yaw	16
Left INS processed roll rate	SS2_Left_ProcessedIMU_RollRate	17
Left INS processed pitch rate	SS2_Left_ProcessedIMU_PitchRate	17
Left INS processed yaw rate	SS2_Left_ProcessedIMU_YawRate	17
Right INS processed roll rate	SS2_Right_ProcessedIMU_RollRate	17
Right INS processed pitch rate	SS2_Right_ProcessedIMU_PitchRate	17
Right INS processed yaw rate	SS2_Right_ProcessedIMU_YawRate	17
Left INS unprocessed roll rate	SS2_Left_gyro_x_raw	17
Left INS unprocessed pitch rate	SS2_Left_gyro_y_raw	17
Left INS unprocessed yaw rate	SS2_Left_gyro_z_raw	17

Table 7. SS2 Euler angle and rate parameters from TM data set presented in this *Study.*

SS2 Load Factor Parameters		
Parameter description	**Parameter name (plot label)**	**Figure #**
X Accelerometer data from pilot's headrest	SS2_Accel_Pilot_Seat_XDIR	18
Y Accelerometer data from pilot's headrest	SS2_Accel_Pilot_Seat_YDIR	18
Z Accelerometer data from pilot's headrest	SS2_Accel_Pilot_Seat_ZDIR	18
Left INS processed n_x	SS2_Left_ProcessedIMU_Accel_X	18
Right INS processed n_x	SS2_Right_ProcessedIMU_Accel_X_in_g	18
Left INS processed n_y	SS2_Left_ProcessedIMU_Accel_Y_in_g	18
Right INS processed n_y	SS2_Right_ProcessedIMU_Accel_Y_in_g	18
Left INS processed nlf	NLFleft	18
Right INS processed nlf	NLFright	18
Left INS unprocessed n_x	SS2_raw_nx	18
Left INS unprocessed n_y	SS2_raw_ny	18
Left INS unprocessed nlf	SS2_raw_nlf	18

Table 8. SS2 load factor parameters from TM data set presented in this *Study.*

SS2 Flight Control Parameters		
Parameter description	**Parameter name (plot label)**	**Figure #**
Pitch force load cell measurement	SS2_Pitch_Load_Cell	19
Stick string potentiometer output in Pitch axis	SS2_Stick_Pitch_Stringpot_Position	19
Derived roll force from horizontal stabilizer controllers and elevon position	SS2_Roll_Stick_Force	19
Stick string potentiometer output in roll axis	SS2_Stick_Roll_Stringpot_Position	19
Derived pedal position from left and right string potentiometers attached to left and right pedals	SS2_Pedal_Position	19
Left rudder position calculated from string potentiometer attached at rudder surface	Left Rudder Position	19
Right rudder position calculated from string potentiometer attached at rudder surface	Right Rudder Position	19
Average of left and right rudder positions	Average Rudder Position	19
Effective rudder indication	Effective Rudder	19
Left rudder lock valve enabled discrete	SS2_Left_Rudder_Lock_Enable	19
Right rudder lock valve enabled discrete	SS2_Right_Rudder_Lock_Enable	19
Left horizontal stabilizer position calculated from string potentiometer attached to stab surface	Left Stab position	20
Right horizontal stabilizer position calculated from string potentiometer attached to stab surface	Right Stab position	20
Left elevon position calculated from string potentiometer attached at elevon surface	Elevon position (left)	20
Right elevon position calculated from string potentiometer attached at elevon surface	Elevon position (right)	20
Left elevon position calculated from string potentiometer attached at elevon surface, recalibrated for GF04[17]	Elevon position GF04 (left)	20
Right elevon position calculated from string potentiometer attached at elevon surface, recalibrated for GF04	Elevon position GF04 (right)	20
Left horizontal stabilizer effective position	Left Stab Effective position	20
Right horizontal stabilizer effective position	Right Stab Effective position	20
Left stabilizer effective position recalibrated for GF04	Left Stab Effective position GF04	20
Right stabilizer effective position recalibrated for GF04	Right Stab Effective position GF04	20
Average of left and right horizontal stabilizer positions	Stabilizer Pitch	21
Average differential position between L and R stabilizers	Stabilizer Roll	21
Average elevon postion between left and right elevons	Elevon Pitch	21
Average differential position between left and right elevons	Elevon Roll	21
Elevon pitch recalibrated for GF04	Elevon Pitch GF04	21
Elevon roll recalibrated for GF04	Elevon Roll GF04	21
Average of L & R stabilizer effective pitch values	Effective Stabilizer Pitch	21
Average of L & R stabilizer effective roll values	Effective Stabilizer Roll	21
Average of L & R stabilizer effective pitch values, recalibrated for GF04	Effective Stabilizer Pitch GF04	21
Average of L & R stabilizer effective roll values, recalibrated for GF04	Effective Stabilizer Roll GF04	21

Table 9. SS2 flight control parameters from TM data set presented in this *Study.*

[17] GF04 = Glide Flight #4 (a test flight on which the rocket motor was not ignited).

SS2 Atmospheric Parameters		
Parameter description	**Parameter name (plot label)**	**Figure #**
Left ADC total pressure	PTOTleft	22
Left ADC static pressure	PMABleft	22
Left ADC static air temperature	SS2_Left_Static_Temp	22
Left ADC total air temperature	SS2_Left_TOAT	22
Right ADC total pressure	PTOTright	22
Right ADC static pressure	PAMBright	22
Right ADC static air temperature	SS2_Right_Static_Temp	22
Right ADC total air temperature	SS2_Right_TOAT	22
Estimated static air temperature based on preflight winds and left INS inertial altitude lookup table	SS2_Static_Temperature_Preflight_ Est_Left_INS	22
Left ADC dynamic pressure	SS2_Left_Dynamic_Pressure	22
Right ADC dynamic pressure	SS2_Right_Dynamic_Pressure	22

Table 10. SS2 atmospheric parameters from TM data set presented in this *Study.*

SS2 aerodynamic control system parameters

The parameters describing the positions of the aerodynamic control surfaces on SS2 are listed in Table 9, and plotted in Figures 19-21. Since SS2's aerodynamic configuration differs from that of a conventional airplane, the vehicle's aerodynamic control system and surfaces warrant further explanation. The following selections from the "Flight Controls" section of Reference 1 provide a brief overview of the system:

CTRL – Flight Controls

General

The primary flight control system of SpaceShipTwo is a mechanical reversible system consisting of pitch and roll elevons and yaw rudders. Cockpit control is by a yoke shaped center stick and rudder pedals. There is a dual set of connected controls for the pilot and co-pilot. Pitch and roll are trimmed via electric horizontal stabilizer actuators. There is no rudder trim. Secondary flight control is solely a ventral speed brake to provide glide path control during the landing approach. Primary pitch and roll trim controls are located on the stick grips.

…

(b) (4)

Stabilator Control System

Overview

Pitch trim, roll trim, supersonic pitch control, and supersonic roll control (roll boost) functions are provided by a pair of (b) (4) internally redundant (dual ended) electric mechanical actuators ….

The actuators drive the all flying horizontal tails (stabilators), which are moved symmetrically to affect pitch and differentially to control roll (when Roll Boost is enabled). The actuators are located one in each boom.

…

(b) (4)

Since the left and right elevons and horizontal stabilizers (or stabilators) combine to produce pitching and rolling moments, SC uses a number of additional parameters to measure the "effective" pitch and roll commands produced by these surfaces. The elevons are flaps on the trailing edges of the stabilizers, and so their deflections change the total stabilizer lift. The lift of a stabilizer with a deflected elevon can be thought of as "equivalent" to the lift of a stabilizer with a faired elevon, but at a different incidence (stabilizer) position. The stabilizer positon with the faired elevon is the "effective" stabilizer position. The difference between the actual stabilizer position and the effective stabilizer position depends on the amount of elevon deflection, and the Mach number. 1° of elevon deflection is roughly equivalent to (b) (4) of stabilizer deflection below Mach 1, and to (b) (4) of stabilizer deflection above Mach 1.[18] The effective stabilizer positon parameters recorded in the TM data file are listed in Table 9 and plotted at the bottom of Figure 20.

Both the elevons and stabilizers move differentially to produce rolling moments. The difference between the left and right elevon positions is a measure of the rolling moment due to differential elevon deflection (by itself). Similarly, the difference between the left and right stabilizer positions is a measure of the rolling moment due to differential stabilizer deflection (by itself). In addition, the pitching moments produced by differential motion of the elevon and stabilizer surfaces can be different than those produced when these surfaces move symmetrically. The total roll and pitch commands (expressed in degrees of surface deflection) produced by the combination of left and right elevon (by itself) are shown in the top plot of Figure 21. The total roll and pitch commands (expressed in degrees of surface deflection) produced by the combination of left and right stabilizer (by itself) are shown in the middle plot of Figure 21.

As described above, the elevon positions can be combined with the stabilizer positions to produce "effective" stabilizer positions. The total roll and pitch commands (expressed in degrees of surface deflection) produced by the combination of left and right effective stabilizer are shown in the bottom plot of Figure 21.

Significant SS2 release, rocket motor, and feathering system events

Many of the Figures in this *Study* contain notes or symbols denoting significant mission events, including the release of SS2 from WK2, the firing of SS2's rocket motor, and the unlocking and movement of SS2's feathering system. For example, Figures 4 and 5 denote these events as markers along SS2's flight track, and Figures 13-22 denote these events as vertical green lines positioned at the time of occurrence of the events, as determined from the TM data. The events depicted in this way are summarized in Table 11.

[18] Email from SC Vehicle Performance Group Member to VPGC, dated 02/17/2015.

Event	Time (HH:MM:SS PDT)
Release from WK2 discrete = 1 (SS2_RMC_carrier_separated)	10:07:19.1
Rocket fire command discrete = 1 (SS2_RMC_SV_A1_open_fire_pilot_cmd)	10:07:21.6
Feather lock state discrete = 0 (SS2_Left_Feather_Lock_State)	10:07:29.5
Feather movement (based on Feather Position parameter)[19]	10:07:30.6
Last apparently valid point in TM data file (based on left INS vertical load factor)*	10:07:33.1
Last data point in TM data file*	10:07:35.0

Table 11. Significant release, rocket motor, and feather system events denoted in the Figures in this *Study*. *These events not depicted in Figures 4 or 5.

Cockpit Image Recorder (CIR) data

As mentioned above, an over-the-shoulder camera mounted in SS2's cockpit captured video and audio data during the accident flight. This data is documented in Reference 11, which includes a transcript of the recorded communications, and descriptions of non-verbal sounds and of the images captured by the video camera. Selected events from this transcript are shown in Table 12. The paraphrased version of the events shown in Table 12 are also depicted in Figures 4 and 5 (the text "[CV]" before the event text in these Figures indicates that the text is from the cockpit video; "[TM]" denotes information from the TM data). For the complete list of transcript events, see Reference 11.

Time (PDT)	Full CIR transcript text	Paraphrased text on plots
09:28:29.7	*SS2 Cockpit [Center MFD fades to black.]*	Center MFD malfunctions.
09:29:17.5	*SS2 Cockpit [Center MFD finishes rebooting]*	Center MFD finishes rebooting.
09:29:49.8	HOT-2 alright thirty thousand foot checks. ready for that?	Comment indicating being ready to begin 30,000 foot checks.
09:58:41.0	HOT-1 roger, Spaceship commencing L minus ten.	Start of L minus 10 checks.
10:03:26.4	HOT-2 alright. rocket burn timer?	Start of L minus 4 checks.
10:06:52.7	HOT-2 L minus thirty.	Comment indicating being 30 seconds from release.
10:06:57.3	HOT-1 stick is forward.	Comment that the control stick is in forward position.
10:07:26.9	HOT-2 [strained voice] point eight.	Mach point eight callout.
10:07:28.4	[HOT-2] [straining] unlocking.	Comment about unlocking the feather system.
10:07:32.8	SS2 Cockpit *[End of recording. End of Transcript]*	End of recording.

Table 12. Full CIR transcript text corresponding to paraphrased text on plots in this *Study*.

Video data from NASA Dryden Long Range Optics video camera

One of the ground-based cameras that captured data from the accident flight was the NASA Dryden Aeronautical Test Range / Edwards AFB Long Range Optics (LRO) video camera. This camera and its location are described in Reference 12. Selected still images from the video recorded by the LRO, including time stamps at the top of the frames, are presented in Figures 23(a)-(l). The times of these images correspond to the significant events listed in Table 11, as well as to images recorded every 0.25 seconds from the start of feather movement up until the breakup of the vehicle is evident.

[19] The VPGC selected 10:07:30.7 as the time of feather movement based on the rise of the Feather Position parameter above any previously recorded position. The Systems and Structures Groups selected the time of feather movement as 10:07:30.6 based on the time that the rate of feather movement becomes and remains positive. The 10:07:30.7 time is shown in the plots in this *Study*, but the text cites the 10:07:30.6 time.

Correlation of radar, TM, CIR, and LRO times

The EDW RIR and ASR radars, SODAS TM file, CIR, and LRO camera all record their information with respect to UTC time, and so are all nominally aligned (i.e., an event labeled with a certain time in one of these sources should be synchronized with events with the identical time label in the other sources). In fact, the synchronization of the EDW RIR position data with the TM data, for example, is apparent in Figure 14. [20] References 10-12 describe how the data sources listed above obtain the UTC time for their recordings. Seven hours are subtracted from the UTC times to convert them to PDT for presentation in this *Study*.

V. Additional performance parameters computed using recorded data

Overview

The flight parameter data set recorded in the TM data is quite comprehensive, and includes almost all vehicle performance parameters of interest, including those parameters that are direct recordings of sensor signals (such as accelerometer and control position signals), and parameters that are the result of computations performed by either vehicle systems or the SODAS using sensor signals (such as most of the air data parameters, including calibrated airspeed, true airspeed, Mach number, etc.). Nonetheless, additional computations using the recorded data are of interest for the accident investigation, for the following reasons:

- To compute winds aloft using data recorded by WK2.
- To confirm the consistency between the recorded air data parameters.
- To confirm the consistency between the recorded inertial data parameters, and if necessary, to correct accelerometer bias errors, and derive a kinematically consistent set of acceleration, velocity, and position parameters defining the trajectory of the center of gravity (CG) of the vehicle.
- To use the computed winds and SS2's velocity relative to the Earth to calculate SS2's true velocity through the air mass, and true Mach number, angle of attack, and flight path angle relative to the air mass.
- To determine the feather moment acting to open or close the feather.

The methods used to derive additional parameters from the TM data are described below, and the results of the calculations are presented and discussed at appropriate points throughout the *Study*.

Wind calculations

True airspeed, groundspeed, and wind speed are related as follows:

$$\vec{V}_W = \vec{V}_G - \vec{V}_T \qquad [1]$$

where $\vec{V}_T$ is the true airspeed vector, $\vec{V}_G$ is the groundspeed vector and $\vec{V}_W$ is the wind vector. These are three-dimensional vectors, but for the purposes of this *Study* the vertical wind is

[20] Several Figures in this *Study* have an "a" and a "b" version, which present the same information but at different scales, or with different background images. When the *Study* refers to a Figure with two or more versions without specifying the version, all versions are meant to be included in the reference.

assumed to be negligible and only the horizontal components of Equation [1] need to be considered. The north and east components of the groundspeed are

$$V_{G,N} = \frac{dN}{dt} = V_G \cos \psi_T \quad [2a]$$

$$V_{G,E} = \frac{dE}{dt} = V_G \sin \psi_T \quad [2b]$$

Where N and E are the north and east coordinates of the vehicle, t is time, and ψ_T is the track angle over the ground. Similarly, the north and east components of true airspeed are

$$V_{T,N} = V_T \cos \psi \quad [3a]$$

$$V_{T,E} = V_T \sin \psi \quad [3b]$$

Where ψ is the vehicle's true heading.[21] Once the north and east components of groundspeed and airspeed are computed using Equations [2] and [3], the north and east components of the wind can be computed using Equation [1]. The total wind magnitude (V_W) and direction (ψ_W) can then be computed as

$$V_W = \sqrt{{V_{W,N}}^2 + {V_{W,E}}^2} \quad [4]$$

$$\psi_W = \tan^{-1}\left(\frac{V_{W,E}}{V_{W,N}}\right) + 180° \quad [5]$$

Note that the signs of $V_{W,N}$ and $V_{W,E}$ must be examined to determine the proper quadrant for the inverse tangent in Equation [5]. Also, because 180° is added to the inverse tangent, ψ_W is the direction the wind blows *from* (per aeronautical convention), not the direction the wind vector points *to*.

Latitude, longitude, altitude, true heading, and true airspeed data from WK2 during the climb from KMHV to the maximum altitude obtained by WK2 were used to compute the north and east coordinates of WK2 relative to the KMHV runway 30 threshold, and the wind profile as a function of altitude, per Equations [1] - [5]. The results of these calculations are shown in Figure 24 as the lines labeled "NTSB calculation using WK2 data."

Similar wind calculations are performed on-board WK2 using that airplane's ADC and INS data. These calculations are also recorded, and are shown in Figure 24 as the "WK2 winds" lines. The two wind calculations are in good agreement (generally within 5 knots of wind speed and 5° of wind direction).

Figure 24 also shows lines labeled "Fit of NTSB calculation." These fits of the calculated wind speed and direction are used to compute true airspeed from inertial groundspeed per Equation [1], as described further below in the sub-section titled "*Wind-corrected inertial speed, Mach number, α, β, and γ calculations*."

[21] These relationships also assume the vehicle is flying at zero sideslip angle (β) (i.e., coordinated flight).

Air data calculations and consistency checks

The Air Data System (ADS) on SS2 (described above) measures total and static pressures, and total air temperature. The ADCs use this information to compute barometric altitude, airspeeds, dynamic pressure, and Mach number. To confirm the consistency between the pressure and temperature data sensed by the ADS and the parameters computed by the ADCs, barometric altitude, airspeeds, dynamic pressure and Mach number were computed independently by the VPGC using the recorded ADS pressure and temperature data. These calculations are outlined below.

The pressure altitude is the altitude in the standard atmosphere corresponding to the static air pressure sensed by the ADS, as determined by equations or tables defining the standard atmosphere. The barometric altitude is pressure altitude corrected for non-standard day sea level pressure. The correction is a constant altitude increment determined by the altimeter setting:

$$h_b = h_p + 145427.1\left[\left(\frac{ALTSET}{29.92}\right)^{0.190283} - 1.0\right] \quad [6]$$

Where h_b is the barometric altitude in feet, h_p is the pressure altitude in feet, and $ALTSET$ is the altimeter setting in inches of mercury (“Hg).

The Mach number can be determined from the total and static pressure:

$$M = \sqrt{\frac{2}{\gamma-1}\left[\left(\frac{P_T-P}{P}+1\right)^{\frac{\gamma-1}{\gamma}}-1\right]} \quad [7]$$

Where M is the Mach number, P_T is the total pressure, P is the static pressure, and γ is the ratio of constant-pressure to constant-volume specific heats for air (= 1.4).

The static air temperature can be determined from the total air temperature and Mach number:

$$T = \frac{T_T}{1+\left(\frac{\gamma-1}{2}\right)M^2} \quad [8]$$

Where T is the static air temperature, and T_T is the total air temperature.

The speed of sound can be computed using the static air temperature:

$$a = \sqrt{\gamma R T} \quad [9]$$

Where a is the speed of sound, and R is the gas constant for air (1716.56 (ft./s)^2/°Rankine).

The true airspeed follows from the Mach number and speed of sound:

$$V_T = aM \quad [10]$$

The static air density can be found from the gas equation of state:

$$\rho = \frac{P}{RT} \quad [11]$$

The dynamic pressure is given by

$$\bar{q} = \frac{1}{2}\rho {V_T}^2 \quad [12]$$

The equivalent airspeed is the true airspeed at standard sea-level conditions that results in the same dynamic pressure with the same true airspeed at the actual altitude and atmospheric conditions, and is given by

$$V_E = V_T\sqrt{\frac{\rho}{\rho_0}} \quad [13]$$

Where V_E is the equivalent airspeed, and ρ_0 is the standard-day sea-level static air density.

Finally, the calibrated airspeed (the airspeed that would be displayed by an aircraft's airspeed indicator, after correcting for static pressure position error) can be computed as

$$V_C = \sqrt{\frac{2\gamma RT_0}{\gamma - 1}\left[\left(\frac{P_T - P}{P_0} + 1\right)^{\frac{\gamma-1}{\gamma}} - 1\right]} \quad [14]$$

Where V_C is the calibrated airspeed, and T_0 and P_0 are the static air temperature and pressure at standard-day sea-level conditions.

The TM data altitude, temperature, pressure, airspeed, and Mach number parameters are plotted in Figures 14, 15 and 22. The NTSB calculations of these parameters based on the TM data total pressure, static pressure, and total temperature (as outlined above) match the parameters plotted in the Figures, confirming the internal consistency of the SS2 ADC data.

Accelerometer data corrections and integration

The usefulness of the calculations that use the ADS pressure and temperature data as inputs is limited by the accuracy of that data, particularly in the transonic region as shocks start to form over the vehicle. As mentioned above, for PF04 the distortion of the ADS-based parameters due to shock effects becomes apparent after about 10:07:27, as SS2 accelerates through Mach 0.8.

The data from the vehicle's INS is not affected by compressibility or shock effects, and so is a better source of position and speed information after the ADS data becomes unusable. However, as noted above, the INS measures the vehicle's velocity relative to the Earth, not the air mass, and so airspeeds and Mach numbers based on the INS data can be in error as a result of wind effects (see Equation [1]), though this error becomes quite small as the vehicle accelerates and the flight path angle becomes vertical after the "gamma-turn" (the pitch maneuver in which the flight path angle (γ) of SS2 transitions from nearly horizontal to nearly vertical).

A better estimate of the true airspeed and Mach number of SS2 on PF04 after 10:07:27 can be computed by solving Equation [1] for $\overrightarrow{V_T}$, with $\overrightarrow{V_G}$ determined from inertial parameters, and $\vec{V}_W$ determined from the "Fit of NTSB calculation" lines plotted in Figure 24.

The INS position and speed solution is obtained by processing multiple Inertial Measurement Unit (IMU) inputs – including linear accelerations and angular rates – through a Kalman filter algorithm. The INS solution includes "processed" accelerations and angular rates, as well as the vehicle position (latitude, longitude, and altitude) and attitude (pitch (θ), roll (ϕ), and yaw (ψ) Euler angles). The processed accelerations and angular rates are included in the TM data set provided by the Data Group.

To confirm the consistency between the accelerations (expressed as load factors) and angular rates sensed by the IMU and the final INS solution, SS2's position and speed were computed independently by the VPGC using the recorded INS load factor and attitude data. As part of this process, the calculations indicated that the recorded attitude parameters were kinematically inconsistent with the processed angular rates, but were consistent with the unprocessed (or "raw") angular rates.[22] The Euler angles and angular rates are kinematically related as follows:

$$\begin{Bmatrix} P \\ Q \\ R \end{Bmatrix} = \begin{bmatrix} -\sin\theta & 0 & 1 \\ \sin\phi\cos\theta & \cos\phi & 0 \\ \cos\phi\cos\theta & -\sin\phi & 0 \end{bmatrix} \begin{Bmatrix} \dot{\psi} \\ \dot{\theta} \\ \dot{\phi} \end{Bmatrix} \qquad [15]$$

Where P, Q, and R are the body-axis roll, pitch, and yaw rates, respectively, and the dot-accent denotes the first time derivative (e.g., $\dot{\psi} \equiv d\psi/dt$). Comparing the processed and raw angular rate data (see Figure 17), it appears that the processed rates are the result of filtering the raw rates to remove high-frequency content, which also results in a time lag in and attenuation of the true signal. However, computing the angular rates from the recorded pitch, roll, and yaw parameters (using Equation [15]) results in a good match of the raw angular rates, indicating that the latter are consistent with the recorded attitude of the vehicle (see Figure 17).

In a similar way, the processed load factors appear to be the result of filtering the raw accelerations (see Figure 18). For the NTSB calculation of inertial position and speed, the raw load factor data was used, as well as angular rates calculated using the recorded attitude data and Equation [15]. The resulting vehicle positions and speed match the recorded INS positions and speed very well. The NTSB calculation is outlined below.

An accurate calculation of the flight path of the vehicle during relatively short intervals (up to about 100 seconds) can be obtained by integrating the accelerations recorded at the CG. However, the accelerometers are generally not located exactly on the CG, and so the accelerations at the CG must be computed by adjusting the recorded load factors for the effects of angular rates and accelerations. Furthermore, accelerometers generally contain small offsets, or "biases," that produce large errors in speed and position if not removed prior to integration.[23] In addition, the initial values of speed, rate of climb, and track angle are

[22] The VPGC requested the raw angular rates from SC after observing the inconsistency between the processed angular rates and the recorded attitude data; the raw rates and accelerations are not in the original TM data set.
[23] For details about the equations to be integrated and the bias correction technique described in this *Study*, see Appendix A of Reference 13.

required during the integration process (these are essentially the “constants of integration” when integrating acceleration to get speeds). The constants of integration and the values of the accelerometer biases can be estimated by selecting them such that the vehicle position that results from the integration agrees with known positions determined from another source. In many cases, the alternative altitude source could be ADS altitude data, if that data is reliable at the beginning and end of the integration segment (as would be the case, for example, in the analysis of a stall maneuver, in which inertial data is used to compute the vehicle motion between the pre- and post- stall periods). In the SS2 accident case, however, the ADS data becomes and remains unreliable from 10:07:27 until the end of the data, and so cannot serve as the “target” for the integration. Furthermore, one of the objectives of the integration is to obtain an independent confirmation of the consistency of the INS solution with the recorded accelerations, and using the final INS position solution as the “target” implies that these data are in fact consistent – thereby assuming what is to be proven.

To overcome this difficulty, in this *Study* the accelerometer biases for the portion of the flight from the release of SS2 from WK2 to the end of the recorded data are assumed to be identical to the biases for the 30 seconds prior to release. The biases for this 30-second “pre-release” segment are computed, and then used for integrating the accelerations for the remainder of the flight. During the pre-release segment, the ADS data are reliable, and the ADS barometric altitude is used as the altitude target for the integration. The horizontal target positions are those defined by an integration of the recorded INS groundspeed and track angle data (which are in good agreement with the RIR positions prior to release).

Accelerations at the CG

The accelerations at the CG can be computed from the recorded load factors as follows. The acceleration at any point *P* on the vehicle, $\vec{a}_P$, is given by

$$\vec{a}_P = \begin{Bmatrix} \dot{u} + wQ - vR \\ \dot{v} + uR - wP \\ \dot{w} + vP - uQ \end{Bmatrix} + \begin{Bmatrix} Q(yP - xQ) + R(zP - xR) + \left(z\dot{Q} - y\dot{R}\right) \\ R(zQ - yR) + P(xQ - yP) + \left(x\dot{R} - z\dot{P}\right) \\ P(xR - zP) + Q(yR - zQ) + \left(y\dot{P} - x\dot{Q}\right) \end{Bmatrix} = \vec{a}_{CG} + \Delta\vec{a} \qquad [16]$$

Where:

$\{u, v, w\}$ = components of inertial velocity in the vehicle body axes
$\{P, Q, R\}$ = components of angular velocity in the vehicle body axes
$\{\dot{P}, \dot{Q}, \dot{R}\}$ = time derivatives of $\{P, Q, R\}$
$\{x, y, z\}$ = coordinates of point *P* in the vehicle body axes

(see Figure 25). Since by definition $\{x, y, z\}$ at the CG = {0,0, 0}, the first term in brackets in Equation [16] is the acceleration of the CG ($\vec{a}_{CG}$), and the second term is the increment in acceleration due to the point *P* being away from the CG ($\Delta\vec{a}$).

A three axis accelerometer at point *P* will measure load factors as follows:

$$\vec{n}_P = \frac{\vec{a}_P - \vec{g}}{g} = \frac{\vec{a}_{CG} + \Delta\vec{a} - \vec{g}}{g} = \vec{n}_{CG} + \frac{\Delta\vec{a}}{g} \qquad [17]$$

Where $\vec{g}$ is the gravity vector, g is the acceleration due to gravity (32.17 ft/s^2), and Equation [16] has been used to substitute for $\vec{a}_P$. The components of $\vec{n}$ are $\{n_x, n_y, n_z\}$. The normal load factor (nlf) is

$$nlf = -n_z \quad [18]$$

The raw n_x, n_y, and nlf from PF04 are plotted in Figure 18. The values of $\{n_x, n_y, n_z\}$ at the CG can be found using the raw data and Equations [18], [17], and [16], with $\{x,y,z\}$ in [16] being the distance of the accelerometer unit from the CG.

The angular rates and accelerations used to evaluate Equation [16] are computed from the recorded θ, ϕ, and ψ angles. These Euler angles are presented in Figure 16.

Accelerometer bias calculations

The accelerometer biases are not necessarily constant over an entire flight, but can drift over time. It is for this reason that integrating the accelerometers works best over relatively short intervals, during which the accelerometer biases are approximately constant. When the period of interest is lengthy, an integrated flight path for the entire length can be obtained by dividing it into shorter segments, and integrating the accelerometer data separately over each segment. In this case, however, the period of interest is only 34 seconds long, and a satisfactory integration can be obtained with a single segment.

The accelerometer biases are chosen to minimize the root-mean-square difference between the integrated north and east position and the north and east position obtained from an integration of the INS groundspeed and track angle data, and the difference between the integrated altitude and the recorded barometric altitude, during the 30 second segment preceding the release of SS2 from WK2. The constants of integration (the initial groundspeed, track angle, and rate of climb) are set equal to the INS groundspeed and track angle, and time derivative of barometric pressure, at the beginning of the integration segment.

The beginning and end times and accelerometer biases for the integration segment are shown in Table 13. The north and east positions, MSL altitude, and speeds resulting from the accelerometer integrations are shown in Figures 5, 8-10, 14b, and 15. The raw and processed load factors recorded in the TM data, and the raw load factors corrected with the biases listed in Table 13, are plotted in Figure 18.

Item	Value
Start time (PDT)	10:06:49
End time (PDT)	10:07:32
n_x bias, G's	0.000582
n_y bias, G's	0.001896
nlf bias, G's	-0.004269

Table 13. Biases and constants of integration for accelerometer integration segment.

Wind-corrected inertial speed, Mach number, α, β, and γ calculations

As mentioned above, after 10:07:27 the SS2 ADS parameters become unreliable because of shock effects, and a better estimate of the true airspeed and Mach number can be computed by solving Equation [1] for $\vec{V}_T$, with $\vec{V}_G$ determined from inertial parameters, and $\vec{V}_W$ determined from the "Fit of NTSB calculation" lines plotted in Figure 24. Once $\vec{V}_T$ is computed, the true Mach number can be calculated using Equations [9] and [10].

The results of these calculations, using the accelerometer integration results to determine $\vec{V}_G$, are shown in Figure 15. The wind-corrected $\overline{q}$ is shown in Figure 22. The true airspeed and Mach number, accounting for winds, are 62 to 66 KTAS or 0.12 to 0.13 Mach higher than the values computed using inertial data without the wind correction. Figure 15 indicates that at the time the feather was unlocked (at 10:07:29.5), the true Mach number was about 1.02, and at the time the feather started to move (at 10:07:30.6), the Mach number was about 1.08.

The components of $\vec{V}_T$ (in Earth axes) resulting from the wind correction calculation can also be used to calculate the vehicle's angle of attack (α) and sideslip angle (β). From Figure 25,

$$\alpha = \tan^{-1}\left(\frac{w}{u}\right) \quad [19]$$

$$\beta = \sin^{-1}\left(\frac{v}{V}\right) \quad [20]$$

where V is total true airspeed, and $\{u, v, w\}$ are the components of airspeed in body axes. Per Equation [1], the airspeed and its components in body axes can be computed if the components of both the groundspeed and wind speed (in body axes) are known. The components of $\vec{V}_G$ in body axes result from the integration of the accelerometer data described above. The components of $\vec{V}_W$ in body axes can be calculated by transforming the components of the wind from Earth axes into body axis using the recorded Euler angles (θ, ϕ, and ψ). The total true airspeed V is shown in Figure 15 as the blue line labeled "NTSB TAS from inert. + winds."

The results of the inertial α and β calculations are shown in Figure 16 as lines labeled "NTSB α from inert. + winds" and "NTSB β from inert. + winds," respectively. Note that the "inert. + winds" α agrees well with the SS2 INS-derived α and the "SS2_Left_Angle_of_Attack" and "SS2_Right_Angle_of_Attack" parameters where the flight path angle is zero, but is slightly lower than those parameters during the drop from WK2. This difference is due to the true airspeed being higher than the inertial speed, and (equivalently) the aerodynamic flight path angle (γ) relative to the air mass being shallower than the inertial γ relative to the Earth. In other terms, since the true airspeed is higher, the α required to produce the same lift is lower; at the same time, since when wings-level $\alpha = \theta - \gamma$, a less-negative γ results in a lower α. The calculation of γ (aerodynamic and inertial) is described below.

The "NTSB β from inert. + winds" in Figure 16 appears to be biased by about +2°; if the sideslip were really 2°, one would expect the lateral load factor (n_y) in Figure 18 to be non-zero at the same time, but the n_y is close to zero during the drop from WK2, and so the true β is also likely close to zero. The apparent bias or offset in β is likely due to inaccuracies in the assumed wind direction.

Notice in Figure 24 that between 46300 and 46600 ft. MSL, there are two solutions for the wind direction, corresponding to WK2's climb and then descent between these altitudes. The wind direction during the descent is about 5° less (more southerly) than during the climb. The curve fit of wind direction vs. altitude used for the airspeed calculations described above passes through the wind calculation for the climb portion only; but SS2 is released from WK2 following the descent from 46600 ft., and so the wind direction that would more likely apply to SS2's flight is the one encountered during the descent. A 5° shift in the wind direction towards the south (left of the flight path) would decrease the computed sideslip by about 2°.

Even with a 2° offset, the computed β is a good indicator of *changes* in β during the flight, which appear to be less than ±1°, until the end of the integration segment, where the increment reaches -2°.

The flight path angle is defined by

$$\gamma = \sin^{-1}\left(\frac{\dot{h}}{V}\right) \qquad [21]$$

where $\dot{h}$ is the rate of climb, and V is speed. The γ relative to air mass (aerodynamic γ) results from using the true airspeed as V in Equation [21]. The γ relative to the Earth (inertial γ) results from using the inertial speed as V in Equation [21].

The γ relative to the air mass resulting from using $\dot{h}$ and V_T from wind-corrected integrated accelerometer data is shown in Figure16 as the dashed blue line labeled "NTSB γ rel. air from inert + winds." As mentioned, the aerodynamic γ is slightly higher (less negative) than the inertial γ during the drop from WK2.

Feather moments on SS2 powered flights

As stated in Section D-I, during a nominal mission, at the end of the boost phase and near apogee, SS2 is put into the "feathered" (feather extended) configuration to provide a stable attitude for reentry and increase drag so as to reduce reentry speeds and associated structural loads and heating. The vehicle must remain in the "unfeathered" (feather retracted) configuration until the intended feather extension conditions[24] are attained, so as to avoid possible loss of control and catastrophic structural failure. The feather system and its operating procedures are designed to ensure that the feather remains retracted until it is intended to be extended.

The "feather moment" is the moment, or torque, that aerodynamic and inertial forces produce about the feather hinge, acting to either extend the feather (opening moment) or retract the feather (closing moment). The feather system includes feather locks for the unfeathered configuration, which are required because the feather actuators (which extend and retract the feather during normal operation) are not designed to keep the feather retracted against the opening feather moments encountered during the transonic boost phase and gamma-turn.

Just as it is critical that the feather remain retracted during the boost phase, it is also critical that the feather be extended for the reentry phase. Otherwise, reentry in the low-drag unfeathered configuration would result in the vehicle over-speeding and exceeding its design

[24] Per SS2 normal procedures, the feather would be extended once the airspeed decayed below 20 KEAS.

limitations, which could lead to structural overload and / or excessive heating. Consequently, a failure of the feather system to unlock could also result in catastrophic failure. To mitigate this risk, the feather is intended to be unlocked early enough in the boost phase that a failure to unlock can be detected and the boost aborted in time for the vehicle to be flown back to base in the unfeathered configuration without exceeding its operating limitations.

Consequently, SC selected the intended feather unlock point so as to satisfy two competing requirements: (1) unlocking the feather later in the boost phase in order to guarantee that the feather moment at the unlock point would be a closing moment and keep the feather retracted, and (2) unlocking the feather as soon as possible during the boost phase so that, in case the feather fails to unlock, the mission can be aborted safely.

The brief description of the design and intended operation of the feather system provided above is a summary of the following information that SC provided to NTSB in response to questions about the system (Reference 15):

> Scaled designed the reentry system (comprising the feathers, the actuators, and the locks) for SpaceShipOne. Basic design parameters were derived from design trade studies. The selected design included actuators for extending and retracting the feathers and locks to maintain the feathers in the retracted position during most portions of the planned trajectory.
>
> As part of the design process, design/engineering team members … analyzed the planned flight trajectory and computed loads that would be encountered by the aircraft during a variety of flight conditions using a variety of aerodynamic analysis tools. The design parameters for the feather actuators were selected such that the feather retracting forces provided by the actuators were adequate to retract the feathers during the recovery phase of flight (after reentry) and *less* than the feather extending forces caused by aerodynamic loads during the transonic flight regime and gamma-turn maneuver. The design parameters of the locks were selected so that they would maintain the feather in the retracted position during the portions of the trajectory when the feather was not intended to be extended, including the transonic flight regime and the gamma-turn maneuver. Feather locks were *not* added as a mitigation against the inability of the feather actuators to hold the feather retracted during all flight phases. They were a design feature to hold the feathers in the retracted position during all phases of flight except when the feathers were intended to be extended.
>
> The basic design elements of SpaceShipOne, and the design of the feather system, including the feather locks and feather actuators, were carried forward to SpaceShipTwo …
>
> … The expected aerodynamic feather extending forces were described in a number of documents including "*SS2-90E200 Feather Unlock Study, [Former Chief Aerodynamicist], 1/9/2007.*" The latter document shows (and states) the expected aerodynamic feather extending forces are larger than the feather retracting forces supplied by the actuators. These documents served as inputs to the detail design of the feather system, so the feather system's need for locks during the transonic flight regime and the gamma-turn maneuver was well understood ….
>
> … Scaled employed aerodynamic analysis to model the loads SpaceShipTwo would encounter during flight, including the transonic flight regime and the gamma-turn maneuver. Through this process, Scaled selected design parameters for the feather system and knew that during these flight phases, the aerodynamic feather extending forces exceeded the feather retracting forces provided by the feather actuators. In the absence of locks, Scaled engineers determined that these loads would result in motion of the feather system which would result in loss of pitch control, which could potentially result in a catastrophic airframe failure. Accordingly, the vehicle was designed and intended to be operated with the locks engaged during the transonic flight regime and the gamma-turn maneuver to prevent deployment of the feather system during these stages.
>
> … Having the feather locks in place during the transonic phase is a design feature, not a procedural mitigation. There *is* a procedural mitigation involving *unlocking* the locks after the transonic region, to address the potential risk of the locks jamming.

> … There were safety margins in place [for procedural mitigations]. For example, with respect to the procedural mitigation to reduce the risk of jammed locks, the Mach 1.4 number for unlocking the feather system was chosen to provide a safety margin at the lower end of the scale to prevent premature unlocking, and at the higher end of the scale to allow adequate time to abort.
>
> … The different flight phases represent different load conditions and different sensitivities to various potential failures. During early, high aerodynamic load boost, the feather locks are intended to be engaged and failures of the feather actuator system cannot immediately lead to adverse consequences. During late, lower aerodynamic force boost, the feather locks are intended to be released and failures in the feather actuator system lead to adverse consequences in the reentry phase. Correspondingly, if the feather locks do not release after the early boost phase, there is the risk of an unfeathered reentry. After reentry, the failure of the locks presents risk of un-commanded feather motion during glide and landing.

Reference 16 describes SS2's aerodynamic response (static and dynamic handling qualities) during the transonic boost phase, and explains the source of the large opening feather moments in that regime. According to that document,

> As SS2 goes supersonic, the center of pressure of the wing moves forward, then aft. During boost the timing of this nose up then nose down pitch is similar in frequency to the short period response of the vehicle. As a result as SS2 accelerates to supersonic speeds, there is a nose up then nose down motion, or bobble in pitch. This response is well damped, with approximately two oscillations lasting 4 seconds from the initial disturbance.
>
> … As SS2 accelerates supersonically, more nose-up trim is required, and the turn to a vertical flight path is initiated.

The forward movement of the center of pressure (CP) of the wing, necessitating increased (upward) lift from the tail to trim, increases the opening feather moment. After the CP of the wing moves back aft, the required tail lift to trim, and associated opening feather moment, are also reduced.

As SS2 decelerates from supersonic speeds back through the transonic regime during the coast portion of the ascent following the burn-out of the rocket motor, the feather moment again increases and becomes an opening moment. Since in this regime the feather is unlocked (having been unlocked while supersonic), the feather is held in the retracted position by the feather actuators. As described further below, in the most demanding circumstances, the opening feather moment can approach the limits of the actuators' ability to keep the feather closed. Even so, an un-commanded extension of the feather in this regime would not be catastrophic (as it was on PF04), because at the higher altitudes (and thinner air) involved, the vehicle would be within its feather operating envelope and remain intact.

One of the primary analysis tools SC uses to understand SS2's handling qualities and feather moments during the vehicle's flight (including the transonic phase and gamma-turn) is a *MATLAB* – based 3 degree-of-freedom (DOF) simulation program called the "Trajectory Code" (TC). In addition to flight simulation routines, the TC includes routines for computing vehicle loads, including the feather moments. The aerodynamic database underlying the TC, which defines SS2's aerodynamic coefficients for the simulation and aerodynamic loads calculations, is rooted in Computational Fluid Dynamics (CFD) studies updated with flight test data from SS2 glide and powered test flights. The TC aerodynamic database is populated with data for a combination of Mach number, α, and stabilizer positions, at three different feather positions: retracted (b) (4) extended (b) (4) and a mid-feather position (b) (4) The database was not designed to model small feather deflections.

The TC is designed to compute loads as part of a simulation run, in which the vehicle state as a function of time is determined within the simulation, and is not specifically designed to compute loads using a pre-defined vehicle state (such as a flight test record) as an input. For the accident investigation, however, it is of interest to confirm that the predicted opening feather moments encountered by SS2 during PF04 were sufficient to overcome the expected retracting moments provided by the feather actuators at the time that the feather was observed to extend during the accident. To this end, the VPGC used selected routines from the TC to compute the feather moments, using the vehicle state from PF04 as input to those routines.

The parameters required by the TC for the feather moment calculation, and the source of these parameters for PF04, are shown in Table 14.

TC input parameter	Definition / source
xcg	Longitudinal CG position in feet, from the PF04 test card (see Reference 4)
zcg	Vertical CG position in feet (provided by SC)
stab	Horizontal stabilizer position, from TM parameter “SS2_Stabilizer_Pitch”
elevon	Elevon position, from TM parameter “SS2_Elevon_Pitch”
feather	Feather position in degrees, from parameter “Feather Position” multiplied by 0.6 to convert position units from % to degrees
mach	Mach number, from parameter “NTSB mach from inert. + wind” in Figure 15
q	Dynamic pressure in lb/ft^2, from parameter “NTSB dyn. Press. from inert. + winds” in Figure 22
alpha	Angle of attack, from parameter “NTSB α from inert. + winds” in Figure 16
thetadotdot	Pitch acceleration in deg/sec^2, from parameter “Time derivative of 3 Hz low-pass FFT filter of raw Q” in Figure 26 (see discussion in text below)
Nx	Longitudinal load factor in G’s, from parameter “NTSB n_x” in Figure 18
Nz	Vertical load factor in G’s, from parameter “NTSB nlf” in Figure 18, multiplied by -1

Table 14. Input parameters for Trajectory Code feather moment calculation.

The “thetadotdot” (pitch acceleration) parameter listed in Table 14 requires some explanation. This parameter is required to compute the inertial component of the feathering moment, and is equal to the second time derivative of the pitch angle:

$$\ddot{\theta} \equiv \frac{d^2\theta}{dt^2} = \frac{dQ}{dt} \qquad [22]$$

Where the pitch rate $Q = d\theta/dt$ for the case where the bank angle (ϕ) and yaw rate ($\dot{\psi}$) are zero (see Equation [15]). Taking derivatives of discretely sampled data introduces noise into the results, and so it is preferable to take as few derivatives as possible to obtain $\ddot{\theta}$. Both the pitch angle θ and pitch rate Q are recorded directly in the TM data, and so it is preferable to use Q to compute $\ddot{\theta}$ instead of θ, since then only one derivative is required, instead of two.

As discussed above, the “processed” Q recorded in the TM data is not consistent with the recorded Euler angles, and appears to lag and be attenuated compared to the true signal (see the top plot in Figure 26). The “unprocessed” Q is consistent with the Euler angles, and so is the preferred parameter for determining $\ddot{\theta}$. However, the unprocessed Q is much noisier than the processed Q, and taking its derivative would exacerbate the noise. To reduce the noise in the derivative calculation while preserving the true shape of the unprocessed Q, this parameter was passed through a low-pass Fast Fourier Transform (FFT) filter with a cutoff frequency of 3 Hz. The filtered result is shown as the line labeled “3 Hz low-pass FFT filter of raw Q” in Figure 26. The first time derivative of this parameter is plotted in the second plot in

Figure 26, and is the $\ddot{\theta}$ parameter used as input to the TC feather moment calculation. (In any case, as shown in the bottom plot of Figure 26, the contribution of the dynamic inertial moment to the total feather moment is very small, reducing the significance of the $\ddot{\theta}$ calculation for PF04.)

The results of the TC feather moment calculation are shown in the bottom plot of Figure 26. The static and dynamic components of the inertial moment,[25] the aerodynamic moment, and the total feather moment are shown. Clearly, the important contributors to the total moment are the aerodynamic moment and the static inertial moment. Also shown in Figure 26 is the total closing moment provided by the feather actuators ((b) (4) per SC and the NTSB Systems Group Chairman[26]).

Note in Figure 26 that at the time the feather is unlocked (at 10:07:29.5), the total feather moment is about (b) (4) (opening), which exceeds the closing moment capability of the actuators, but decreases to about (b) (4) at 10:07:30, which is within the actuator capability. The moment then increases above the actuator capability again, and is about (b) (4) and increasing when the feather starts to open at 10:07:30.6.[27] This oscillation in moment is consistent with the approximately 1.1 second delay between the unlocking of the feather and the movement of the feather towards the extended position. Furthermore, the TC results confirm that the predicted opening feather moment at the time the feather extended is sufficient to overcome the closing moment provided by the feather actuators. Consequently, the extension of the feather after unlocking at about Mach 1 is consistent with SC's modeling and understanding of the feather moment behavior at transonic speeds.

As mentioned above, the aerodynamic database underlying the TC was not designed to model small feather deflections; consequently, the feather moments computed by the TC once the feather starts to move become unreliable. For this reason, In Figure 26 the computed feather moments are only shown up until 10:07:31.0, when the feather position reaches about 0.6% (0.36°).

Figure 26 also shows the feather moments for PF04 resulting from a "tail strain computation" performed by SC. These are the moments derived from a combination of stabilizer loads measured using strain gauges, and aerodynamic analyses of the contributions of the feather flap and boom strakes to the feather moment. Since part of this calculation uses measured flight loads, it approximates a flight-test validation of the moments computed using the TC. The shape of the curves computed using tail strains and the TC match well, though the tail-strain curve shows larger opening moments than the TC code, except for the period between 10:07:28 and 10:07:29.5.

Comparisons of the tail-strain and TC feather moment computations for flights PF01, PF02, and PF03 are shown in Figure 27. Again, the shape of the curves match well, though some offsets in the absolute levels of the feather moments can be observed.

The total feather moments for the four SS2 powered flights (PF01 – PF04), as computed using the TC,[28] are compared in Figure 28. The middle graph in Figure 28 plots the moments

[25] The static inertial moment is the moment produced primarily by the weight of the feather (multiplied by the normal load factor) "cantilevered" out from the feather hinge.
[26] Email from NTSB Systems Group Chairman to NTSB VPGC dated February 5, 2015.
[27] As noted earlier, the start of feather movement is at 10:07:30.6, but is depicted at 10:07:30.7 in the Figures.
[28] The TC calculations for PF01-PF03 were provided to the VPGC by both TSC and SC.

vs. time from SS2's release from WK2, and the bottom graph plots the moments vs. Mach number. The top graph shows Mach number vs. time for each flight. Figure 28 shows that, at the higher Mach numbers where the feather is intended to be unlocked, the feather moment is a closing moment, and the feather is held in the retracted position by aerodynamic forces.[29]

As noted above, as SS2 decelerates from supersonic speeds back through the transonic regime, the feather moment increases and becomes an opening moment. Figure 28 indicates that on PF02, although the feather moment was a large closing moment at the time the feather was unlocked, as SS2 decelerated through the transonic regime, large opening moments were produced. In fact, between time 35 and 38 seconds, the opening moment exceeded the actuator capability (while the feather was unlocked), and resulted in a small, un-commanded feather motion. The VPGC asked SC to comment on this situation, presuming that un-commanded feather motion is generally undesirable. SC noted (in References 17 and 18) that on PF02, SS2 was deliberately operated near the edge of the feather-unlocked operating envelope in order to collect transonic test data at high α and lower $\bar{q}$, and to validate normal and emergency procedures:

> During PF01, tail lift was higher than expected in the transonic regime, and drove an improvement in the aero model. To verify the new model, the PF02 deceleration test point (Release + 33 to 38 seconds) was designed to explore high alpha transonic stability at a lower dynamic pressure. During this test, the feather opened slightly (estimated at 0.8 degrees) for less than a second. Feather motion was not planned during the test, but this motion was consistent with the high tail loads expected during the test point. The feather motion occurred at (b) (4) KEAS, less than the (b) (4) KEAS maximum feather speed (from the Pilot Operating Handbook …), and at about ¼ the dynamic pressure of the PF04 feather event ((b) (4) KEAS.) After gathering the PF02 high alpha transonic data, PF03 returned to normal operating procedures, and targeted a lower flight path angle after burnout. [Reference 17.]

> SC structured its flight test data cards and procedures, to the extent possible, using the expected Normal Procedures for future flights where a full rocket burn was planned. That continuity was intended to improve crew training as well as confidence in the Normal Procedures. The feather was unlocked at Mach 1.2 during the PF02 boost phase, rather than Mach 1.4 to assure unlock occurred before burnout. Furthermore, by unlocking the feather during PF02 consistent with the Normal Procedures for the boost phase, SC also validated the powered flight abort procedure in the SS2 Emergency Procedures. PF02 served to refine the limiting parameters for an abort with the feather unlocked, targeting the upper range of the predicted feather opening moments during an abort. Flying the PF02 profile with the feather locked until the planned feather test would not have fully demonstrated this capability. Many other SS2 system safety mitigations depend on the capability to abort a powered flight as early as the 1.4M point. Unlocking the feather later in the PF02 boost profile would not have fully demonstrated this capability. Aborts later in the burn would produce lower dynamic pressures and less nose up trim than PF02 experienced, and thus would have demonstrated opening moments lower in the predicted range. Likewise, unlocking the feather later in the abort procedure would have exposed the unlocked feather to dynamic pressures much lower than SC needed to flight test. [Reference 18.]

Figure 28 indicates that on PF03, which was operated per normal procedures, an opening feather moment (that was within the feather actuator capability) was present during deceleration through the transonic regime, while the feather was unlocked. On flights with longer rocket motor burns, the deceleration through the transonic regime would occur at higher altitudes and correspondingly lower $\bar{q}$, and consequently the magnitude of the feather moments would be smaller.

[29] The feather was not unlocked or extended on PF01.

VI. Instantaneous Impact Point and key flight-safety event analysis

Relevant FAA regulations concerning public safety

As stated at the top of this *Study*, SC was operating SS2 under an experimental permit issued by the FAA's Office of Commercial Space Transportation (AST) under the provisions of 14 CFR Part 437. Several of the regulations under Part 437 concern protecting the uninvolved public from mishaps that may occur while operating a reusable suborbital rocket under an experimental permit (such as the SS2 accident). Of particular interest in this *Study* are those regulations that aim at protecting the public from impacts with the vehicle or its parts. This section introduces several of these regulations, briefly outlines how SC proposed to comply with those regulations in its experimental permit application (Reference 2), how AST evaluated SC's proposals, and how SS2's "instantaneous impact point" (IIP)[30] and the trajectories of the major components of SS2 following the in-flight breakup compare with the requirements of SC's approved permit.

The regulations of most interest that are concerned with debris from the vehicle following a mishap are 14 CFR Parts 437.25, 437.31, 437.57, and 437.59, presented below:

> **§437.25 Flight test plan.**
>
> An applicant must—
>
> (a) Describe any flight test program, including estimated number of flights and key flight-safety events.
>
> (b) Identify and describe the geographic coordinates of the boundaries of one or more proposed operating areas where it plans to perform its flights and that satisfy §437.57(b) of subpart C. The FAA may designate one or more exclusion areas in accordance with §437.57(c) of subpart C.
>
> (c) For each operating area, provide the planned maximum altitude of the reusable suborbital rocket.
>
> **§437.31 Verification of operating area containment and key flight-safety event limitations.**
>
> (a) An applicant must identify, describe, and provide verification evidence of the methods and systems used to meet the requirement of §437.57(a) to contain its reusable suborbital rocket's instantaneous impact point within an operating area and outside any exclusion area. The description must include, at a minimum—
>
> (1) Proof of physical limits on the ability of the reusable suborbital rocket to leave the operating area; or
>
> (2) Abort procedures and other safety measures derived from a system safety engineering process.
>
> (b) An applicant must identify, describe, and provide verification evidence of the methods and systems used to meet the requirements of §437.59 to conduct any key flight-safety event so that the reusable suborbital rocket's instantaneous impact point, including its expected dispersions, is over unpopulated or sparsely populated areas, and to conduct each reusable suborbital rocket flight so that the reentry impact point does not loiter over a populated area.

[30] 14 CFR 401.5 defines the IIP as "an impact point, following thrust termination of a launch vehicle, calculated in the absence of atmospheric drag effects."

§437.57 Operating area containment.

(a) During each permitted flight, a permittee must contain its reusable suborbital rocket's instantaneous impact point within an operating area determined in accordance with paragraph (b) and outside any exclusion area defined by the FAA in accordance with paragraph (c) of this section.

(b) An operating area—

(1) Must be large enough to contain each planned trajectory and all expected vehicle dispersions;

(2) Must contain enough unpopulated or sparsely populated area to perform key flight-safety events as required by §437.59;

(3) May not contain or be adjacent to a densely populated area or large concentrations of members of the public; and

(4) May not contain or be adjacent to significant automobile traffic, railway traffic, or waterborne vessel traffic.

(c) The FAA may prohibit a reusable suborbital rocket's instantaneous impact point from traversing certain areas within an operating area by designating one or more areas as exclusion areas, if necessary to protect public health and safety, safety of property, or foreign policy or national security interests of the United States. An exclusion area may be confined to a specific phase of flight.

§437.59 Key flight-safety event limitations.

(a) A permittee must conduct any key flight-safety event so that the reusable suborbital rocket's instantaneous impact point, including its expected dispersion, is over an unpopulated or sparsely populated area. At a minimum, a key flight-safety event includes:

(1) Ignition of any primary rocket engine,

(2) Any staging event, or

(3) Any envelope expansion.

(b) A permittee must conduct each reusable suborbital rocket flight so that the reentry impact point does not loiter over a populated area.

SC's Tier 1B experimental permit application

In its *Experimental Permit Application for the Tier 1B Reusable Suborbital System* (Reference 2), SC presents its proposed methods of complying with the regulations presented above. The methods rely on two main principles: (1) the operation of the Tier 1B vehicles within the Restricted Area R2508 operating area and away from populated zones within that area; and (2) the management of SS2's IIP throughout its flight through crew awareness of the IIP via cockpit displays, and crew control of the vehicle so as to keep the IIP within the operating area and away from populated zones.

Regarding the use of R2508 as the Tier 1B operating area, Reference 2 states (Section 2.2):

> The R-2508 complex, created to contain military and civilian flight test activities, is ideal for SS2 test flights:
>
> - It is remote from most high-density population areas
> - It has well-documented procedures and processes for test flights, and air traffic controllers well-trained in test flight operations.

- It has substantial pre-existing environmental information which will simplify the environmental assessment process required for the permit.

All SS2 test flights will land at the Mojave Air and Space Port.

… Within this operating area, Scaled plans to select tracks appropriate to the goals of each specific test flight, giving consideration to population density, wind, expected trajectory dispersion, sensitive areas, exclusion zones, etc. The maximum altitude for any of these tracks is approximately 450,000 feet.

Regarding the management of the IIP by the flight crew, Reference 2 states (Section 3.2.1):

3.2.1. Approach to Protecting the Uninvolved Public

For background, because SS2 is a piloted vehicle the safety analysis shows that *significant* risk to the uninvolved public and their property is prevented for those hazards which leave the vehicle in an adequately controllable state. In those cases the crew can and would pilot the ship so as to avoid injury to the public. Hazards in the catastrophic or hazardous class are required to have very low probability because they may prevent the crew from performing this function (the crew may be disabled or the craft may be uncontrollable) and thus directly present risk to the uninvolved public as well as the crew and the craft.

Hazards in categories less than catastrophic and hazardous *may* present higher risk to the uninvolved public than to the SS2 crew or craft. We have reviewed our system safety analysis to determine if there are cases of this nature and we conclude that there are some. As an example, consider function 14 (Landing Gear) where there are "major" category hazards which might cause the gear doors to be shed. Such an event would not prevent the craft from being controllable but the doors might impact people or property on the ground (but because this would happen during the boost phase of flight, it would happen over sparsely populated areas where there isn't much to hit). We mark these hazards so that they can be easily identified.

Note, however, that there are very few hazards in this category. For example, "incorrect or misleading IIP data" is ***not*** a case where, by itself, the hazard to the public is greater than the hazard to the crew and craft because it has no impact on the controllability of the craft. Even in the event of wildly incorrect or misleading IIP data that was not otherwise caught or corrected, the crew can and would pilot the vehicle to either a normal landing or a landing at a contingency field or to a controlled emergency landing away from the uninvolved public. Also, gross errors in IIP computation are not a significant hazard because:

- IIP is redundantly computed (from redundant sources of information) by the three MFDs.
- Mission rules require abort for significant IIP computation anomalies.
- Small to moderate IIP errors do not prevent a normal approach and landing to the planned airport due to the large glide-cone diameter.
- Gross trajectory errors are detectable visually, again leading to abort.

In addition to these high-level perspectives, Reference 2 describes specific metrics and analyses for ensuring that the IIP and the location of key flight-safety events[31] remain in the operating area:

3.3.1. Key Factors in Operating Area Containment

Scaled uses three key metrics for planning mission tracks:

- The maximum distance the IIP projects ahead of SS2 at any point in the trajectory, and
- The maximum distance the IIP extends downrange from the air-launch point.
- The dispersion affecting key flight points in the trajectory.

[31] Reference 16 defines a key flight-safety event as "a permitted flight activity that has an increased likelihood of causing a launch accident compared with other portions of flight."

… These metrics are based on the concept that after re-entry and de-feather, SS2 is a controllable glider flying as if under 14 CFR 91, and the concept of IIP is no longer relevant.

For a nominal altitude mission, the IIP never projects more than about 12.5 miles in front of SS2, nor travels more than about 20 miles from the air-launch point ….

For the third metric, Scaled uses the simulator and over several runs (with varying wind conditions, thrust asymmetries, and other perturbations) computes the 3 sigma dispersion of the location of key flight [safety] points:

- The air-launch point
- The IIP dwell point. (At all locations other than the dwell point, the IIP rapidly traverses areas on the ground so that the exposure of the uninvolved public at these locations is relatively low. At the dwell point the IIP doesn't move for a relative long time and so the exposure of the uninvolved public is larger.)
- The re-entry point
- The de-feather point

Since some relatively populated areas exist within the R2508 operating area, Reference 2 also describes a method for evaluating the risk to the public within the area, given the IIP and key flight-safety event location metrics described above:

3.3.2. Methodology for Selecting Mission Tracks

Given the three metrics described above, Scaled selects mission tracks using the following methodology:

- Select an acceptable casualty statistic, like 30E-6.
- Using Monte Carlo simulation, determine the rough probability of contact with a person on the ground by an uncontrolled spaceship or fragment. For example, in a 1km square, the probability of an $18m^2$ spaceship (or a reasonable size fragment from that spaceship) hitting a $1m^2$ person is about 3.9%.
- Using the system safety analysis, or engineering judgment, select a probability that the vehicle fail or will become uncontrollable such that the vehicle can impact people or property on the ground. A reasonable probability here would be between the values in the safety analysis (around 1E-6) and some larger value like 1E-3. The latter figure can be supported due to the nearly 7,000 hours of flight-test experience Scaled has using the same design methodology (across many exotic aircraft *and spacecraft*) and flight test practices as used for SS2.
- Using mission test parameters, winds, and other parameters, select a track using the three metrics above that contains the vehicle and IIP, including expected dispersions, within the operating area.
- Using the probabilities above, and the dispersion numbers, verify that the uninvolved public's exposure to casualty for the mission is within the selected value.

During the investigation, the VPGC asked AST and SC to explain the mathematics behind the second bullet above in more detail. AST was unable to do so, but SC provided the following information (in Reference 19):

Scaled is not certain how the number 3.9% came to be in our Application for an Experimental Permit but we suspect it entered during the proofreading process. Experimental Permit applicants are not required to perform Expected Casualty computations and this number was only intended to be a rough estimate to validate the process used to select mission tracks.

Scaled recently performed the Monte Carlo simulation described in the application and found the probability to be approximately 0.00036 or 0.036% using the following methodology:

- Assume a square 18 meters on a side (not 18 meters squared) to represent an impacting SS2.

- Assume a square 1 meters on a side to represent a person.
- Assume the impact zone (the field) to be a square 1000 meters on a side.
- Randomly place both the 18 meter square and the 1 meter square on the field.
- Determine if the squares intersect.

Performing this test 10,000,000 times and dividing the number of intersections by 10,000,000 produces the result of approximately 0.00036 collisions per test, or roughly 1 in 3,000. This analysis implicitly assumes that any contact between a person and any portion of SS2 debris produces a casualty. This number is much larger than the number computed by the Challenger Accident Investigation Board for the probability of a particular person on the ground becoming a casualty in the Challenger accident, namely 1 in 10,000.

AST evaluation of SC's Tier 1B experimental permit application

AST evaluated and approved SC's Tier 1B experimental permit application (Reference 2), as well as two applications for renewal of the permit.[32] The dates of application for and issuance of the permits and renewals, and of SS2 powered flights, are shown in Table 15.

Event	Date
SC submits Tier 1B experimental permit application	01/24/2012
FAA issues SC an experimental permit for the Tier 1B program	05/23/2012
SC submits application for 1st renewal of Tier 1B experimental permit	03/07/2013
SpaceShipTwo Powered Flight #1 (PF01)	04/29/2013
FAA issues SC 1st renewal of the Tier 1B experimental permit	05/22/2013
SpaceShipTwo Powered Flight #2 (PF02)	09/05/2013
SpaceShipTwo Powered Flight #3 (PF03)	01/10/2014
SC submits application for 2nd renewal of the Tier 1B experimental permit	03/17/2014
FAA issues SC 2nd renewal of the Tier 1B experimental permit	05/21/2014
SpaceShipTwo Powered Flight #4 (PF04) (accident)	10/31/2014

Table 15. Dates of Tier 1B experimental permit applications and issuances, and SS2 powered flights.

Appendix A to AST's evaluation of SC's application for the first renewal of the Tier 1B experimental permit application (Reference 20) defines 14 "exclusion zones" within the R2508 operating area, per 14 CFR 437.57(c) and 437.59. One of these zones was subsequently removed. The remaining 13 exclusion zones applied at the time of PF04, and so SS2's IIP and key flight-safety events for that flight were required to remain within R2508, but outside of the 13 exclusion zones.

The latitude and longitude coordinates of the IIP computed by SS2's INS systems are recorded in the TM data. These coordinates, as well as R2508 and the 13 exclusion zones described above, are depicted in Figure 29. The SS2 debris locations defined in Reference 5 are also shown in the Figure.

Figure 29 indicates that throughout PF04, SS2's IIP and key flight-safety events (release from WK2 and rocket-powered flight) remained within R2508 and outside of the exclusion zones, as required. The debris locations are also within R2508 and outside of the exclusion zones[33] except for the distant fragment found on the China Lake Golf Course, which fell inside the Ridgecrest exclusion zone.

[32] AST's permit evaluation process is described in Reference 21.

[33] The regulations in 14 CFR 437 do not require that all debris fragments from a mishap remain outside the exclusion zones; they only require that the IIP and key flight-safety events remain outside these zones. The exclusion zones are intended to protect areas that have a higher population density from direct overflight of the vehicle during hazardous operations.

E. CONCLUSIONS

The debris field, RIR, ASR, TM data, CIR, LRO, and calculated data presented in this *Study* are consistent with the sequence of events summarized in Table 16, concerning the motion of WK2, SS2, N24GA, and the helicopters involved in the rescue of the surviving SS2 pilot. The time range considered in Table 16 extends from the takeoff of WK2/SS2 from KMHV to the departure of Mercy 14 from the accident scene with the surviving SS2 pilot on board.

Before 10:07:18, the SS2 altitude, Mach number and equivalent airspeed values shown in Table 16 are based on recorded INS and ADC data from WK2. At 10:07:18 and onward, these parameters are based on the SS2 wind-corrected integrated accelerometer data, described in Section D-V.

The results presented in this *Study* indicate that shortly after the feather was unlocked, the opening feathering moments (as predicted by SC's Trajectory Code) were sufficient to overcome the closing moment provided by the feather actuators, and open the feather. On the two previous powered flights, the feather was unlocked at points where aerodynamic forces produced a closing feather moment, as intended. However, during PF02, the vehicle's subsequent deceleration through the transonic region while unlocked produced high opening feather moments that resulted in a small amount of feather motion.

On PF04, the flight path of WK2 and SS2, and the debris from the breakup of SS2, remained within the mission's operating area (Restricted Area R2508). The key flight-safety events (release from WK2 and rocket-powered flight), and SS2's predicted instantaneous impact point, remained within the operating area and outside of the mission's exclusion zones.

_____

John O'Callaghan
National Resource Specialist – Aircraft Performance
Office of Research and Engineering

Event	Time (PDT)	Time from SS2 release HH:MM:SS	SS2 Altitude, ft. MSL	SS2 KEAS	SS2 Mach Number
[WK2] Takeoff	09:19:07.00	-00:48:12.10	2741	126	0.20
[CV] Center MFD malfunctions.	09:28:29.70	-00:38:49.40	29186	139	0.37
[CV] Center MFD finishes rebooting.	09:29:17.50	-00:38:01.60	30277	142	0.39
[CV] Comment indicating being ready to begin 30,000 foot checks.	09:29:49.75	-00:37:29.35	31404	137	0.38
[CV] Start of L minus 10 checks.	09:58:40.95	-00:08:38.15	46590	125	0.50
[CV] Start of L minus 4 checks.	10:03:26.41	-00:03:52.69	46331	138	0.55
[CV] Comment indicating being 30 seconds from release.	10:06:52.68	-00:00:26.42	46482	137	0.55
[CV] Comment that the control stick is in forward position.	10:06:57.27	-00:00:21.83	46475	136	0.55
[TM] Release from WK2 discrete = 1	10:07:19.10	00:00:00.00	46431	138	0.55
[TM] Rocket fire command discrete = 1	10:07:21.60	00:00:02.50	46380	137	0.55
[CV] PFD indicates ADC to INS transition.	10:07:26.83	00:00:07.73	45858	212	0.83
[CV] Mach point eight callout.	10:07:26.91	00:00:07.81	45847	214	0.84
[CV] Comment about unlocking the feather system.	10:07:28.39	00:00:09.29	45664	241	0.94
[TM] Feather lock state discrete = 0	10:07:29.50	00:00:10.40	45598	261	1.02
[TM] Feather movement.	10:07:30.60	00:00:11.50	45581	279	1.08
[TM] SS2 peak airspeed	10:07:32.00	00:00:12.90	45662	291	1.14
[ASR] Primary returns appear near breakup point.	10:07:32.63	00:00:13.53	45790	265	1.03
[CV] End of recording.	10:07:32.80	00:00:13.70	45842	247	0.96
[TM] Last apparently valid point in TM data file (based on left INS vertical load factor)	10:07:33.10	00:00:14.00	45908	239	0.93
[RIR] RIR indicates tracked target is on the ground	10:10:58.85	00:03:39.75			
[ASR] Tiger 1 lands near surviving SS2 pilot	10:51:53.00	00:44:33.90			
[ASR] KCFD Helo 408 lands near surviving SS2 pilot	10:56:35.00	00:49:15.90			
[ASR] Tiger 1 takes off from pilot site	11:12:54.00	01:05:34.90			
[ASR] Mercy 14 lands near surviving SS2 pilot	11:16:25.00	01:09:05.90			
[ASR] Mercy 14 takes off with surviving SS2 pilot on board	11:23:20.00	01:16:00.90			

Notes:

Characters in brackets [ ] indicate source of information, as follows:
[WK2] = WhiteKnightTwo recorded data
[CV] = Cockpit Image Recorder ("cockpit video") data
[TM] = SS2 telemetered data
[RIR] = NASA Dryden Range Instrumentation Radar
[ASR] = FAA Airport Surveillance Radar

Table 16. Sequence of events concerning vehicle motions based on the information in this *Study*.

F. REFERENCES

1. Scaled Composites, LLC, *SpaceShipTwo (SS2) Pilot Operating Handbook*, SC document # SS2-90BP001, Rev D, September 3, 2013. (SC Proprietary document).

2. Scaled Composites, LLC, *Experimental Permit Application for the Tier 1B Reusable Suborbital System*, SC document # T1B-90E060 R B.2, January 23, 2012. (SC Proprietary document).

3. National Transportation Safety Board, Office of Aviation Safety, *Propulsion Group Chairman's Factual Report, Virgin Galactic SpaceShipTwo (SS2) rocket plane, registration N339SS, Koehn Lake, CA, October 31, 2014.* NTSB Accident Number DCA15MA019 (Washington, DC: NTSB, March 5, 2015). (Contact NTSB at pubinq@ntsb.gov).

4. National Transportation Safety Board, Office of Aviation Safety, *Operations Group Chairman's Factual Report, Virgin Galactic SpaceShipTwo (SS2) rocket plane, registration N339SS, Koehn Lake, CA, October 31, 2014.* NTSB Accident Number DCA15MA019 (Washington, DC: NTSB, March 16, 2015). (Contact NTSB at pubinq@ntsb.gov).

5. National Transportation Safety Board, Office of Aviation Safety, *Vehicle Recovery Group Chairman's Factual Report, Virgin Galactic SpaceShipTwo (SS2) rocket plane, registration N339SS, Koehn Lake, CA, October 31, 2014.* NTSB Accident Number DCA15MA019 (Washington, DC: NTSB, March 5, 2015). (Contact NTSB at pubinq@ntsb.gov).

6. Interview of Mojave Air & Space Port Firefighter / EMT (attachment to Reference 14).

7. Interview of Mercy Air Flight Paramedic (attachment to Reference 14).

8. Interview of Mercy Air Registered Nurse (attachment to Reference 14).

9. Interview of Mercy Air Helicopter Pilot (attachment to Reference 14).

10. National Transportation Safety Board, Office of Research and Engineering, *Electronic Devices and Flight Data Factual Report, Virgin Galactic SpaceShipTwo (SS2) rocket plane, registration N339SS, Koehn Lake, CA, October 31, 2014.* NTSB Accident Number DCA15MA019 (Washington, DC: NTSB, March 20, 2015). (Contact NTSB at pubinq@ntsb.gov).

11. National Transportation Safety Board, Office of Research and Engineering, *Cockpit Image Recorder Factual Report, Virgin Galactic SpaceShipTwo (SS2) rocket plane, registration N339SS, Koehn Lake, CA, October 31, 2014.* NTSB Accident Number DCA15MA019 (Washington, DC: NTSB, December 16, 2014). (Contact NTSB at pubinq@ntsb.gov).

12. National Transportation Safety Board, Office of Research and Engineering, *External Imagery Factual Report, Virgin Galactic SpaceShipTwo (SS2) rocket plane, registration N339SS, Koehn Lake, CA, October 31, 2014*. NTSB Accident Number DCA15MA019 (Washington, DC: NTSB, March 18, 2015). (Contact NTSB at pubinq@ntsb.gov).

13. National Transportation Safety Board, Office of Research and Engineering, *Group Chairman's Aircraft Performance Study, American Airlines Flight 587, Airbus A300B4-605R, Belle Harbor, New York, November 12, 2001*, NTSB Accident Number DCA02MA001, Docket Item 188 (Washington, DC: NTSB, October 10, 2002). (Contact NTSB at pubinq@ntsb.gov).

14. National Transportation Safety Board, Office of Aviation Safety, *Survival Factors Group Chairman's Factual Report, Virgin Galactic SpaceShipTwo (SS2) rocket plane, registration N339SS, Koehn Lake, CA, October 31, 2014. NTSB Accident Number DCA15MA019* (Washington, DC: NTSB, July 2015). (Contact NTSB at pubinq@ntsb.gov).

15. Scaled Composites, LLC, *Answers to questions submitted by NTSB via email dated 12/18/2014,* January 23, 2015 (SC proprietary document)

16. Scaled Composites, LLC, *PF04 Aerodynamic Response, Rev. B*, February 23, 2015 (SC proprietary document).

17. Scaled Composites, LLC, *Response to the latest draft of the Vehicle Performance Factual Report,* March 17, 2015 (SC proprietary document).

18. Scaled Composites, LLC, *Vehicle Performance Factual Report Comments V3,* March 19, 2015 (SC proprietary document).

19. Scaled Composites, LLC, *AST Experimental Application Note (IIP Calculation),* March 5, 2015 (SC proprietary document).

20. Federal Aviation Administration, Office of Commercial Space Transportation, *Permit Application Technical Evaluation Report For Scaled Composites, LLC, SpaceShipTwo (SS2) Tier 1B* (1st permit renewal), Technical Document PA-12-SCA-016, May 24, 2013. (FAA privileged document).

21. National Transportation Safety Board, Office of Aviation Safety, *System Safety Group Chairman's Factual Report, Virgin Galactic SpaceShipTwo (SS2) rocket plane, registration N339SS, Koehn Lake, CA, October 31, 2014. NTSB Accident Number DCA15MA019* (Washington, DC: NTSB, April 29, 2015). (Contact NTSB at pubinq@ntsb.gov).

G. GLOSSARY OF SYMBOLS AND ACRONYMS

English characters

a	Speed of sound
$\vec{a}$	Acceleration vector
ACP	Azimuth Change Pulse
ADC	Air Data Computer
AFB	Air Force Base
AGL	Above Ground Level
$ALTSET$	Altimeter setting
ASR	Airport Surveillance Radar
AST	FAA Office of Commercial Space Transportation
CFD	Computational Fluid Dynamics
CFR	Code of Federal Regulations
CG	Center of Gravity
CP	Center of Pressure
CIR	Cockpit Image Recorder
C_L	Lift coefficient
DOF	Degree of freedom
E	Distance east of KMHV runway 30 threshold
EDW	Edwards Air Force Base, California
ERT	Emergency Response Team
FAA	Federal Aviation Administration
FBI	Federal Bureau of Investigation
g	Acceleration due to gravity (32.17 ft/s^2)
GPS	Global Positioning System
h_b	Barometric altitude
h_p	Pressure altitude
IIP	Instantaneous Impact Point
IMU	Inertial Measurement Unit
INS	Inertial Navigation System
IRIG	Inter-range instrumentation group
KCAS	Knots calibrated airspeed
KEAS	Knots equivalent airspeed
KMHV	Mojave Air and Space Port, Mojave, California
KTAS	Knots true airspeed
LRO	NASA Dryden Long Range Optics video camera
M	Mach number
MAC	Mean Aerodynamic Chord
MFD	Multi-Function Display

MSL	Mean Sea Level
$\vec{n}$	Load factor vector
nlf	Normal load factor = $-n_z$
n_x	Longitudinal load factor
n_y	Lateral load factor
n_z	Vertical load factor
N	Distance north of KMHV runway 30 threshold
NASA	National Aeronautics and Space Administration
NTSB	National Transportation Safety Board
P	Body-axis roll rate, or static air pressure (dependent on context)
P_0	Standard-day static air pressure at sea-level
P_T	Total air pressure
PF04	Powered Flight #4
POH	Pilot's Operating Handbook
$\bar{q}$	Dynamic pressure
Q	Body-axis pitch rate or dynamic pressure (dependent on context)
QFV	Fremont Valley Common Digitizer ASR
R	Body-axis yaw rate, or gas constant for air (dependent on context)
RIR	Range Instrumentation Radar
S	Wing area
SC	Scaled Composites, LLC
SODAS	Strap-On Data Acquisition System
SS2	SpaceShipTwo
t	Time
T	Static air temperature
T_0	Standard-day static air temperature at sea-level
T_T	Total air temperature
TC	Scaled Composites, LLC *MATLAB* - based Trajectory Code
TSC	The Spaceship Company
u	Velocity component along x-body axis
UTC	Universal Coordinated Time
v	Velocity component along y-body axis
V	Total velocity (inertial speed or airspeed dependent on context)
$\vec{V}$	Velocity vector (inertial speed or airspeed dependent on context)
V_C	Calibrated airspeed
V_E	Equivalent airspeed
$\vec{V}_G$	Groundspeed vector
$\vec{V}_T$	True airspeed vector
$\vec{V}_W$	Wind vector
w	Velocity component along z-body axis
W	Vehicle weight = mg
WK2	WhiteKnightTwo
x	x-coordinate (axis system dependent on context)
y	y-coordinate (axis system dependent on context)
z	z-coordinate (axis system dependent on context)

Greek characters

α	Angle of attack
β	Sideslip angle
γ	Flight path angle, or ratio of specific heats for air (dependent on context)
θ	Pitch angle
ϕ	Roll angle
ψ	True heading (yaw) angle
ψ_T	True track angle
ψ_W	Wind direction (direction wind is blowing *from*)
ρ	Static air density
ρ_0	Standard-day static air density at sea-level

FIGURES

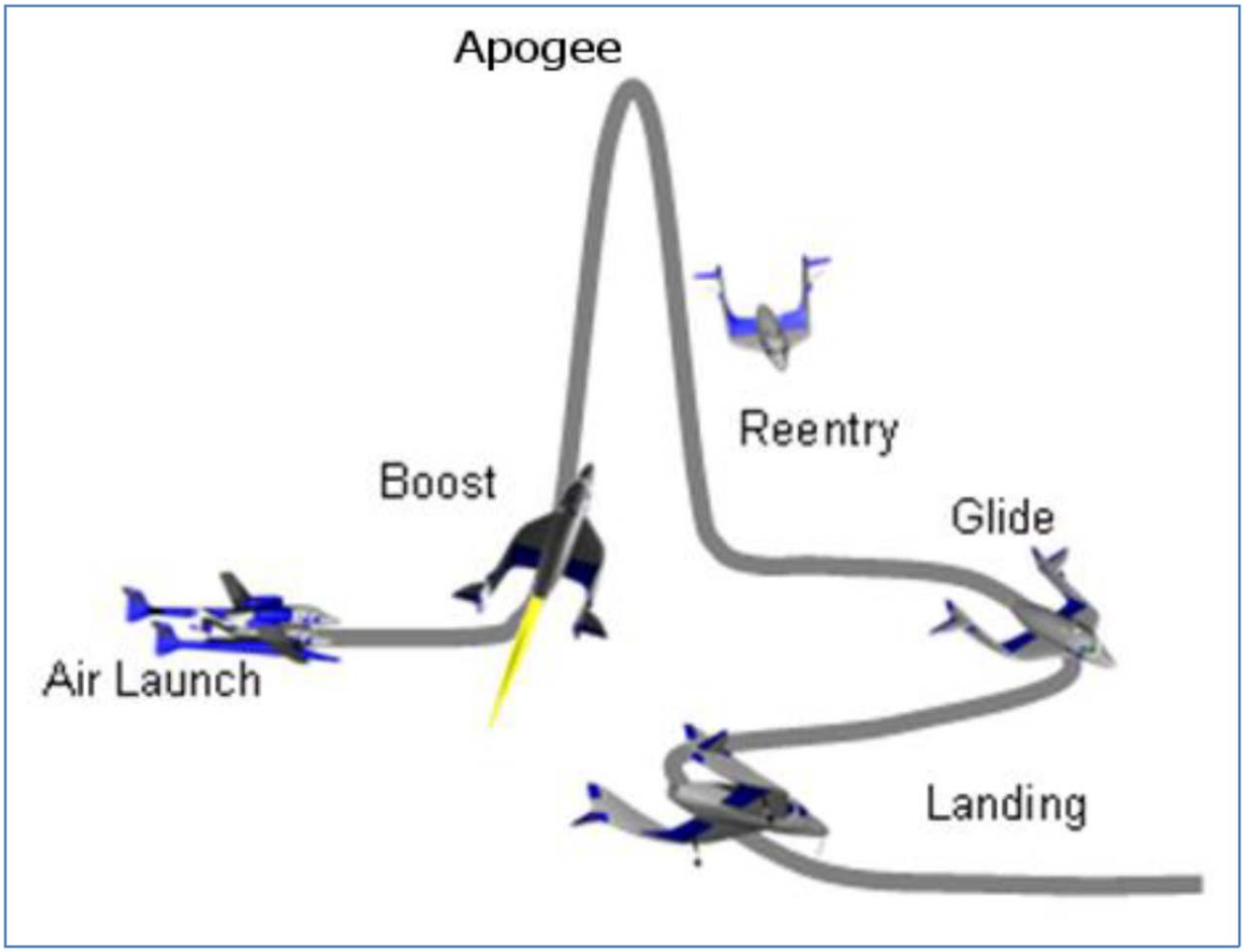

Figure 1: The Scaled Composites Tier 1B design mission (from Reference 2).

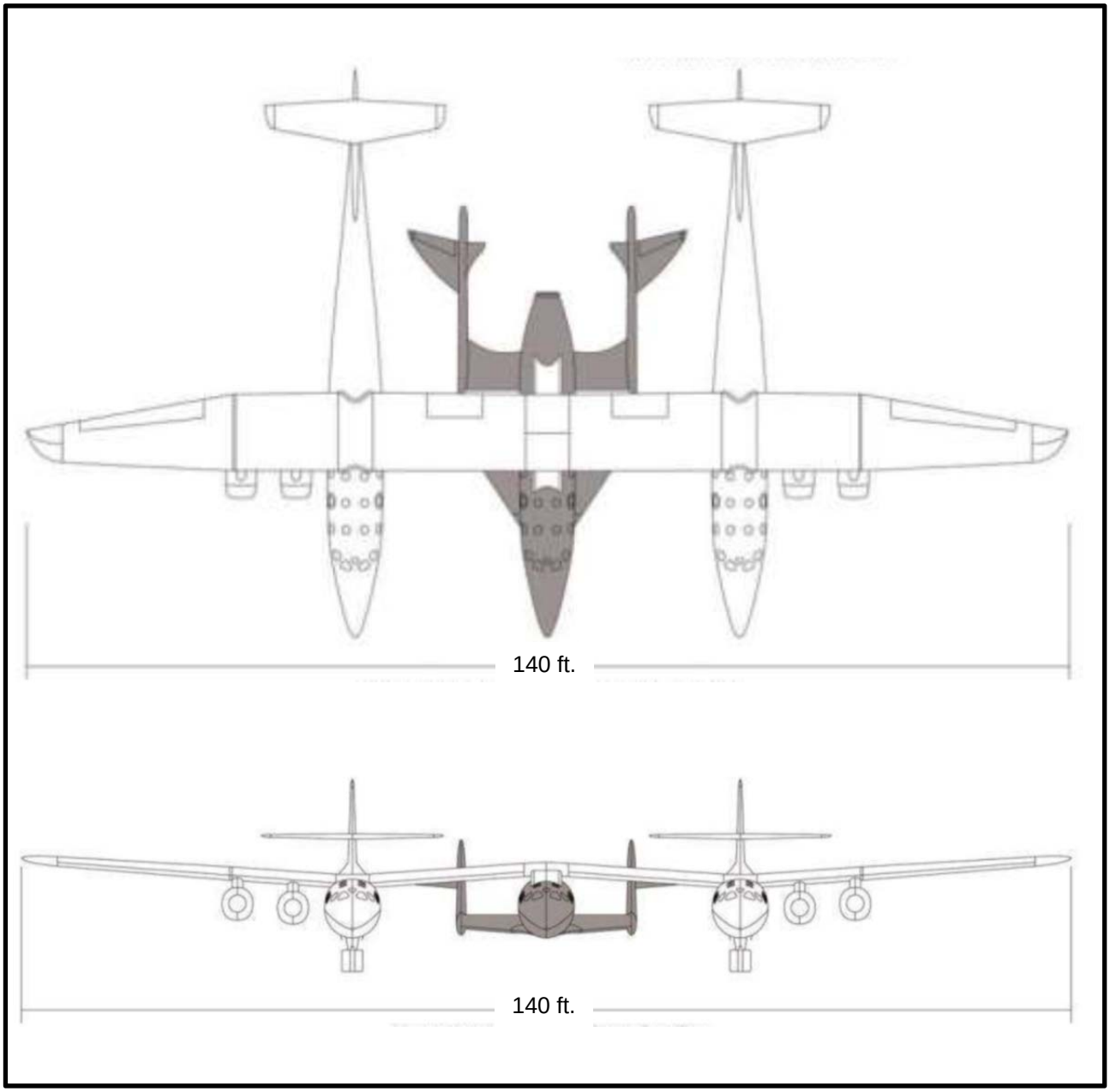

Figure 2. WhiteKnightTwo / SpaceShipTwo mated configuration (from Reference 1).

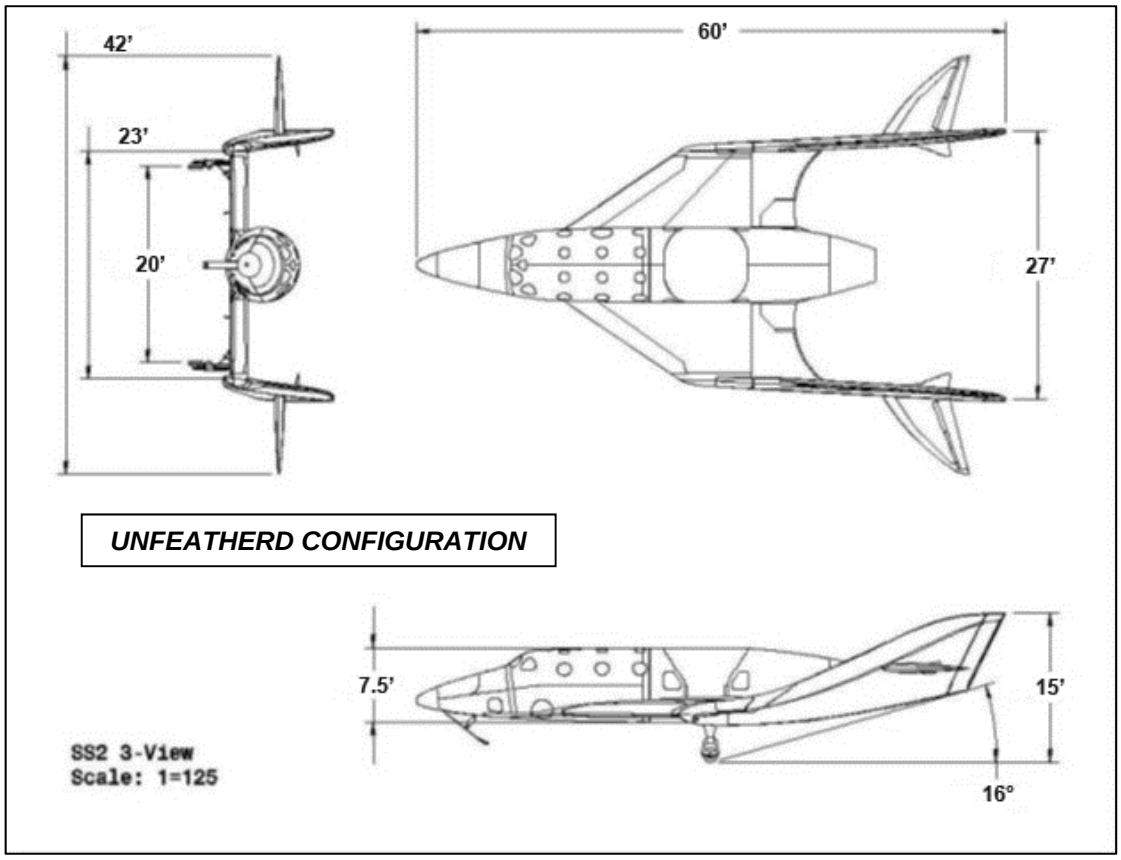

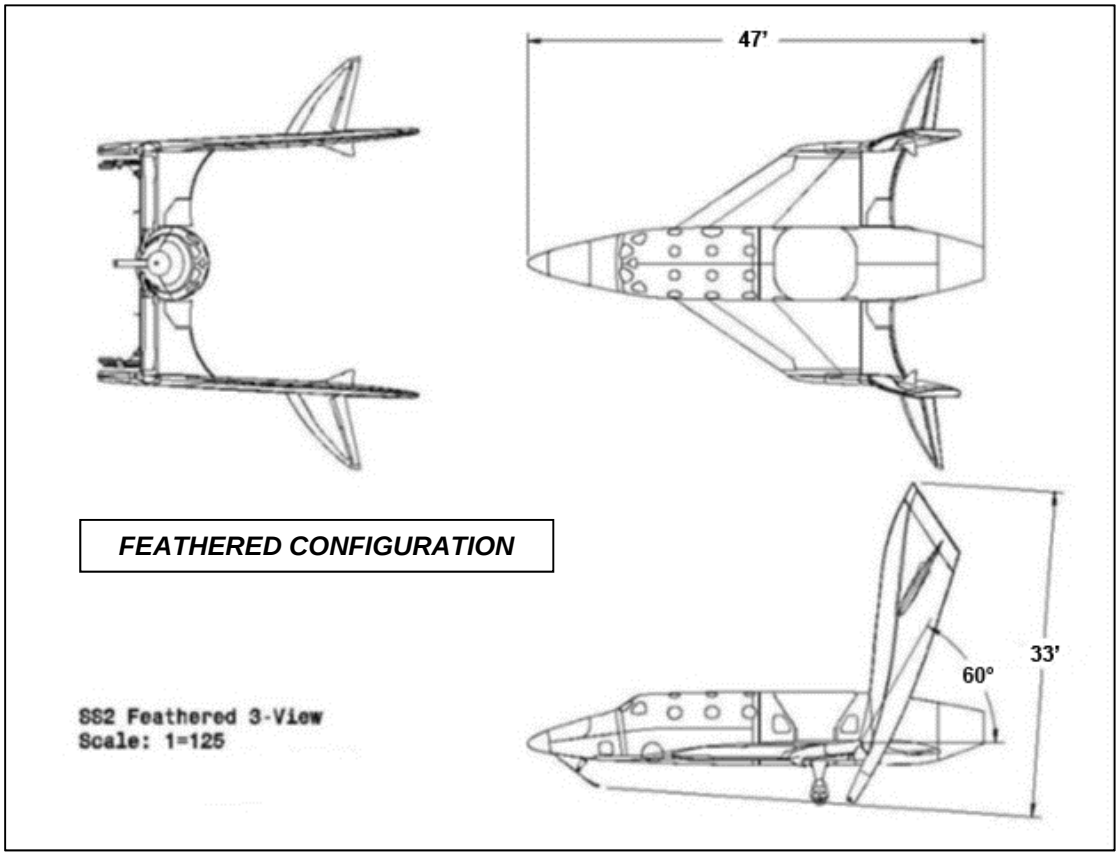

Figure 3. Three-view of SS2 in unfeathered and feathered configurations (from Reference 1).

DCA15MA019: SpaceShipTwo, N339SS, Koehn Dry Lake, CA, 10/31/2014

Plan view of WhiteKnightTwo, SpaceShipTwo, and N24GA flight tracks (09:15:00 - 10:07:35 PDT)

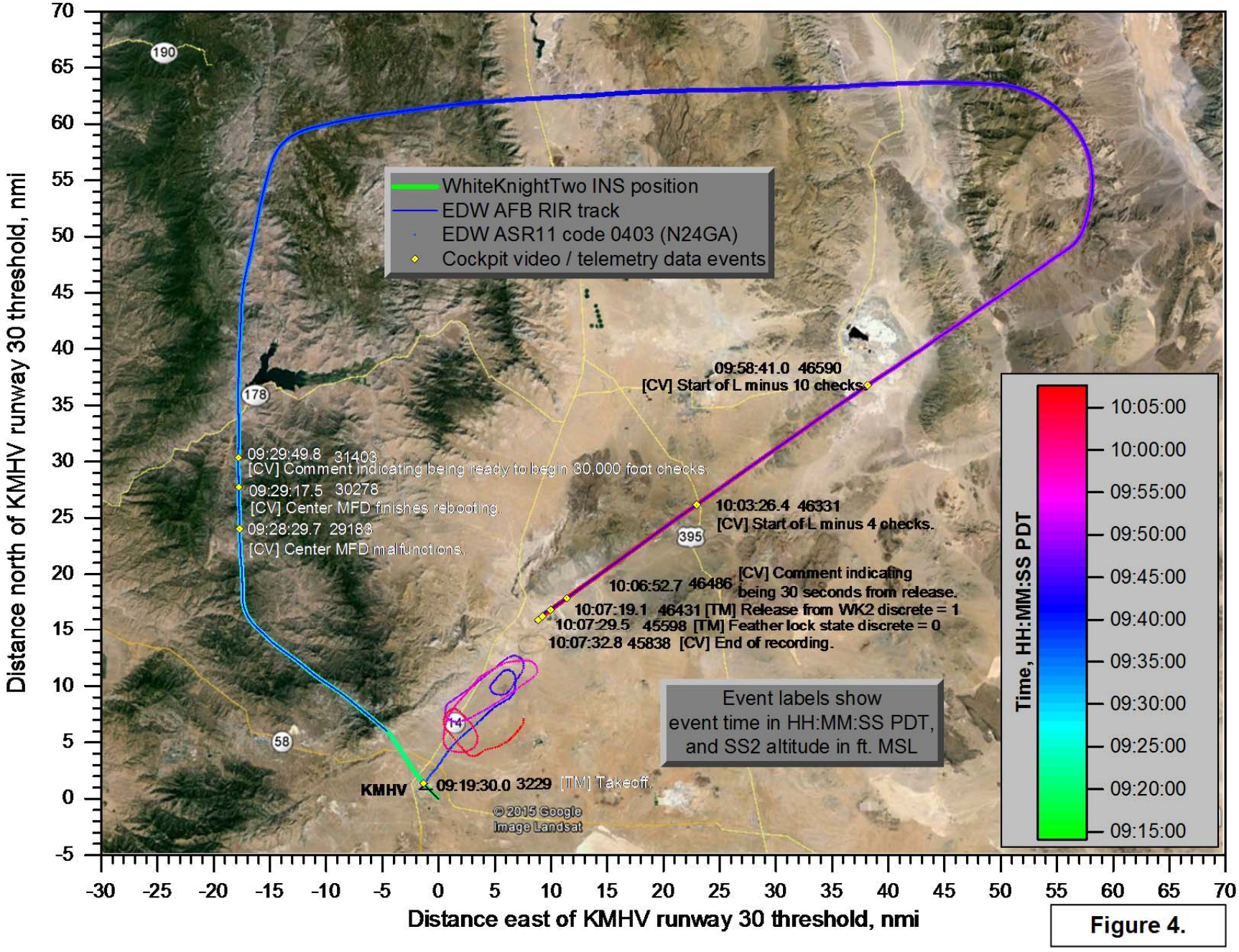

Figure 4.

DCA15MA019: SpaceShipTwo, N339SS, Koehn Dry Lake, CA, 10/31/2014

Plan view of WhiteKnightTwo, SpaceShipTwo, and N24GA flight tracks (10:06:00 - 10:11:00 PDT)

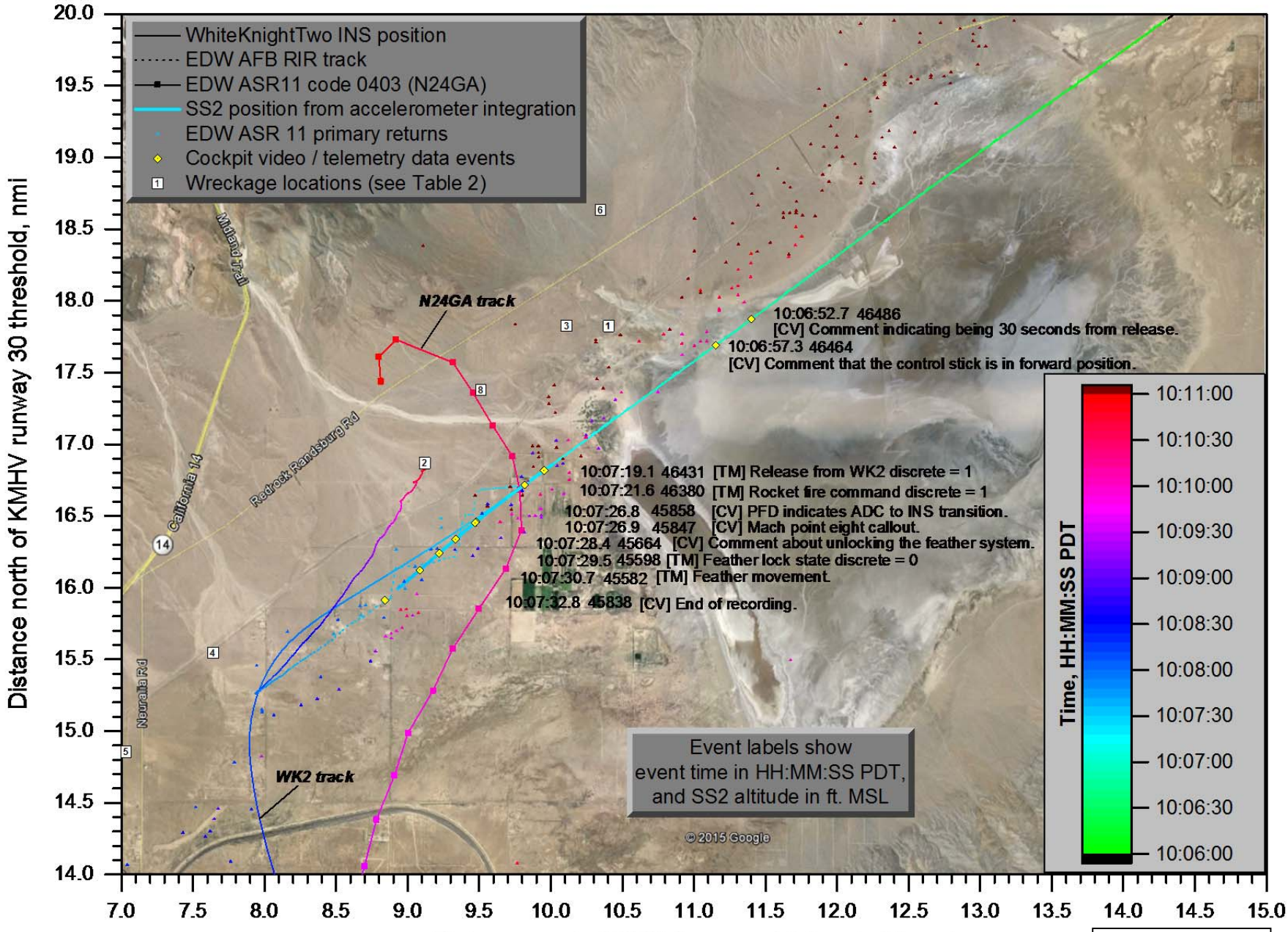

Figure 5.

DCA15MA019: SpaceShipTwo, N339SS, Koehn Dry Lake, CA, 10/31/2014

Plan view of WhiteKnightTwo and N24GA flight tracks (10:07:30 - 11:06:00 PDT)

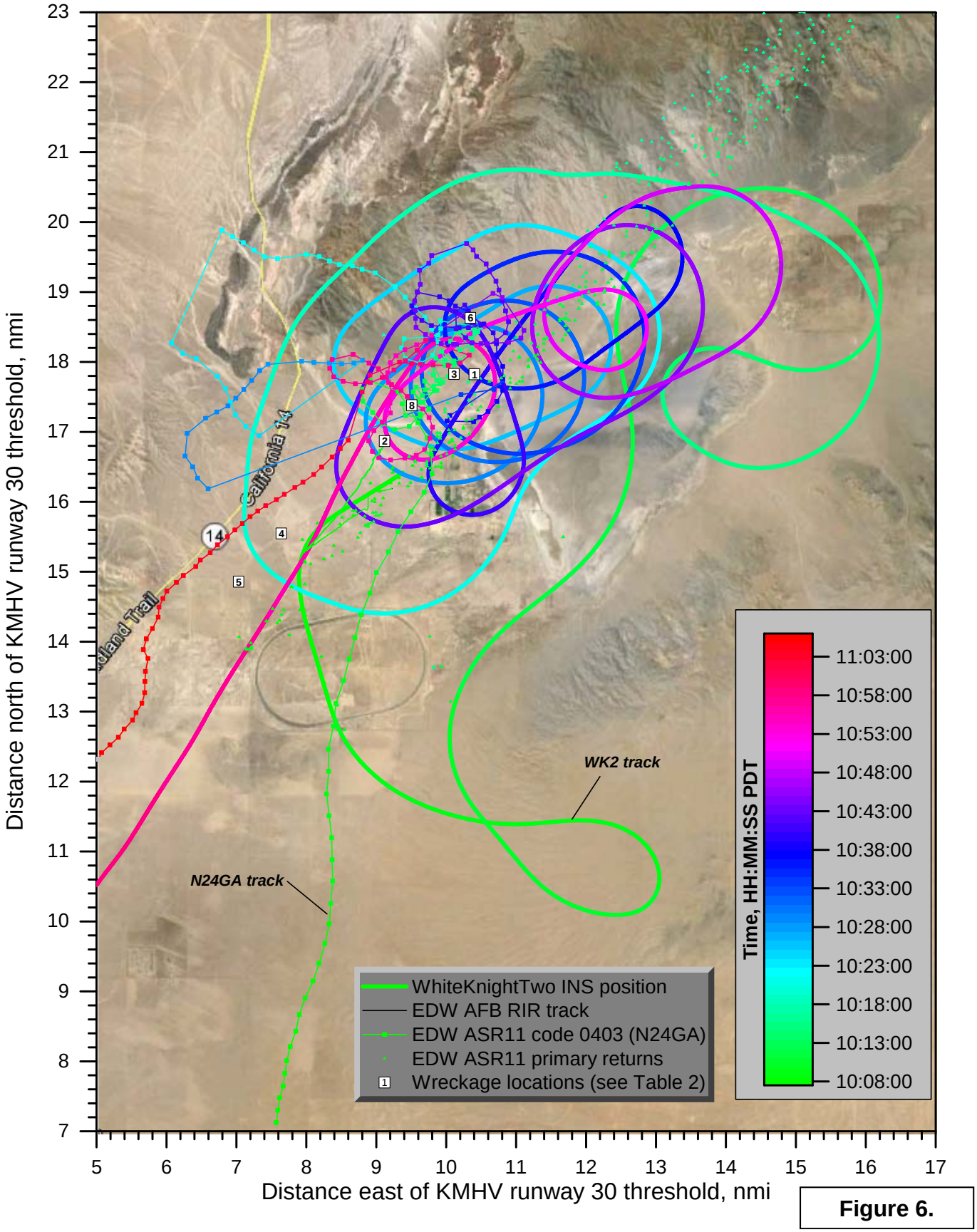

Figure 6.

DCA15MA019: SpaceShipTwo, N339SS, Koehn Dry Lake, CA, 10/31/2014

Plan view of primary returns from EDW ASR11 (10:07:30 - 10:42:00 PDT)

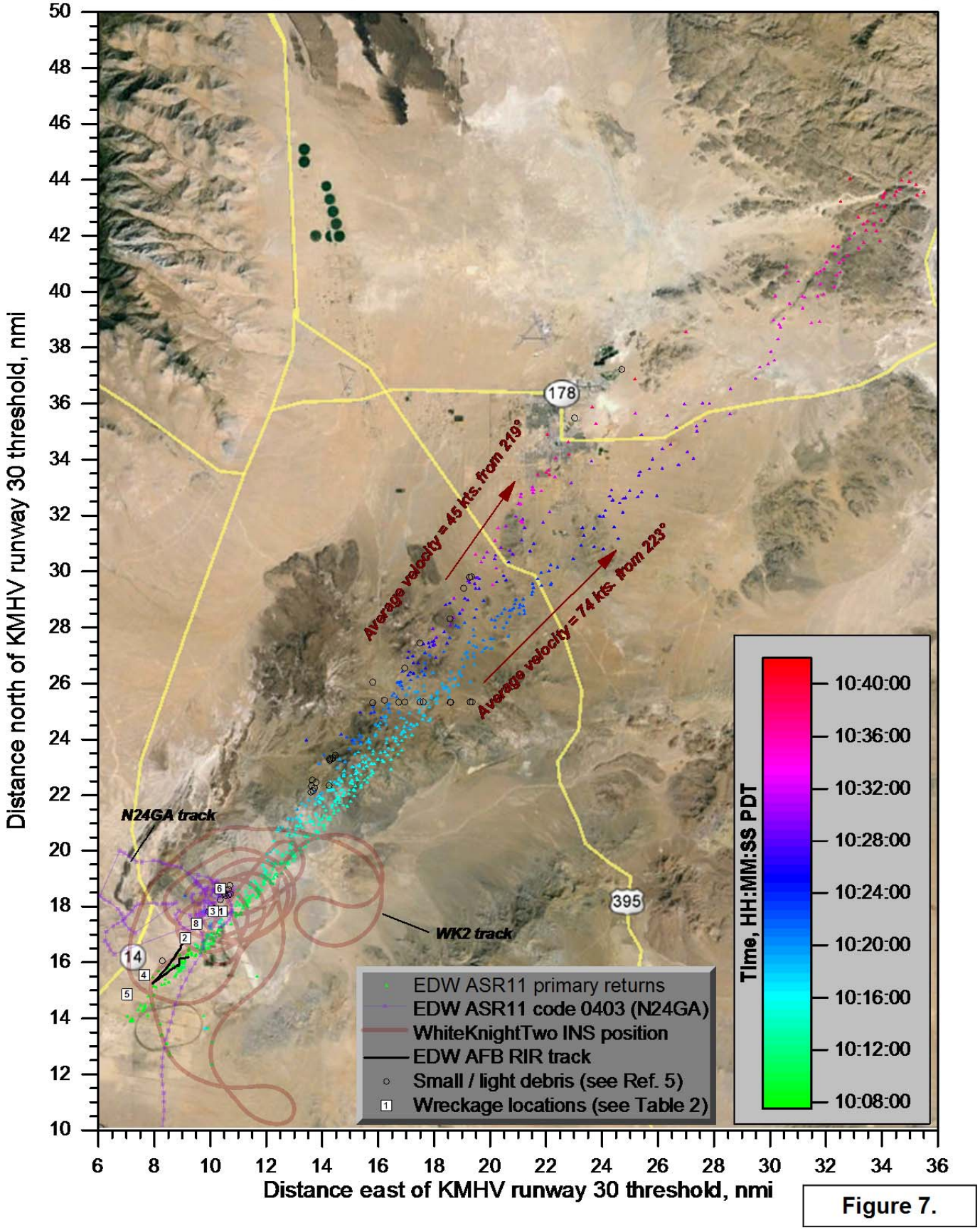

Figure 7.

DCA15MA019: SpaceShipTwo, N339SS, Koehn Dry Lake, CA, 10/31/2014

WhiteKnightTwo, SpaceShipTwo, and N24GA position vs. time (09:18:00 - 10:12:00 PDT)

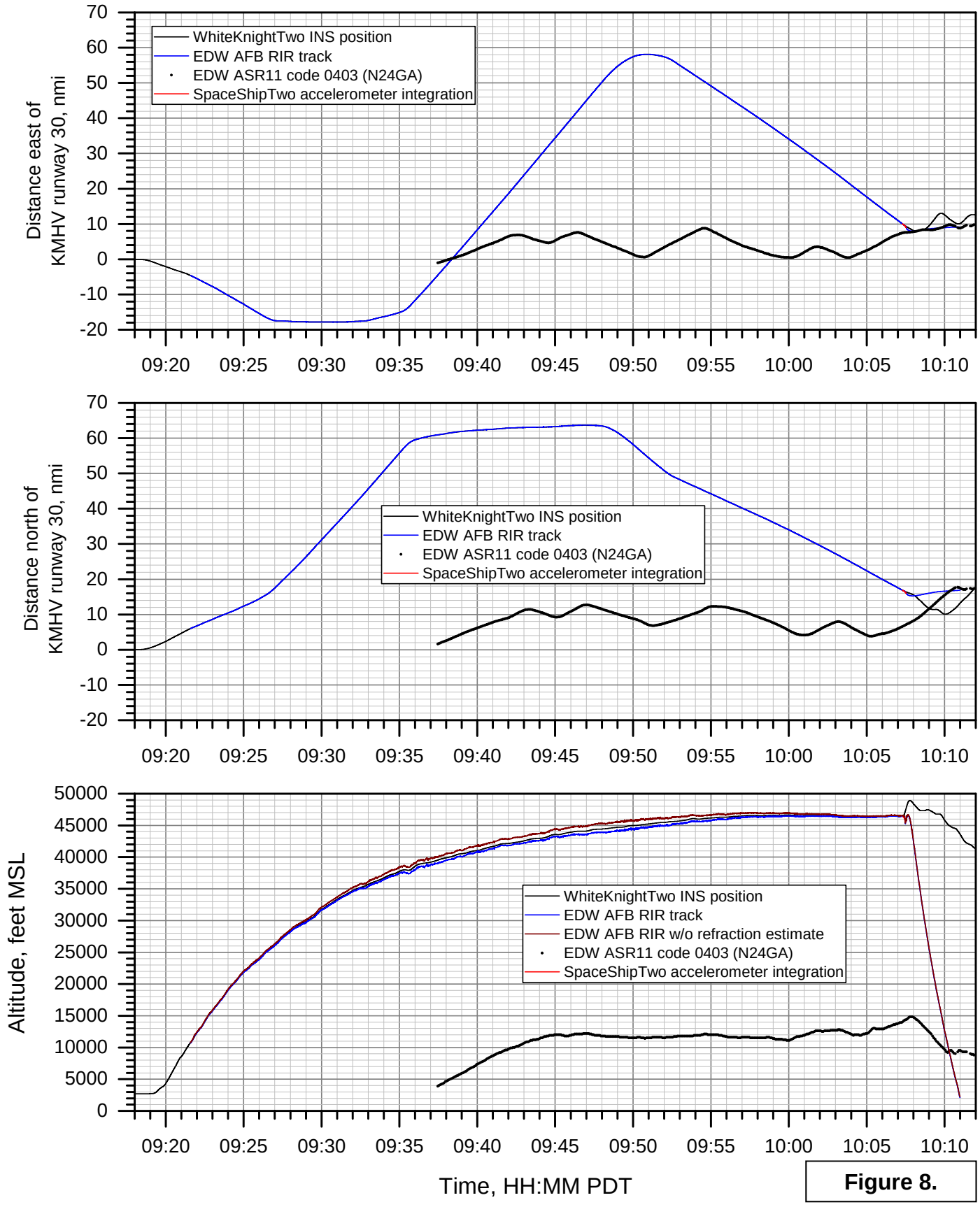

Figure 8.

DCA15MA019: SpaceShipTwo, N339SS, Koehn Dry Lake, CA, 10/31/2014

WhiteKnightTwo, SpaceShipTwo, and N24GA position vs. time (10:07:00 - 10:11:10 PDT)

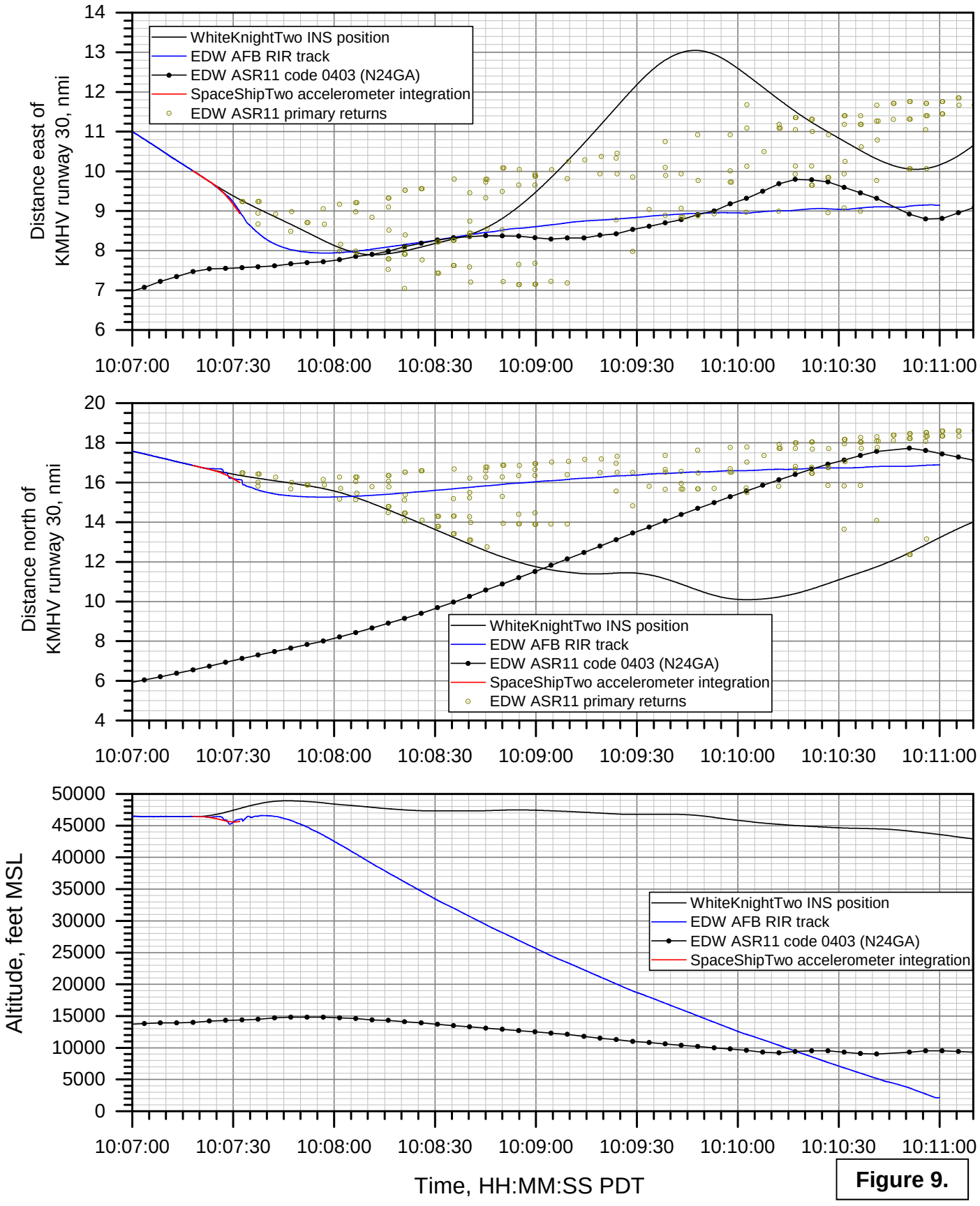

Figure 9.

DCA15MA019: SpaceShipTwo, N339SS, Koehn Dry Lake, CA, 10/31/2014

WhiteKnightTwo, SpaceShipTwo, and N24GA position vs. time (10:07 - 11:13 PDT)

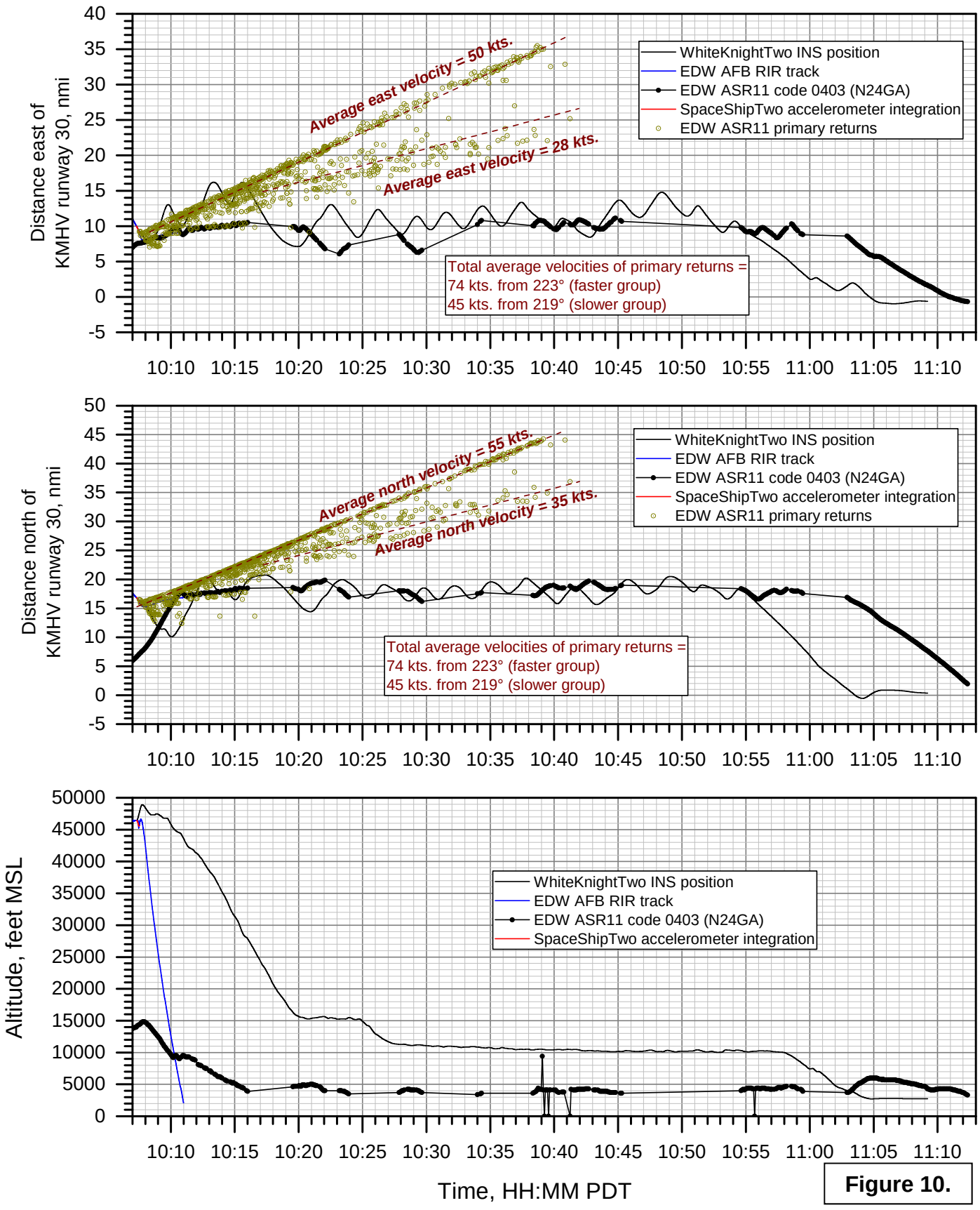

Figure 10.

DCA15MA019: SpaceShipTwo, N339SS, Koehn Dry Lake, CA, 10/31/2014

Plan view of rescue helicopter flight tracks (10:35:00 - 11:35:00 PDT)

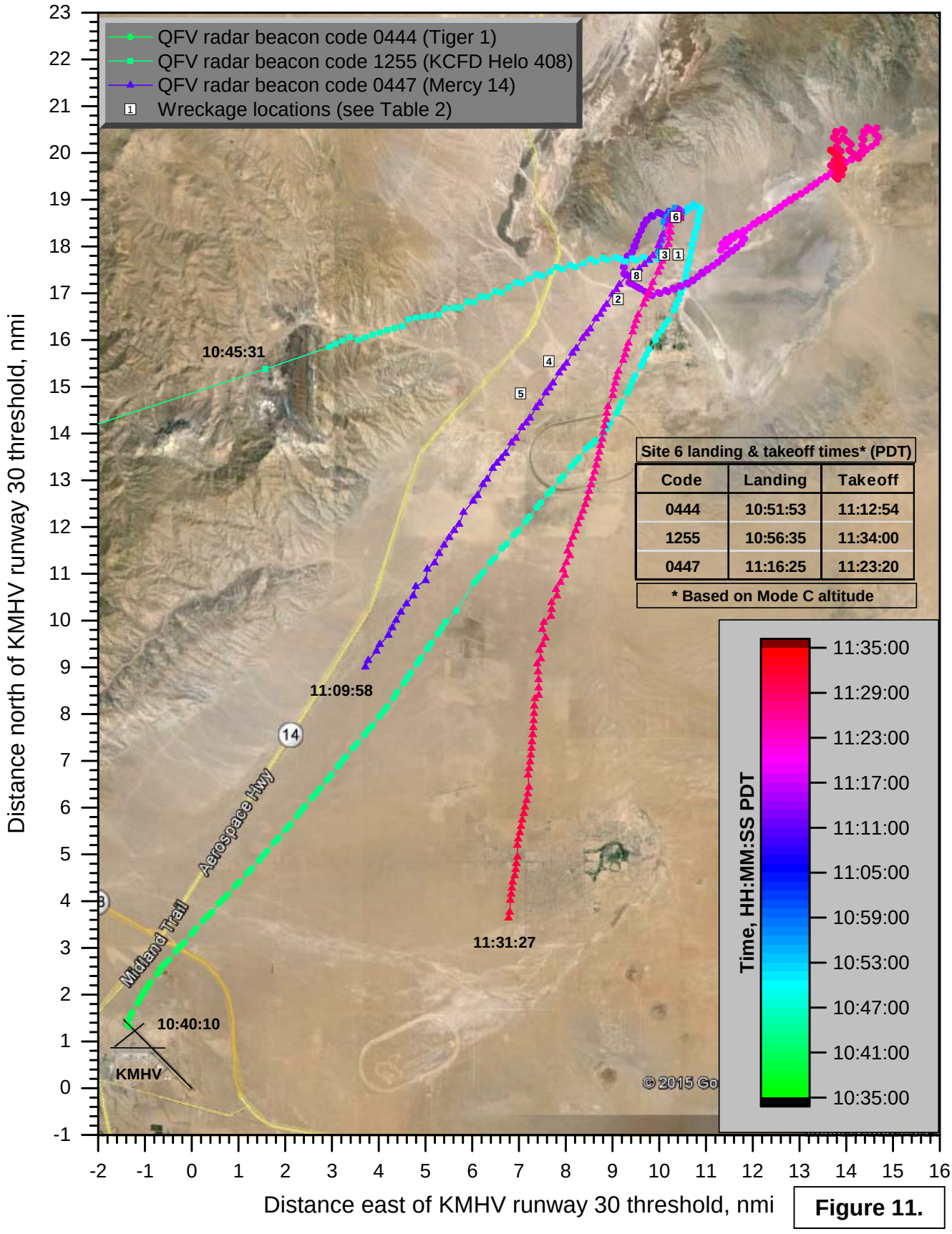

Figure 11.

DCA15MA019: SpaceShipTwo, N339SS, Koehn Dry Lake, CA, 10/31/2014

Rescue helicopter altitudes vs. time (10:35:00 - 11:35:00 PDT)

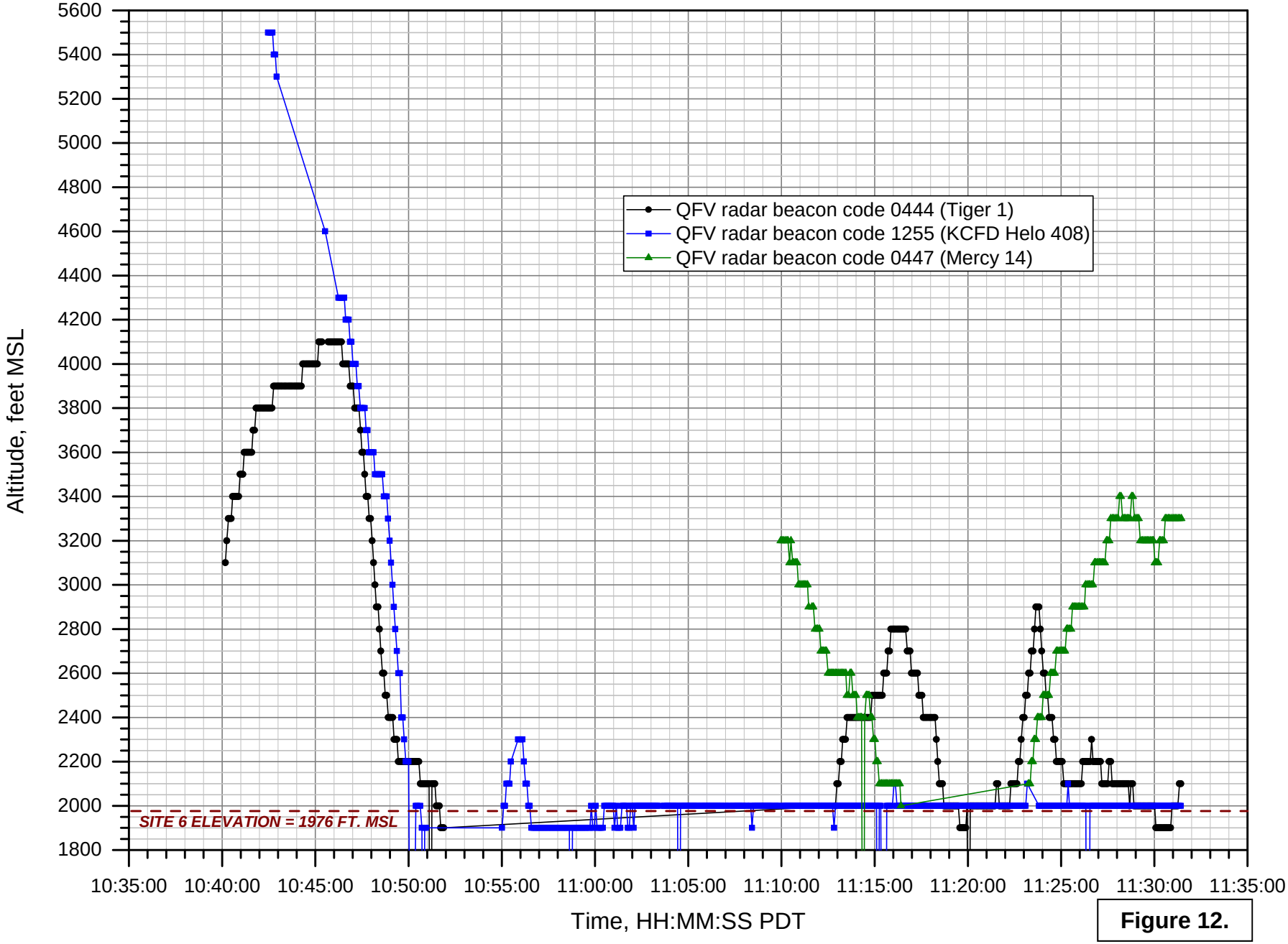

Figure 12.

DCA15MA019: SpaceShipTwo, N339SS, Koehn Dry Lake, CA, 10/31/2014

WK2 release, rocket firing, & feather lock data: release to end of data

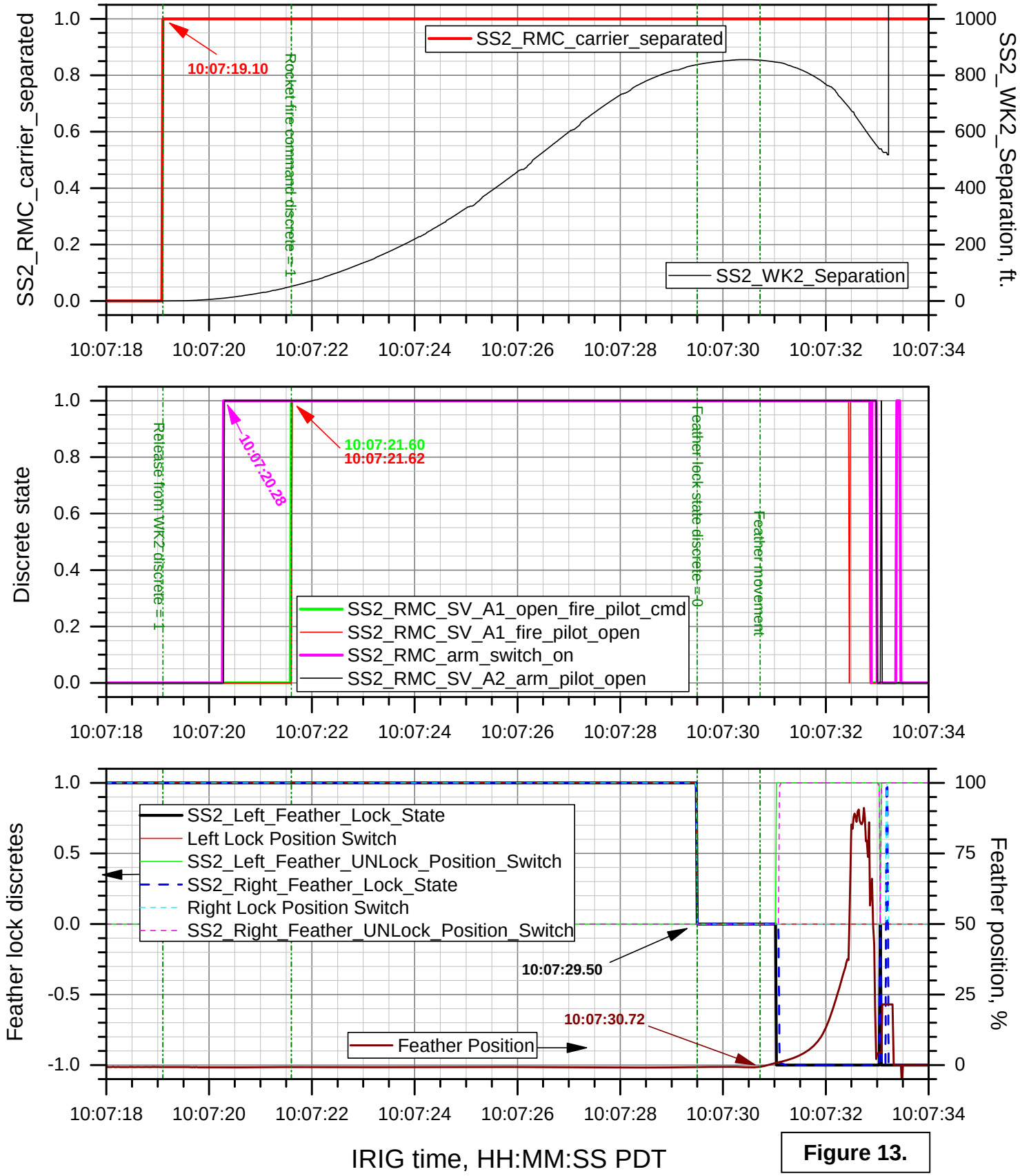

Figure 13.

DCA15MA019: SpaceShipTwo, N339SS, Koehn Dry Lake, CA, 10/31/2014

Position data comparisions: release to end of data (latitude & longitude coordinates)

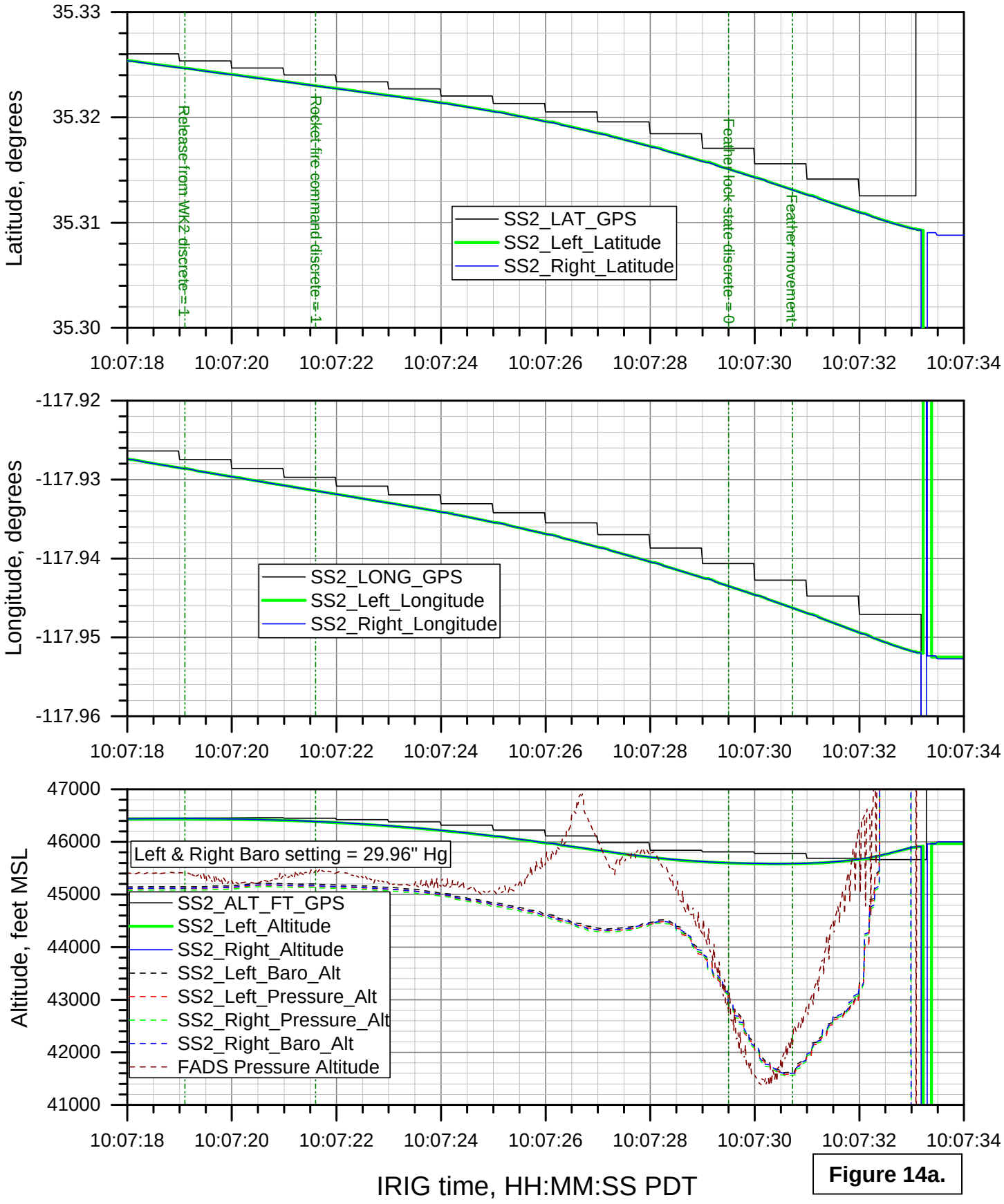

Figure 14a.

DCA15MA019: SpaceShipTwo, N339SS, Koehn Dry Lake, CA, 10/31/2014

Position data comparisions: release to end of data (north & east coordinates)

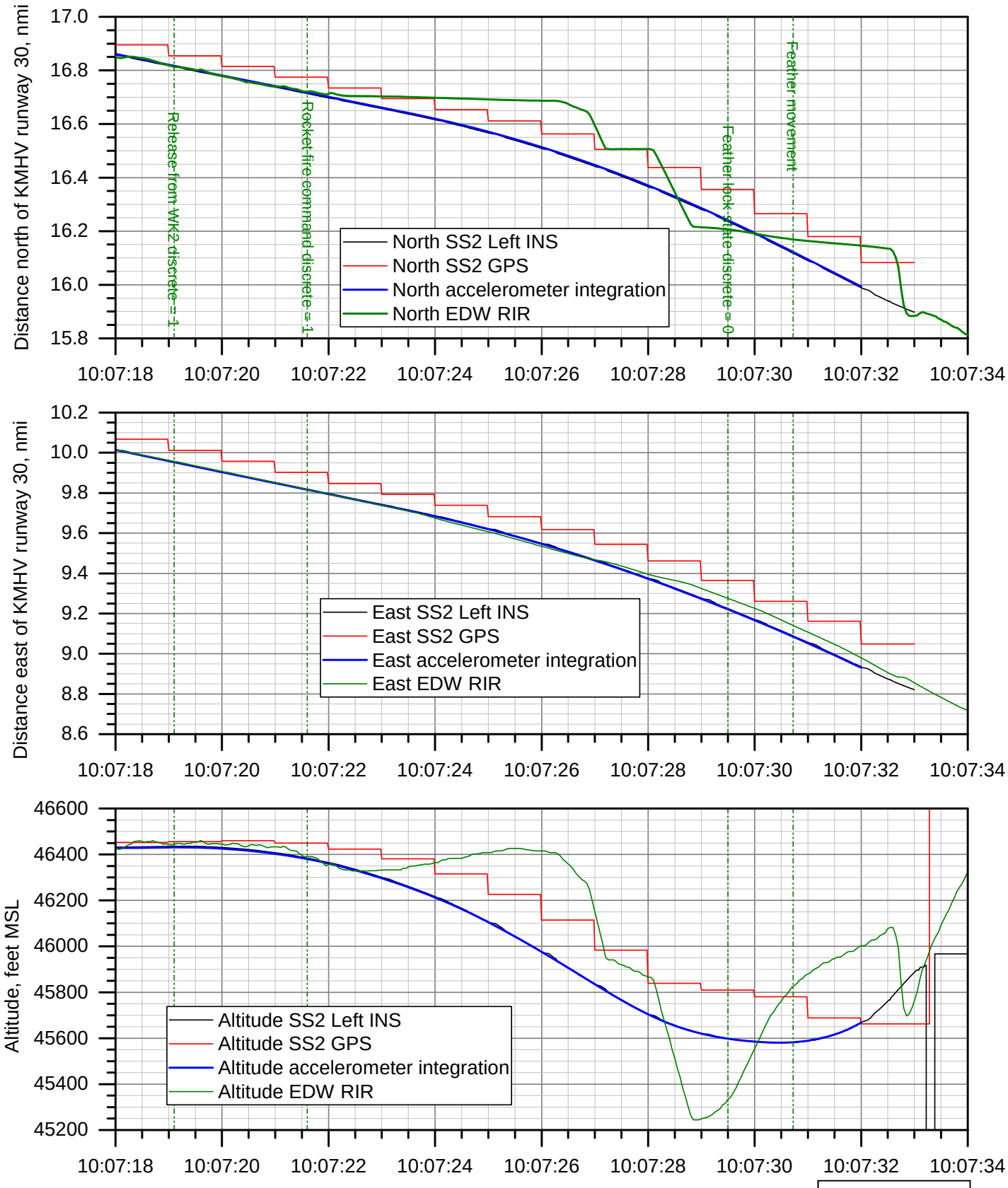

Figure 14b.

DCA15MA019: SpaceShipTwo, N339SS, Koehn Dry Lake, CA, 10/31/2014

Speed data comparisions: release to end of data

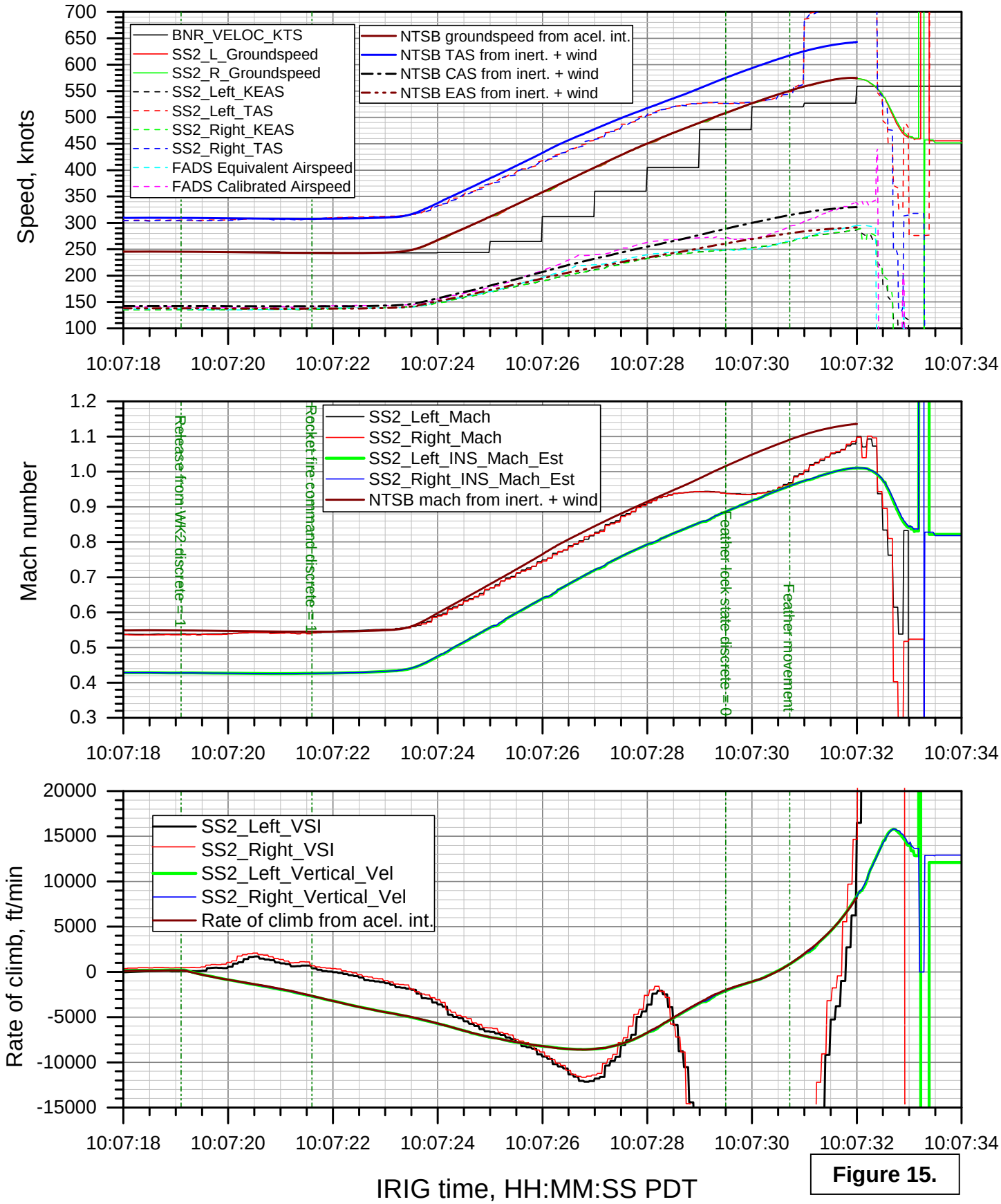

Figure 15.

DCA15MA019: SpaceShipTwo, N339SS, Koehn Dry Lake, CA, 10/31/2014

Euler & flight angles: release to end of data

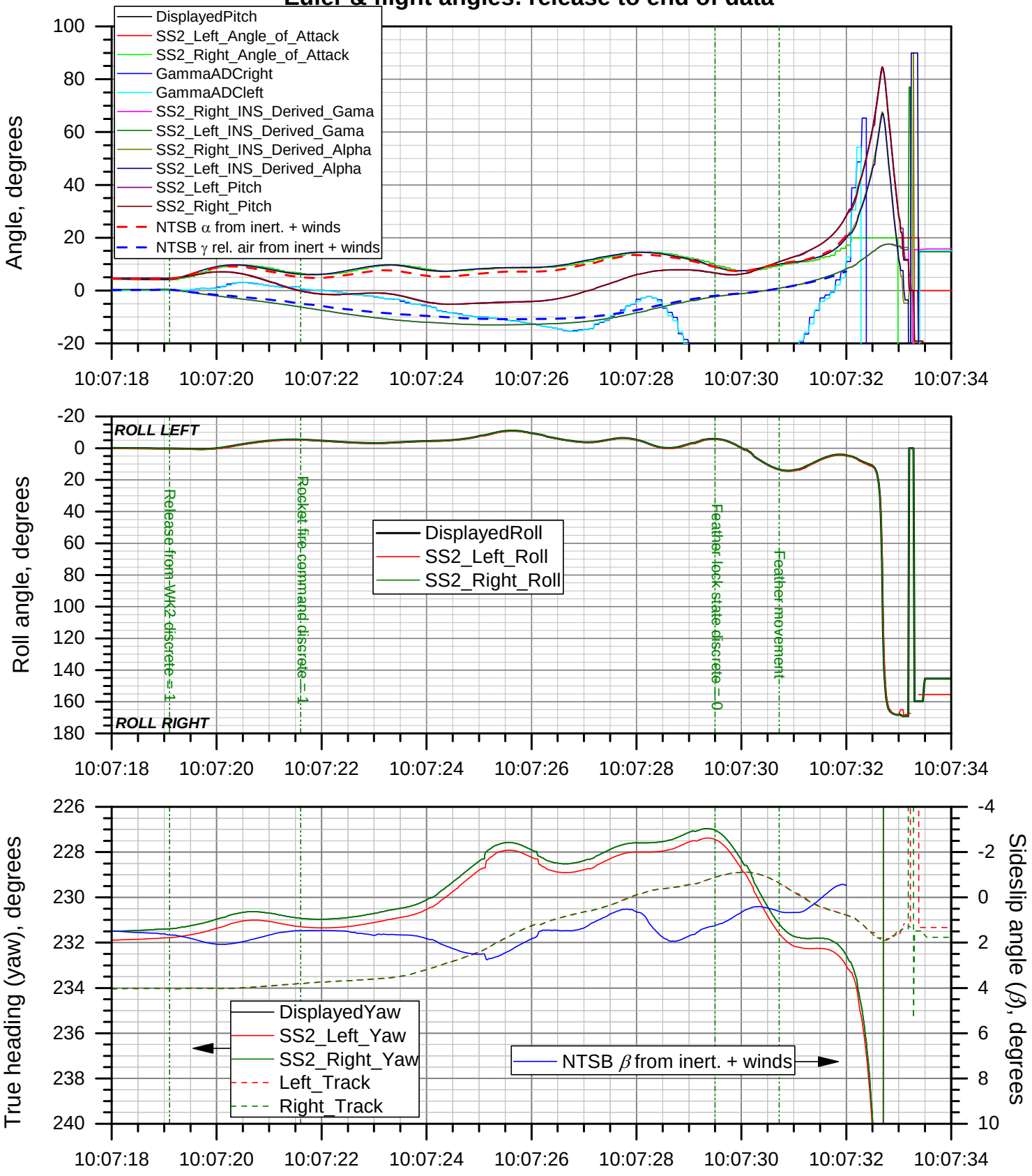

Figure 16.

DCA15MA019: SpaceShipTwo, N339SS, Koehn Dry Lake, CA, 10/31/2014

Angular rates: release to end of data

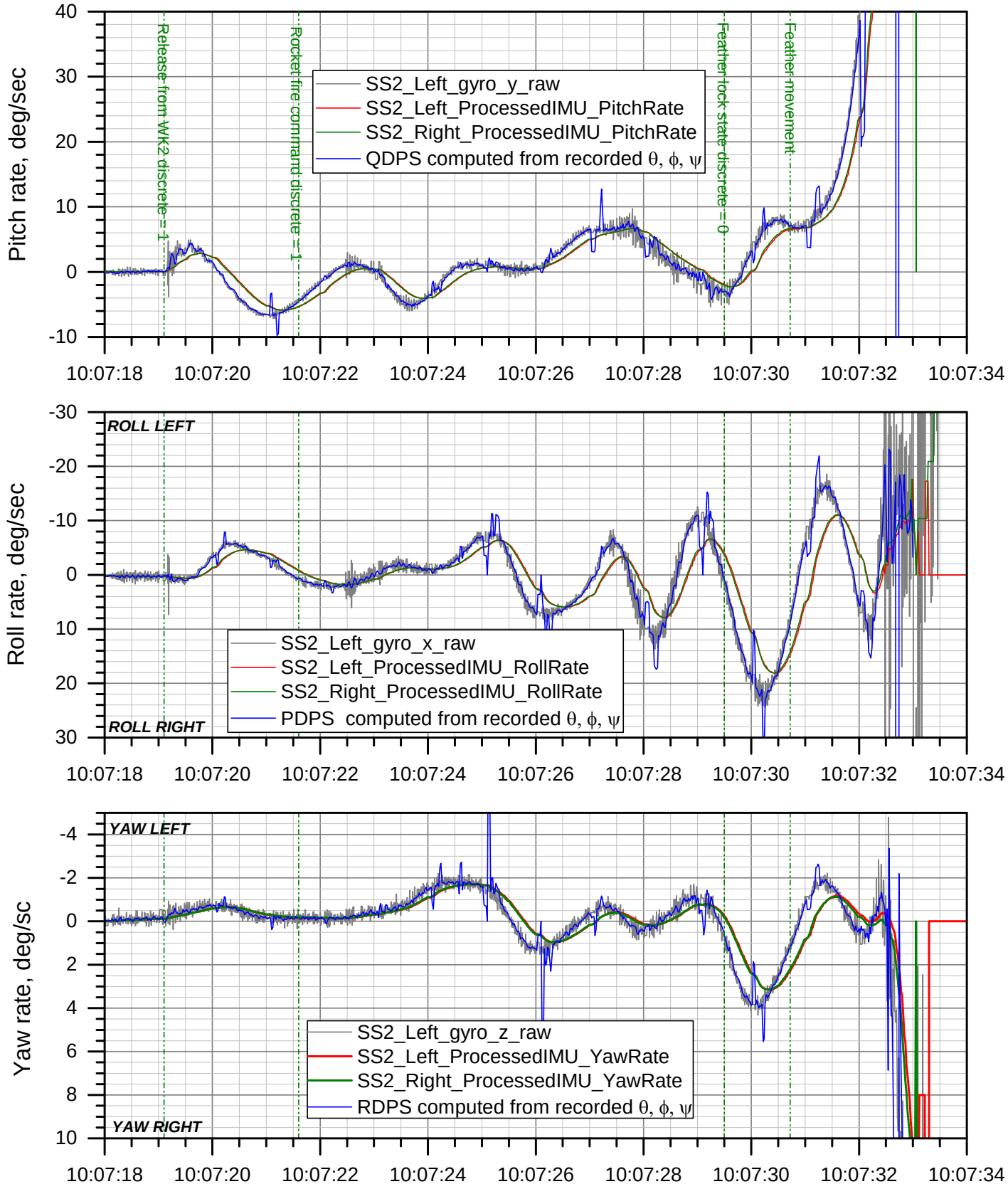

Figure 17.

DCA15MA019: SpaceShipTwo, N339SS, Koehn Dry Lake, CA, 10/31/2014

Load factors: release to end of data

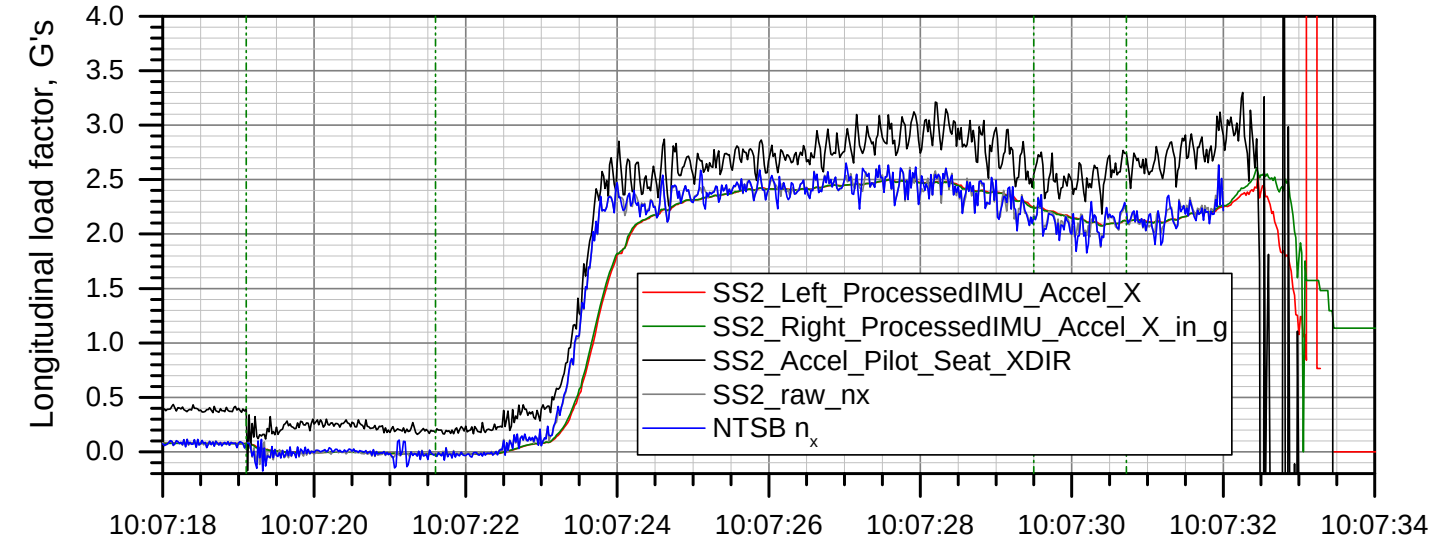

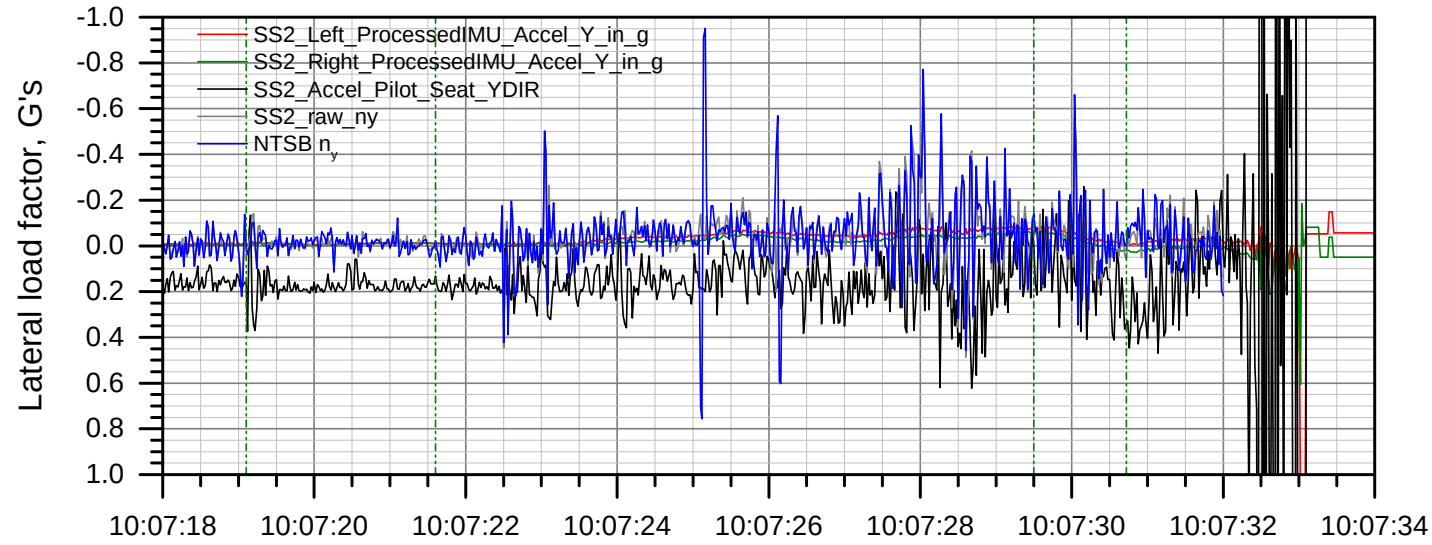

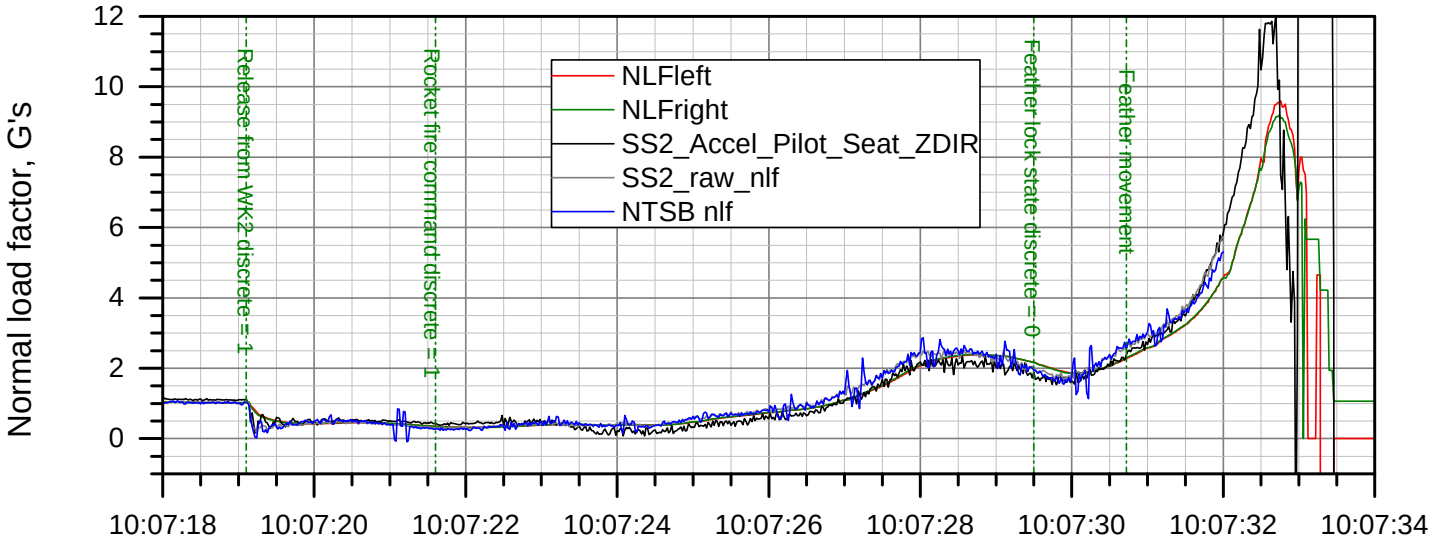

IRIG time, HH:MM:SS PDT

Figure 18.

DCA15MA019: SpaceShipTwo, N339SS, Koehn Dry Lake, CA, 10/31/2014

Stick & rudder positions & forces: release to end of data

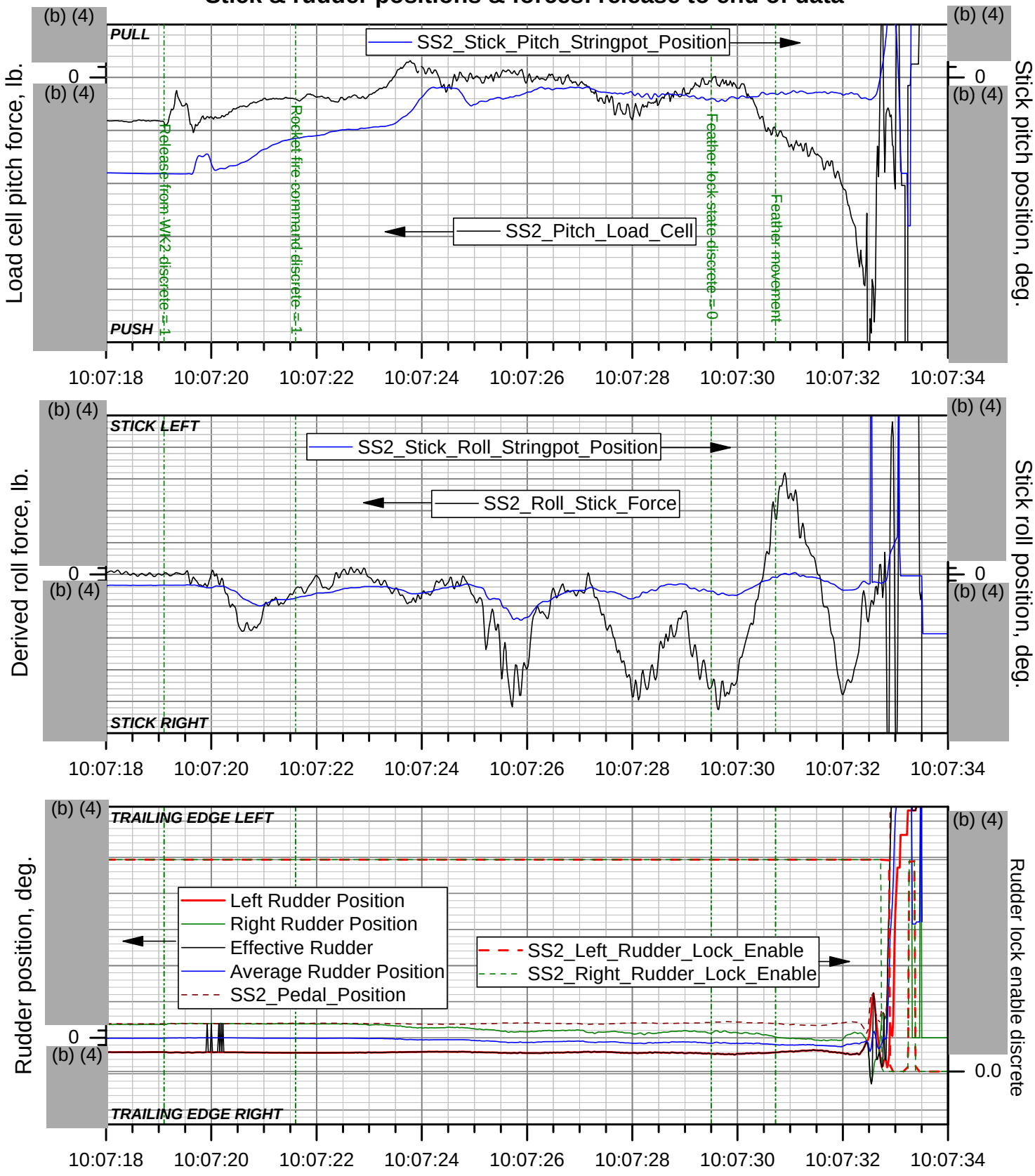

Figure 19.

DCA15MA019: SpaceShipTwo, N339SS, Koehn Dry Lake, CA, 10/31/2014

Stabilizer & elevon positions: release to end of data

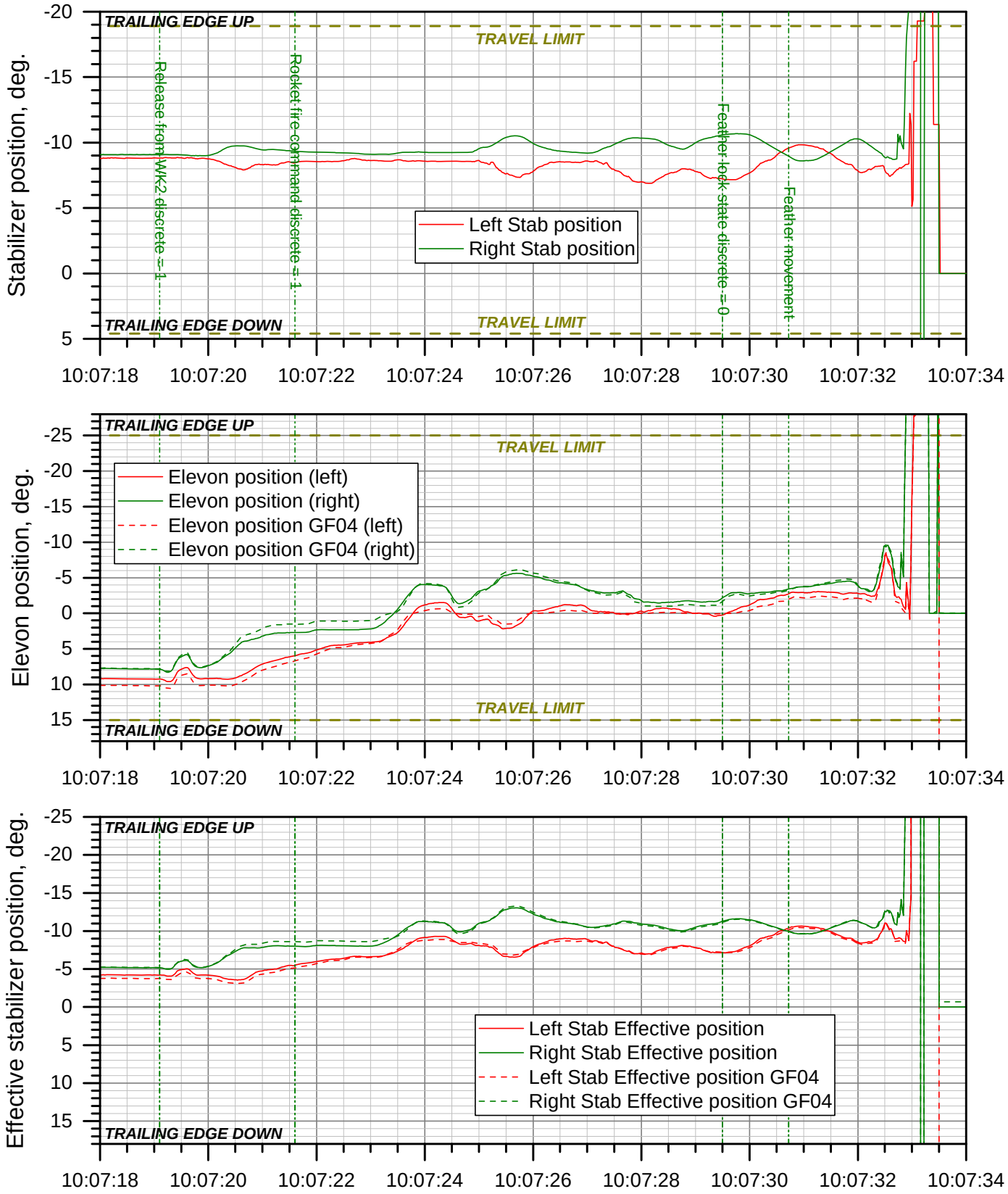

Figure 20.

DCA15MA019: SpaceShipTwo, N339SS, Koehn Dry Lake, CA, 10/31/2014

Stabilizer & elevon pitch & roll commands: release to end of data

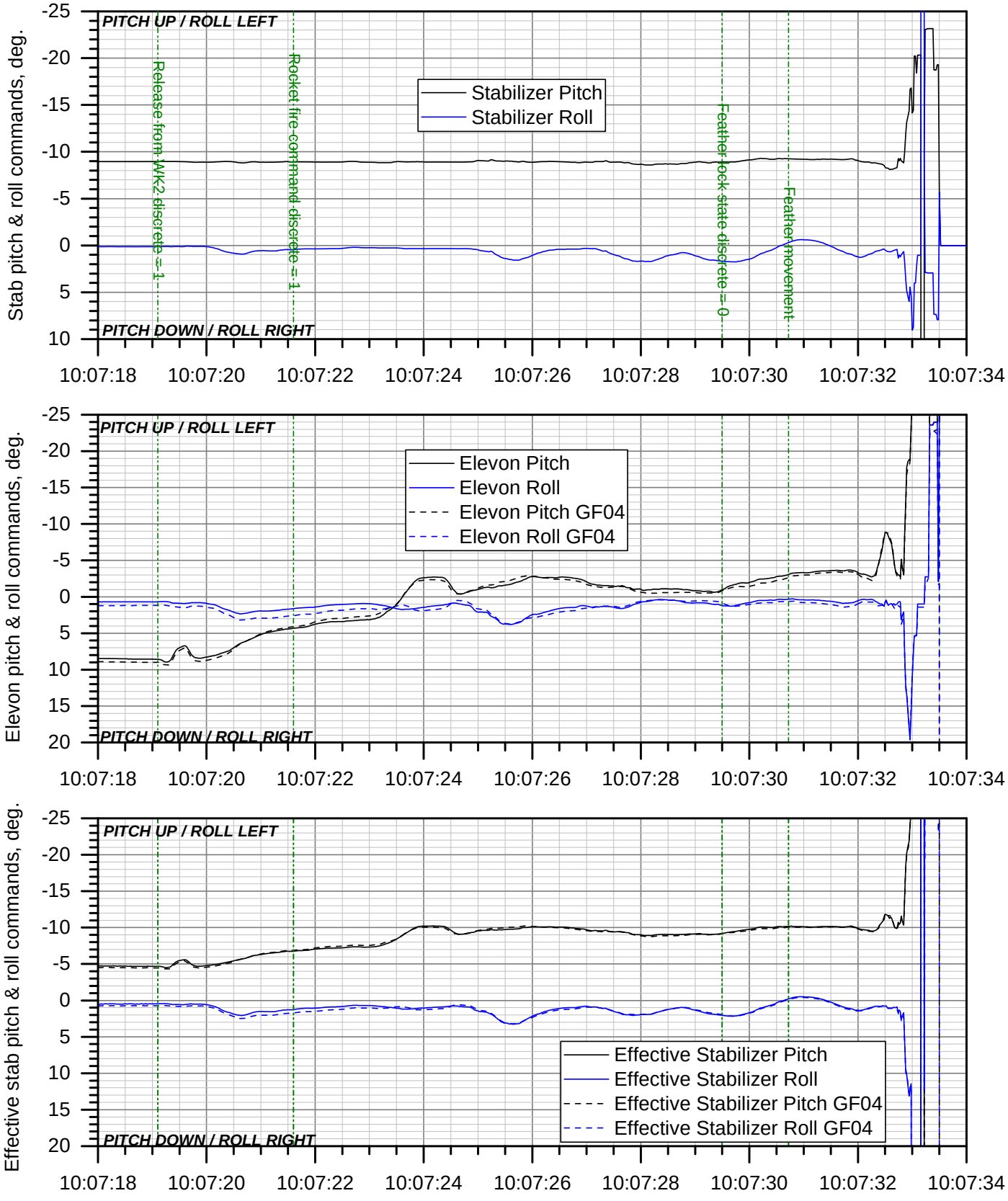

Figure 21.

DCA15MA019: SpaceShipTwo, N339SS, Koehn Dry Lake, CA, 10/31/2014

Atmospheric properties: release to end of data

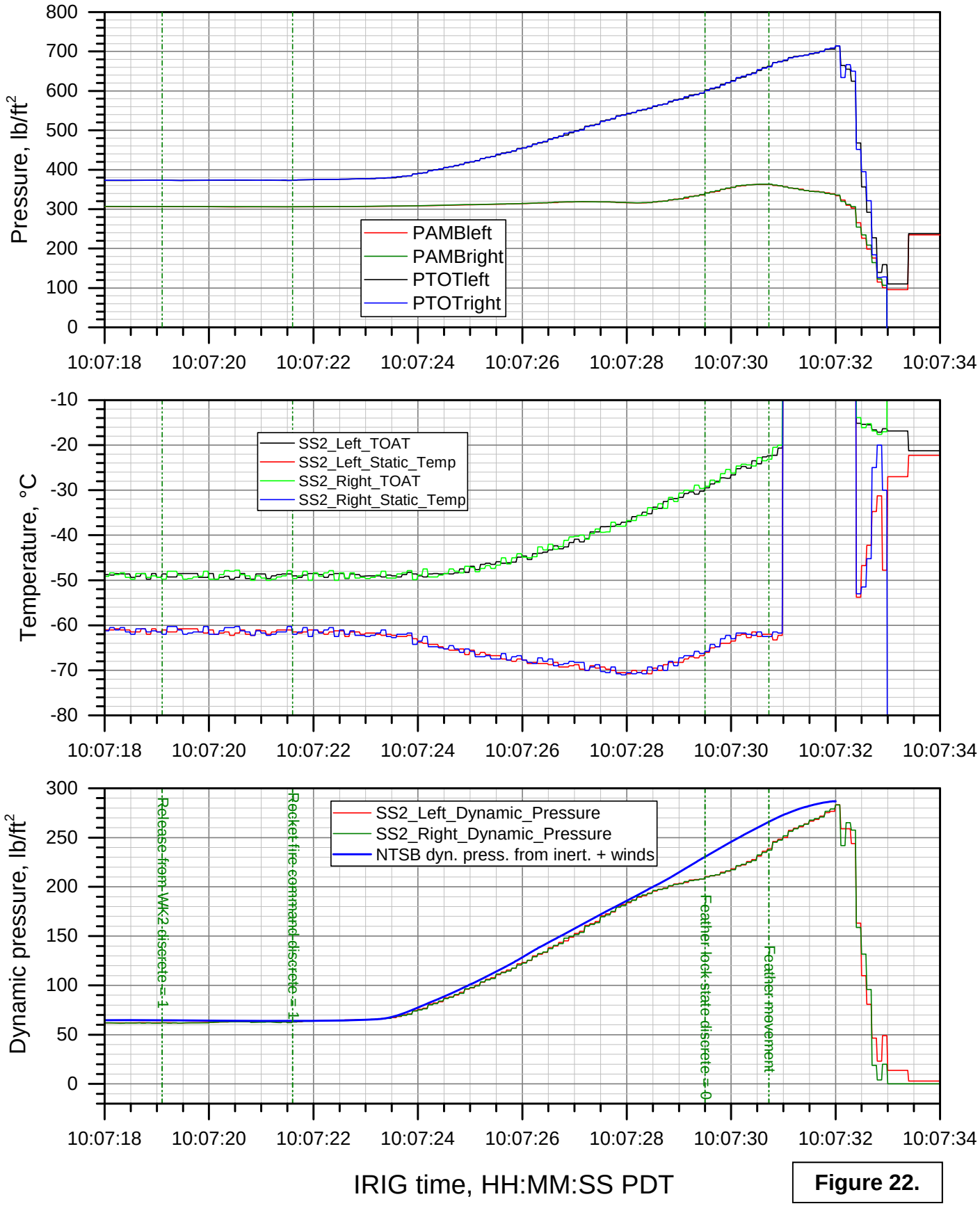

Figure 22.

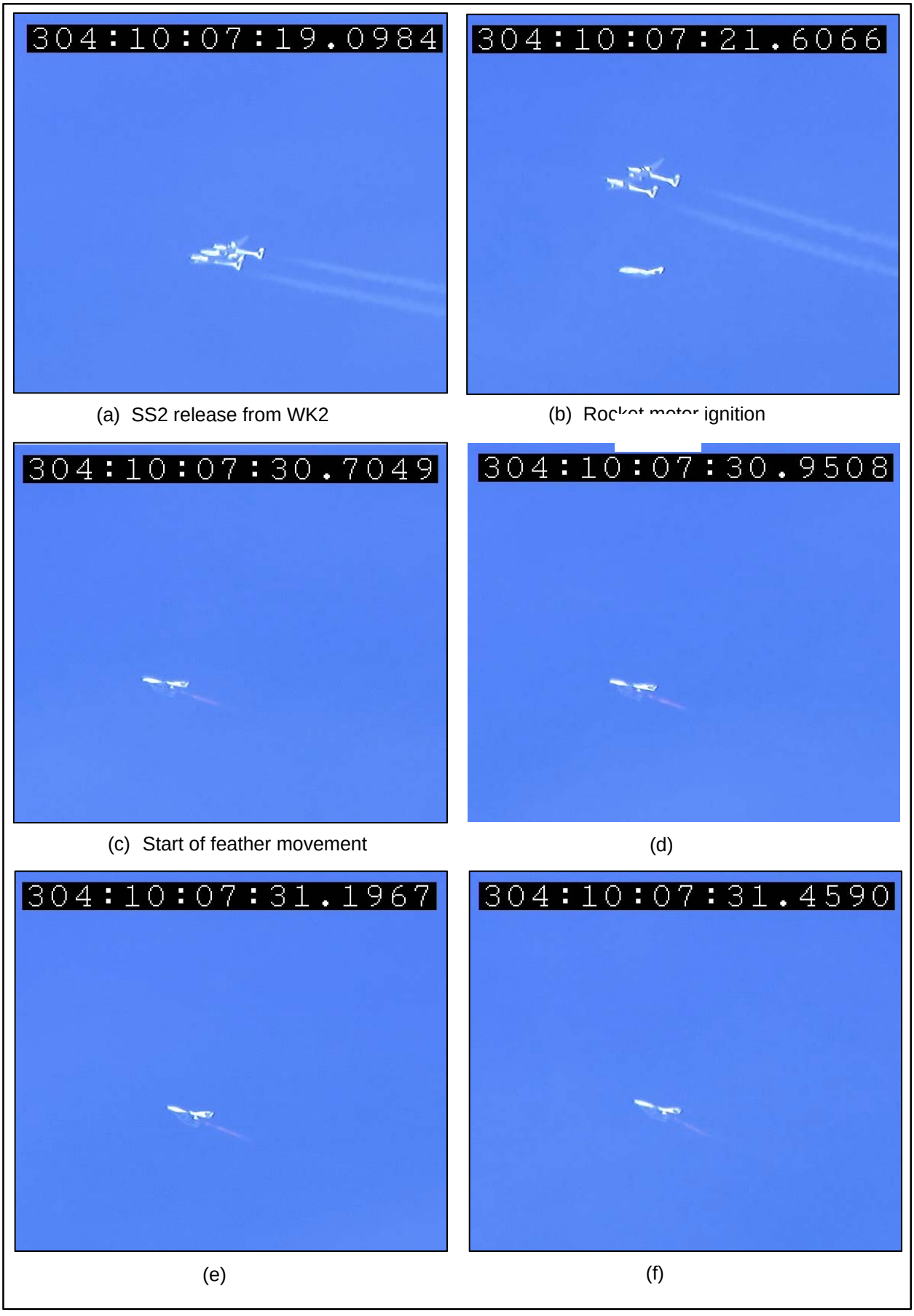

(a) SS2 release from WK2

(b) Rocket motor ignition

(c) Start of feather movement

(d)

(e)

(f)

Figure 23. Selected still images from NASA Dryden LRO camera (page 1 of 2).

Figure 23. Selected still images from NASA Dryden LRO camera (page 2 of 2).

DCA15MA019: SpaceShipTwo, N339SS, Koehn Dry Lake, CA, 10/31/2014

Winds aloft computed from WhiteKnightTwo during climb

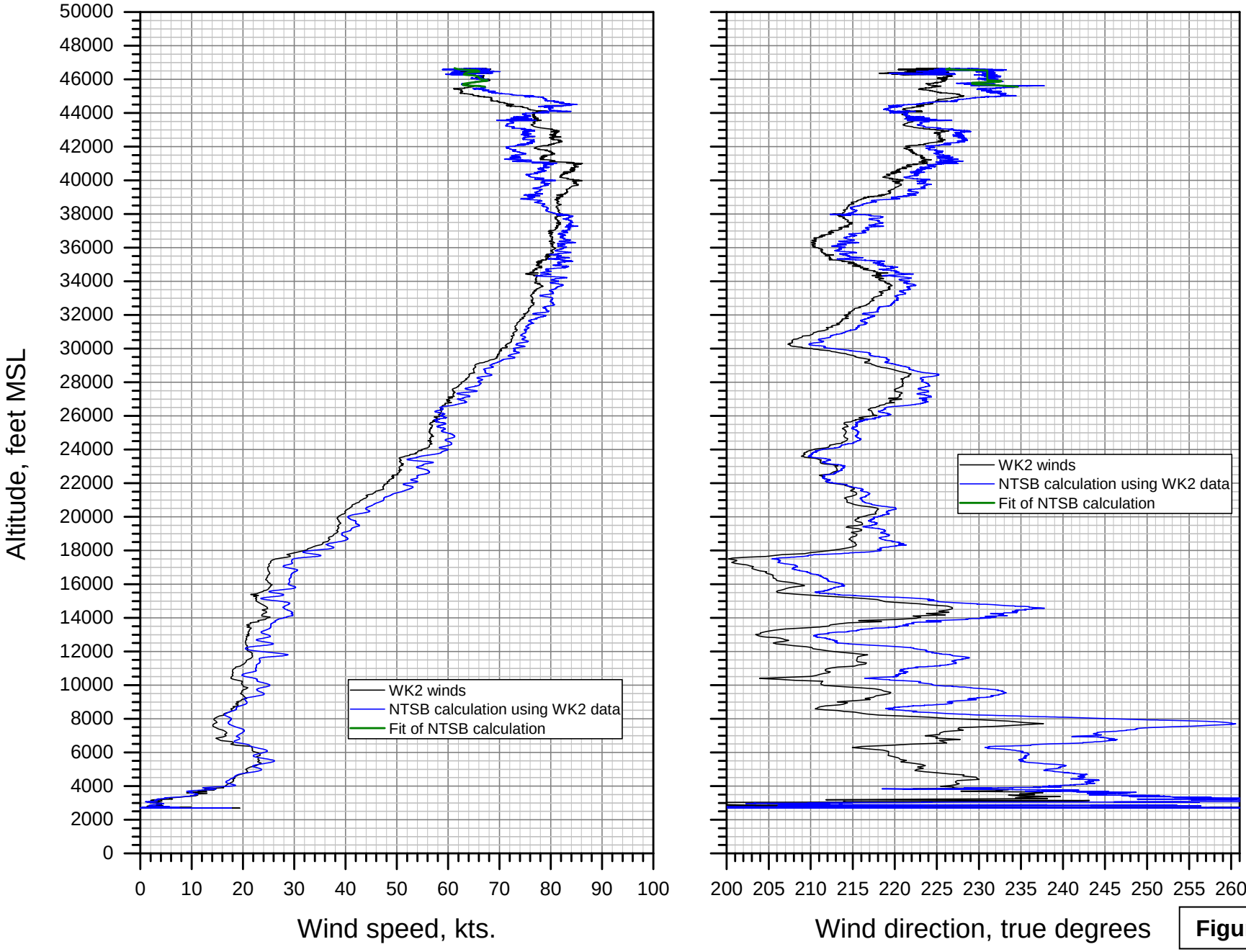

Figure 24a.

DCA15MA019: SpaceShipTwo, N339SS, Koehn Dry Lake, CA, 10/31/2014

Winds aloft computed from WhiteKnightTwo during climb (detail)

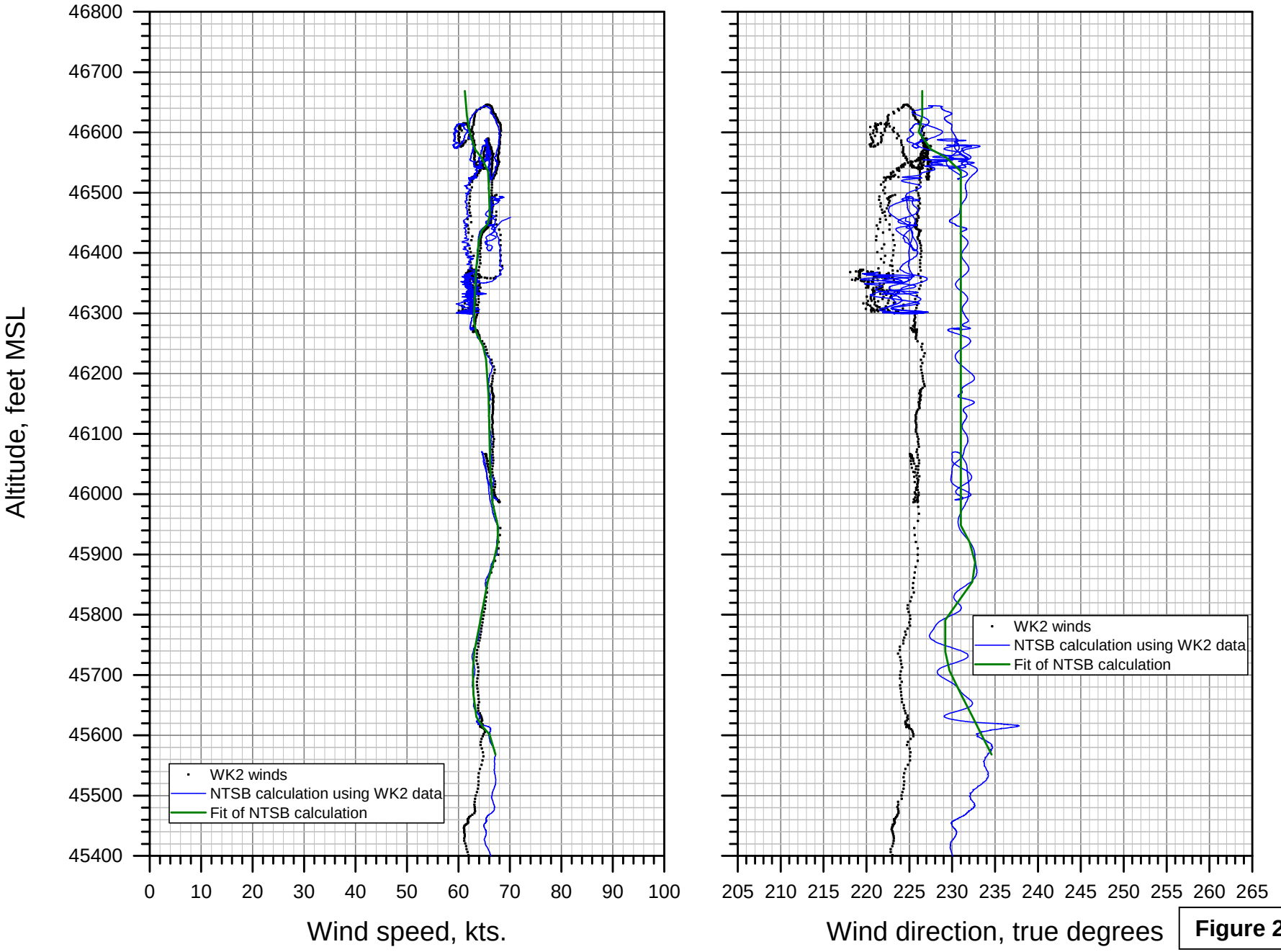

Figure 24b.

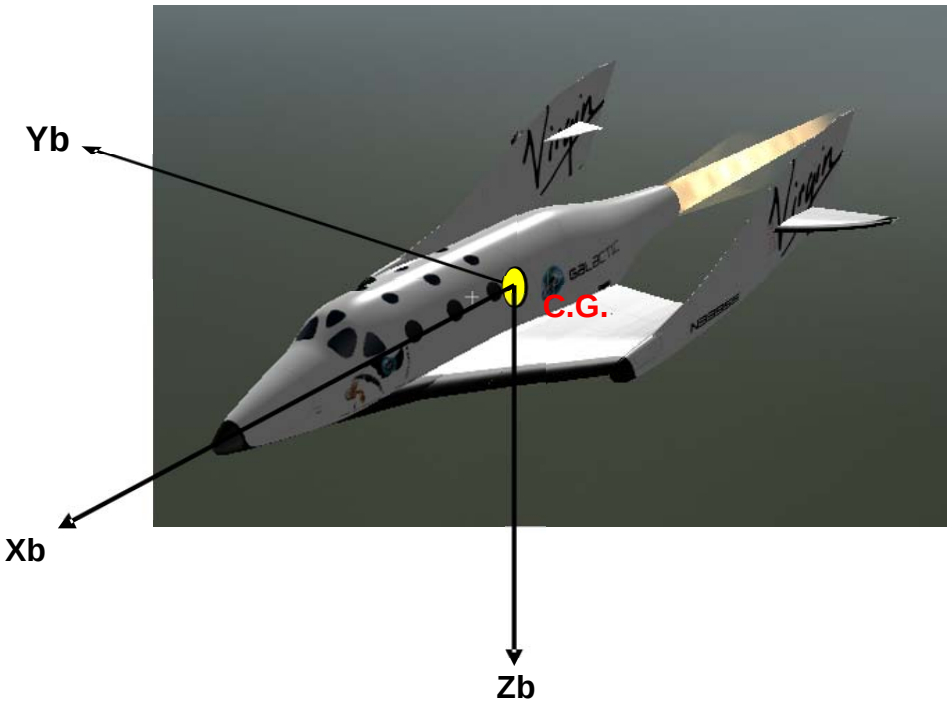

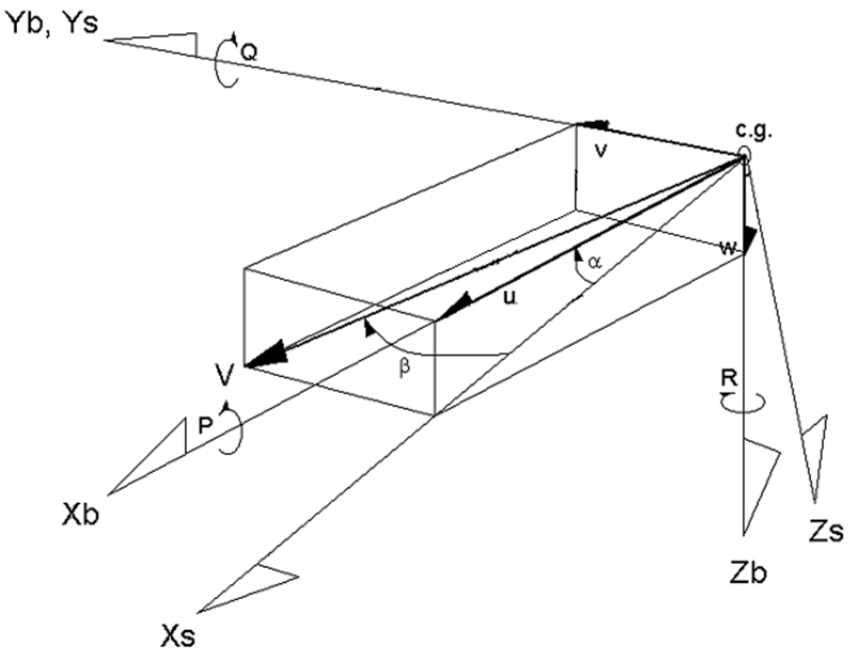

C.G. = center of gravity

{Xb, Yb, Zb} = body axis system

{Xs, Ys, Zs} = stability axis system

V = velocity vector

α = angle of attack

β = sideslip angle

P = body axis roll rate

Q = body axis pitch rate

R = body axis yaw rate

u = component of V along Xb

v = component of V along Yb

w = component of V along Zb

Figure 25.

DCA15MA019: SpaceShipTwo, N339SS, Koehn Dry Lake, CA, 10/31/2014

Feather moment calculation

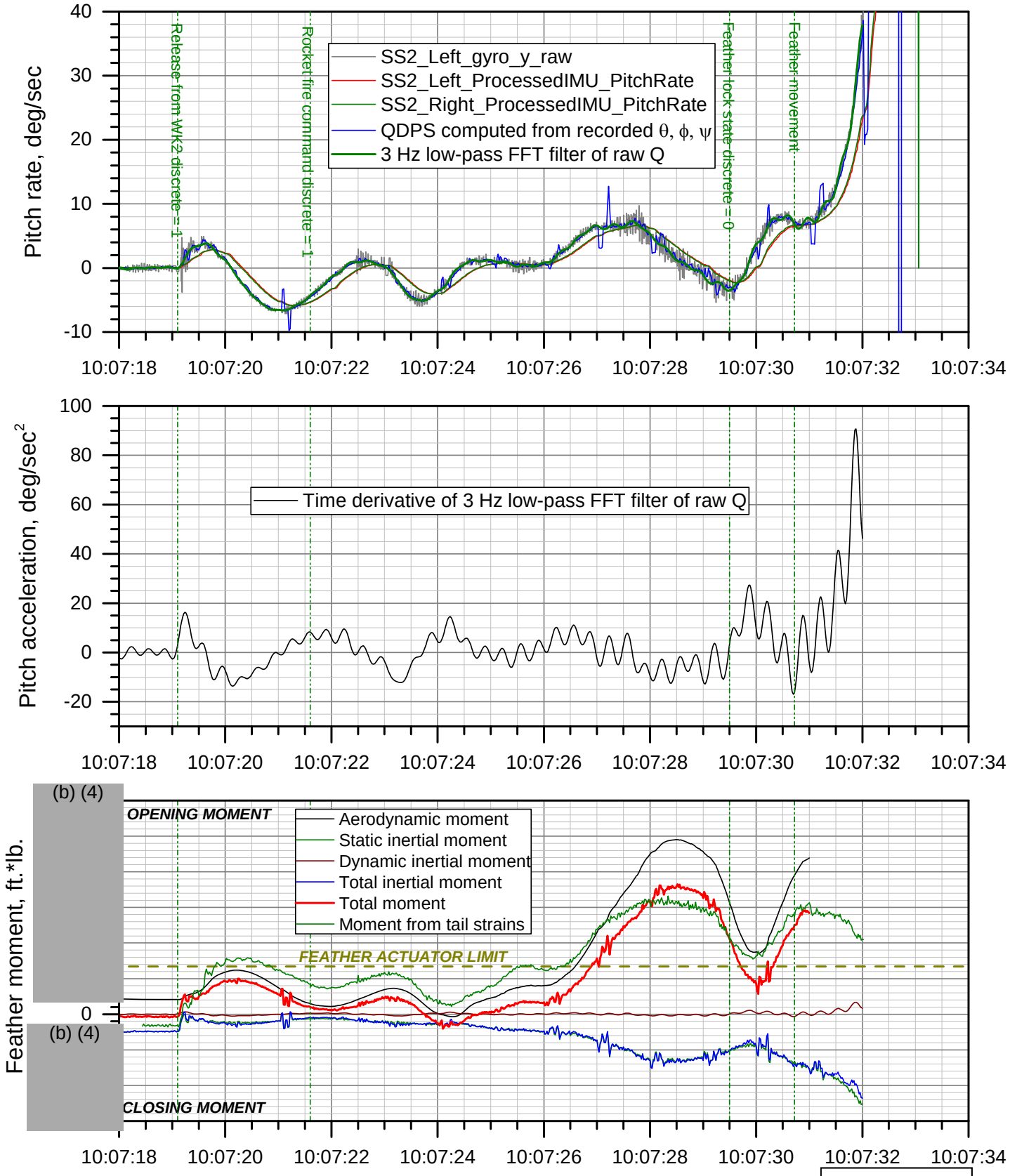

Figure 26.

DCA15MA019: SpaceShipTwo, N339SS, Koehn Dry Lake, CA, 10/31/2014

Comparision of TC & tail strain feather moments for PF01, PF02, & PF03

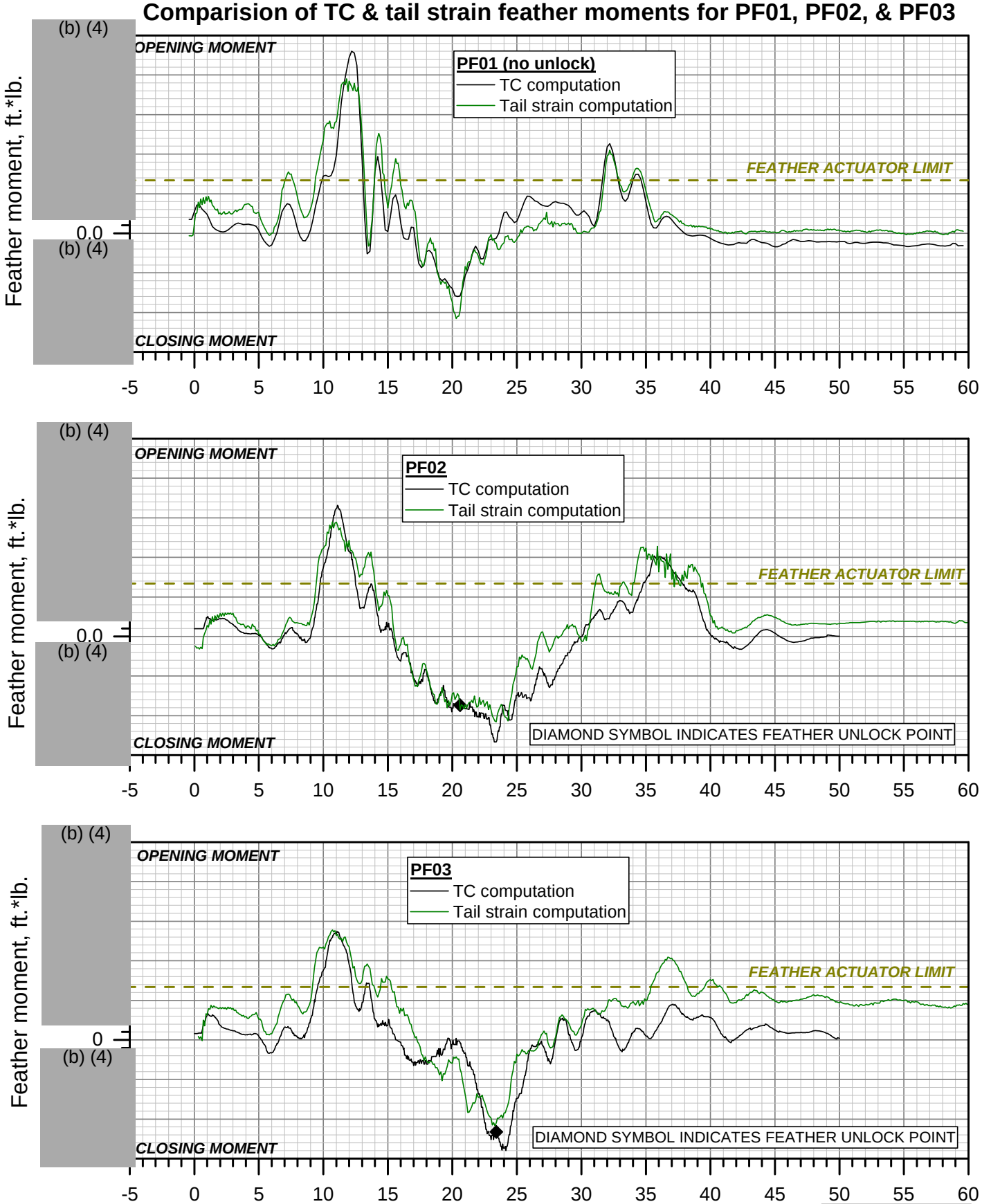

Figure 27.

DCA15MA019: SpaceShipTwo, N339SS, Koehn Dry Lake, CA, 10/31/2014

Comparision of TC feather moments for PF01, PF02, PF03 & PF04

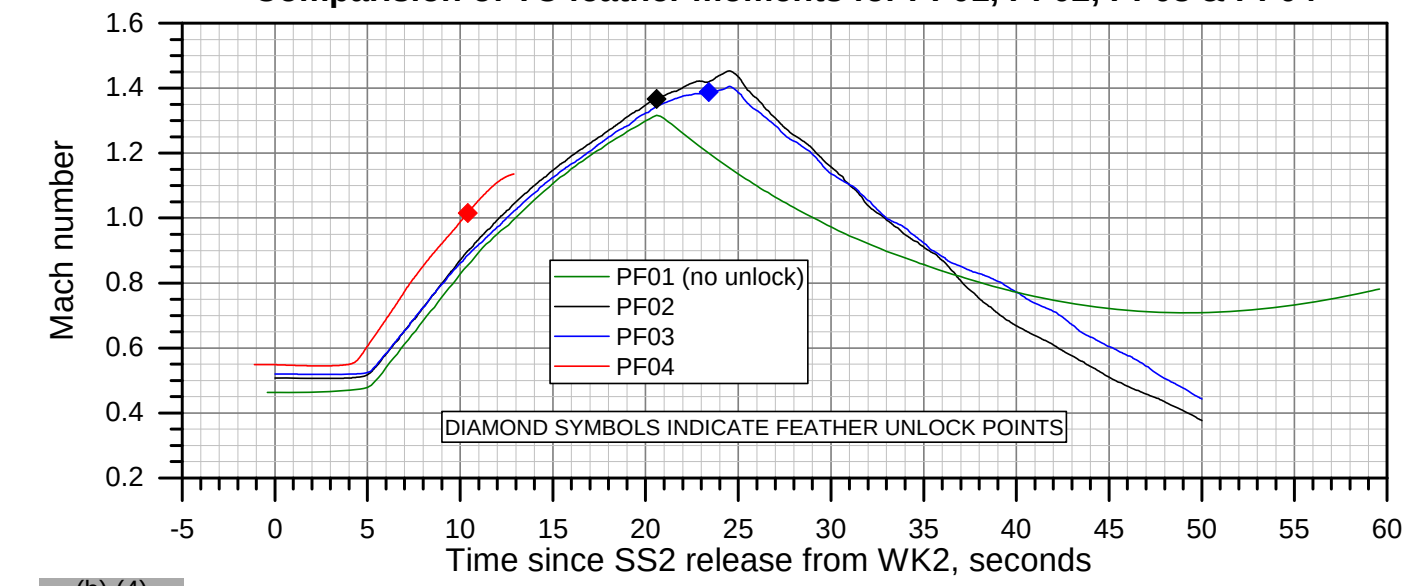

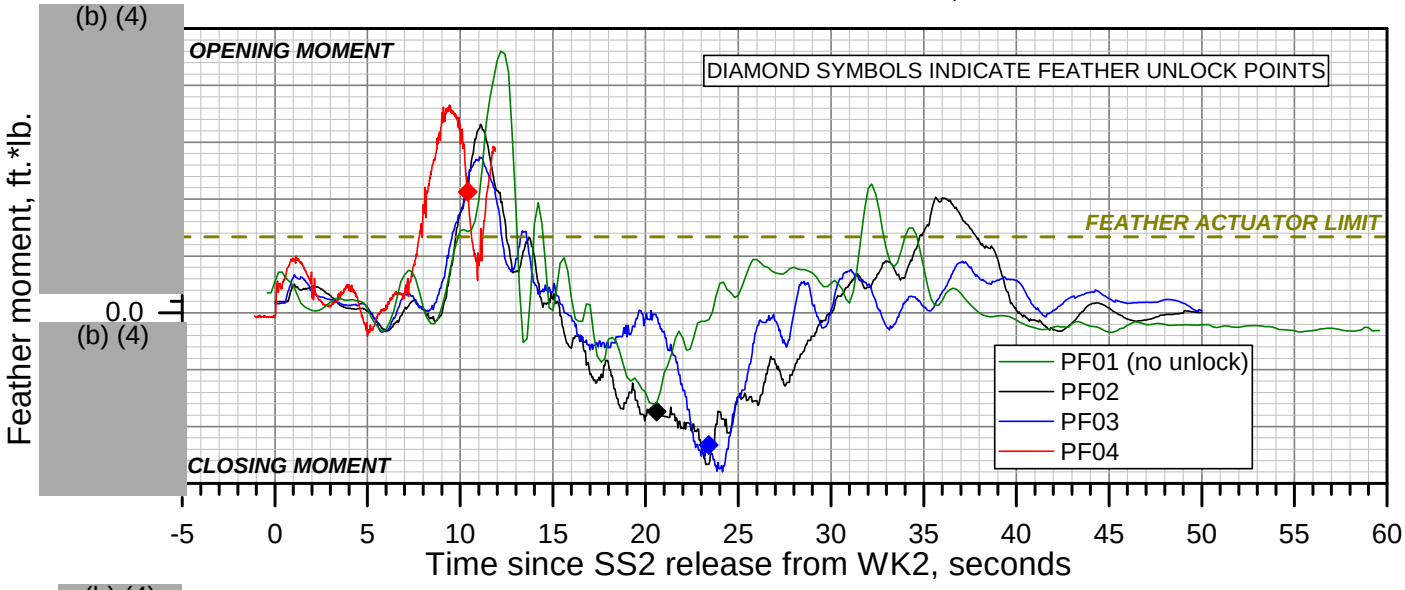

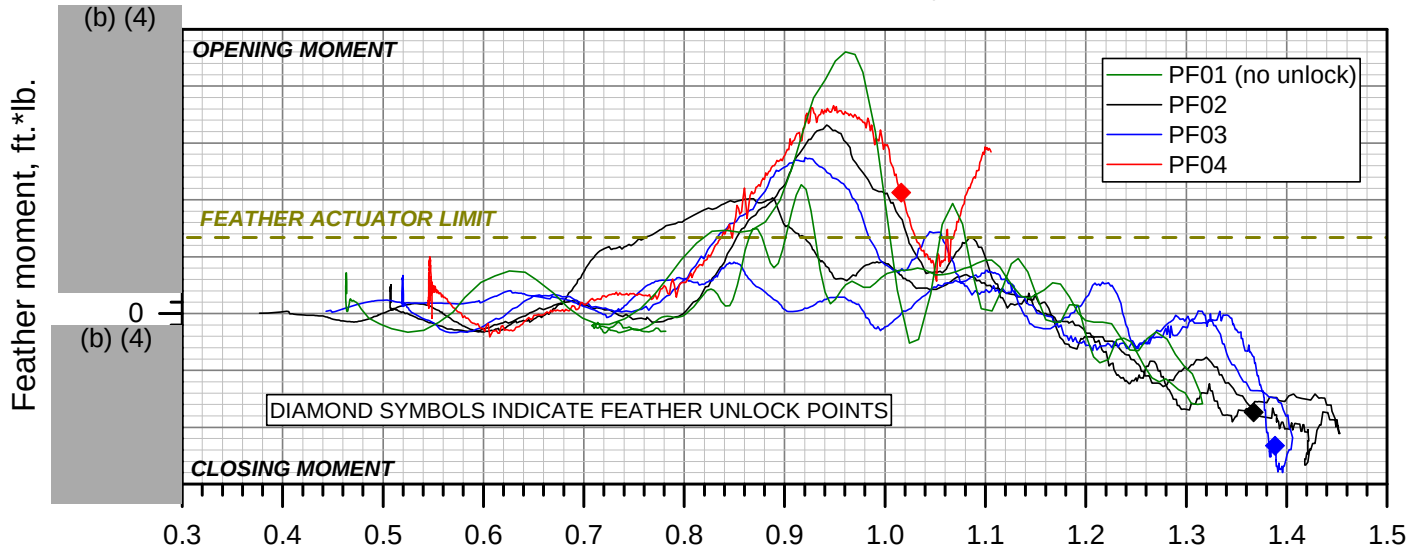

Figure 28.

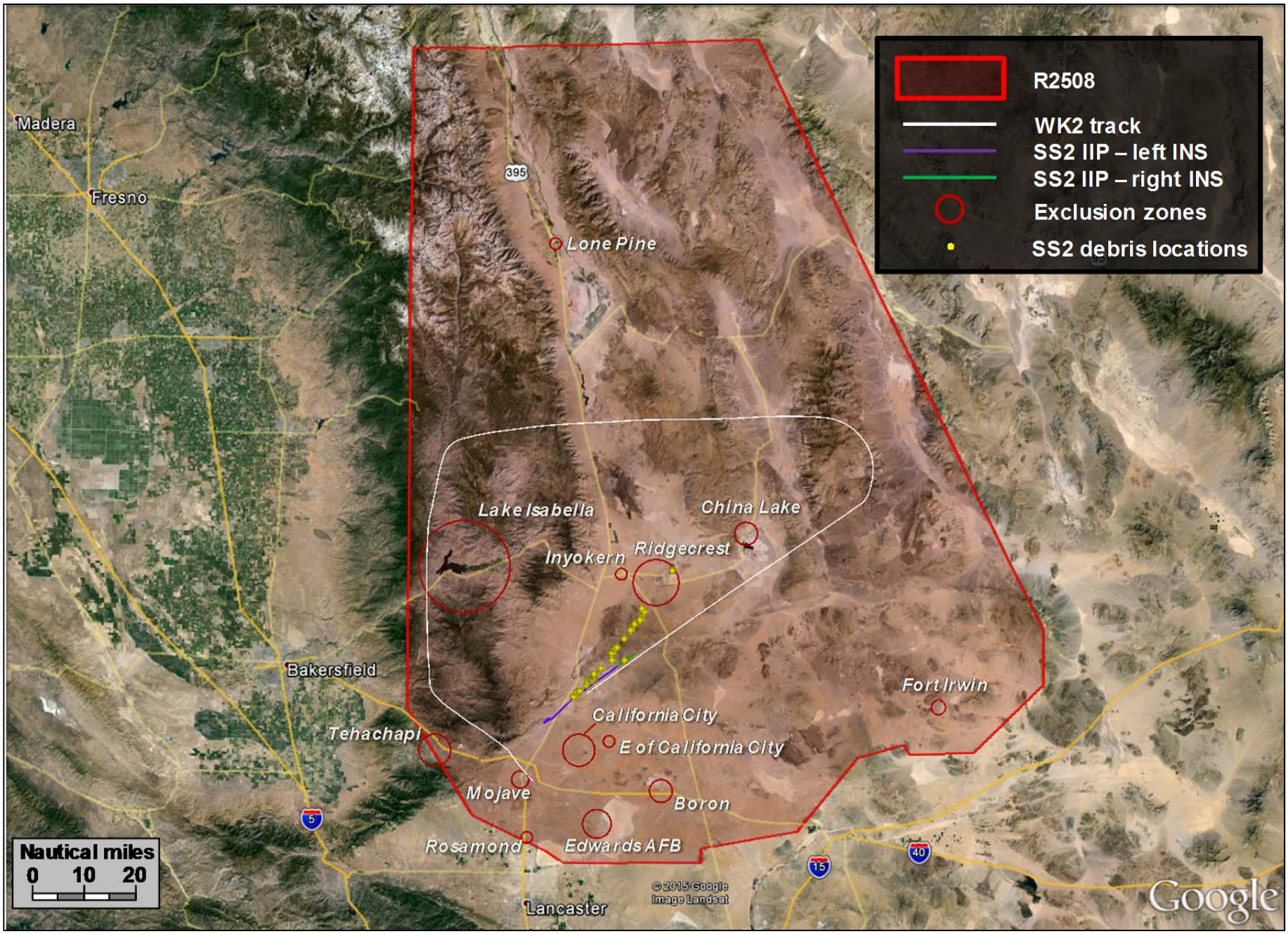
R2508
WK2 track
SS2 IIP – left INS
SS2 IIP – right INS
Exclusion zones
SS2 debris locations
Madera
Fresno
395
Lone Pine
Lake Isabella
China Lake
Inyokern
Ridgecrest
Bakersfield
Fort Irwin
California City
E of California City
Tehachapi
Mojave
Boron
Rosamond
Edwards AFB
Lancaster
5
15
40
Nautical miles
0 10 20
© 2015 Google
Image Landsat
Google

Figure 29.

THIS PAGE INTENTIONALLY LEFT BLANK